

Atmospheric Leaching of Enargite in the Presence of Carbon Based Catalysts

by

Fazlolah Ghazali Jahromi

A thesis submitted to the Robert M. Buchan Department of Mining

In conformity with the requirements for

the degree of Doctor of Philosophy

Queen's University

Kingston, Ontario, Canada

(August, 2018)

Copyright © Fazlolah Ghazali Jahromi, 2018

Abstract

Pyrometallurgy is not the most sustainable option for enargite concentrate treatment due to the environmental limitations on arsenic release. Therefore, developing an effective hydrometallurgical process is a promising solution for enargite treatment. Most hydrometallurgical processes proposed in literature have not reached commercial utilization because of common issues such as slow dissolution rate of the mineral, incomplete copper or precious metals recovery, sulfate generation, arsenic fixation problems, and high capital and operating costs.

In this thesis, the atmospheric leaching of enargite in chloride media was investigated in the presence of activated carbon (AC) and AF 5, a novel carbon based catalyst. Both catalysts were found to be very effective in facilitating the enargite leaching process and improved the oxidation and copper recovery from 65% to 92% (AC) or 96% (AF 5) after 96 hours. The best leaching condition was found to be: ferric and cupric concentrations greater than 5 g/L, concentrate to catalyst mass ratio of 1:2, and a 90 °C working temperature or higher. The elemental sulfur product of the leach reaction did not coat the surface of the partially leached mineral particles. When AF 5 was used as the catalyst in the leaching process, it collected the generated elemental sulfur. The arsenic also precipitated in the form of scorodite, one of the most stable forms of arsenic, during the leaching in chloride media at temperatures higher than 80 °C. The catalytic properties of the carbon-base catalysts (CBC) was due to the oxidation via oxygen functional groups on their surfaces, which were detected by XPS analysis.

The results showed that the chemical pre-treatment of CBC can be effective in increasing its catalytic effect on enargite leaching. The comparison between the chloride and sulfate media showed that the sulfate media has better copper and iron dissolution kinetics and promotes sulfur collection, whereas the remediation of arsenic in the form of scorodite can be superior in chloride media.

Co-Authorship

I have conducted all of the experiments, testing and analysis for these publications. I have also written the manuscript and this document. This work has performed with the assistance of Denver Cowan.

Acknowledgement

First and foremost, I would like to thank my supervisor, Professor Ahmad Ghahreman, for the opportunity he gave me to be part of his group. This thesis would not have been completed without his guidance, assistance, patience and support through my four years of research.

I would like to thank my thesis committee members, Professor Christopher Pickles, Professor Alvaro Videla, Professor Suning Wang, and Professor Jamie Archibald for their valuable comments about my research.

I am truly grateful to Larissa Smith for all of her friendship, help, and support. A special thanks goes to the Robert M. Buchan Department of Mining employees such as Wanda Badger, Oscar Rielo, Kate Cowperthwaite, Tina McKenna, Larry Steele, and Perry Ross for their assistance and support. I would also like to thank Graham Cairns for the ICP analysis and Curtis Macdonald for his help and conducting the SEM analysis.

I would like to thank my colleagues and friends for their support and advice. In particular, Ali S., Rebecca R., Sina J., Sepideh, Pooneh S., Parvin N, Alexander C., Lin L. and all of my fellow hydrometallurgy graduate students. I would also like to thank Milad A., and Denver C., who were like brothers to me. To be surrounded by such loving and caring people is a wonderful gift.

I would like to acknowledge the financial support of the Natural Sciences and Engineering Research Council of Canada through a Discovery Grant RGPIN-2015-05718. I would also like to thank the Ministry of Advanced Education and Skills Development for financial support for the Ontario Trillium Scholarship.

I would like to declare my sincere gratitude to my parents, Fariba and Reza, for their love and always encouraging me to strive to do well in whatever I pursue. Thank you to my sister Farnaz for always being there for me. You guys mean to world to me.

Finally, a huge thank you goes to my best friend, my wife, Fatemeh, for her support, love and encouragement over the course of my research. Thank you for your understanding, your patience, and

always encouraging me in my endeavors. I could not do it without you. To know that I can always count on you is beyond words.

Table of Contents

Abstract	ii
Co-Authorship.....	iii
Acknowledgement	iv
List of Figures	x
List of Tables	xv
List of Abbreviations	xvi
Chapter 1 Introduction	1
1.1 General overview	1
1.2 Research objectives.....	2
1.3 Thesis organization	2
Chapter 2 Literature review	4
2.1 Enargite treatment processes.....	5
2.1.1 Pyrometallurgical methods (roasting)	5
2.2 Hydrometallurgical processes	6
2.2.1 Atmospheric leaching	6
2.2.1.1 Ferric and cupric leaching.....	6
2.2.1.2 Albion process	8
2.2.1.3 Galvanox process	10
2.2.1.4 Silver assisted Galvanox process	12
2.2.1.5 AC assisted leaching	13
2.2.1.6 Alkaline sulfide leaching	14
2.2.2 Pressure oxidation process	14
2.2.2.1 Ammonia pressure leaching.....	15
2.2.2.2 Acidic pressure leaching	15
2.2.3 Biological leaching of enargite	19
2.2.3.1 BioCOP process	20
2.2.3.2 The BacTech/Mintek process.....	21
2.2.3.3 The GEOCOAT process	21
2.3 Activated carbon (AC) properties and catalytic mechanism.....	23
2.4 Arsenic remediation	25
Chapter 3 Materials and experimental methods.....	29
3.1 Materials	29

3.2 Leaching experiments	30
3.3 Oxidation and absorption	32
3.4 Solid analysis	33
3.5 Electrochemical experiments	34
Chapter 4 Catalyst characterization	36
Chapter 5 Lanxess Lewatit ® AF 5 and AC catalysis of enargite leaching in chloride media; A parameters study	40
5.1 Introduction.....	40
5.2 Result and discussion	40
5.2.1 Effect of mixing rate	40
5.2.2 Effect of catalysts.....	41
5.2.3 Effect of concentrate:catalyst mass ratio.....	45
5.2.4 Effect of initial ferric ion concentration.....	48
5.2.5 Effect of temperature	49
5.2.6 Effect of oxygen addition.....	51
5.2.7 Effect of sulfate addition.....	53
5.2.8 Effect of cupric addition	55
5.2.9 Effect of pulp density	57
5.2.10 Effect of retention time	58
5.2.11 SEM study.....	59
5.3 Conclusions.....	60
Chapter 6 The kinetics of enargite dissolution in chloride media in the presence of AC and AF 5 catalysts	62
6.1 Introduction.....	62
6.2 Results and discussion	63
6.2.1 Thermodynamic of enargite dissolution.....	63
6.2.2 Leaching kinetic model.....	66
6.2.3 High pulp density leaching	68
6.2.3.1 Enargite leaching without a catalyst	68
6.2.3.2 Enargite leaching with AC.....	69
6.2.3.3 Enargite leaching with AF 5	69
6.2.4 Low pulp density leach tests	73
6.2.4.1 Effect of particle size	75
6.2.4.2 Effect of initial cupric and ferric ions	76

6.2.5 Chronoamperometry experiments.....	78
6.2.6 SEM analysis	80
6.2.7 Effect of diffusivities	84
6.3 Conclusions.....	86
Chapter 7 Oxidative arsenic precipitation as scorodite during carbon catalyzed enargite leaching process	87
7.1 Introduction.....	87
7.2 Results and discussion	87
7.2.1 Scorodite crystallization during enargite leaching with AC and AF 5	87
7.2.1.1 Effect of temperature on the arsenic recovery	87
7.2.1.2 Effect of carbon-based catalysts on the arsenic recovery	90
7.2.1.3 Effect of ferric ion on the arsenic recovery.....	92
7.2.1.4 Effect of oxygen sparging rate on the arsenic recovery	94
7.2.1.5 Effect of seed addition on the arsenic recovery	95
7.2.1.6 Free acid concentration effect on the arsenic recovery	96
7.2.2 The effect of iron on the precipitation and dissolution	97
7.2.3 Scorodite characterization.....	102
7.3 Conclusions.....	108
Chapter 8 Effect of surface modification with different acids on the catalytic properties of AF 5 during atmospheric leaching of enargite	110
8.1 Introduction.....	110
8.2 Results and discussion	113
8.2.1 Pre-treated AF 5 surface Characterization	113
8.2.1.1 Infrared (IR) Spectroscopy.....	113
8.2.1.2 Surface analysis by XPS	114
8.2.1.3 Sulfur analysis.....	123
8.2.2 Adsorption and oxidation.....	124
8.2.2.1 Adsorption.....	124
8.2.2.2 The AF 5 catalysis of oxidation process	125
8.2.3 Effect of catalyst pre-treatment and leaching media on enargite leaching.....	128
8.2.3.1 Oxidative enargite leaching with AF 5 catalyst	128
8.2.3.2 Arsenic oxidation with AF 5 catalyst.....	129
8.2.3.3 Iron oxidation with AF 5 catalyst	131
8.2.3.4 Elemental sulfur adsorption onto AF 5 during leaching tests	133

8.2.3.5 XPS study of the residue and the post leaching catalysts	134
8.3 Conclusions.....	138
Chapter 9 General conclusions and recommendations	140
9.1 Conclusions.....	140
9.2 Recommendations.....	142
References.....	143

List of Figures

Figure 2-1. Schematic diagram of chalcopyrite electrochemical leaching in the presence of ferric ions (Dixon et al., 2008)	8
Figure 2-2. Schematic diagram of galvanically-assisted electrochemical leaching (Dixon et al., 2008)....	11
Figure 2-3. High temperature pressure oxidation flow sheet to treat copper arsenide minerals (Safarzadeh et al., 2012)	18
Figure 2-4. Copper dissolution rate for mesophiles and thermophiles of a chalcopyrite concentrate (Batty and Rorke, 2006).....	21
Figure 2-5. Galvanic interactions between enargite and AC particles (Ghanad, 2011).....	23
Figure 3-1. Absorption and oxidation experimental setup.....	33
Figure 4-1. Optical microscope image of catalysts (a) AC, (b) AF 5	37
Figure 4-2. Pore volume distribution based on different pore width range (a) AC, (b) AF 5.....	37
Figure 4-3. Nitrogen adsorption isotherm for AC and AF 5.....	38
Figure 4-4. XP C1s core level spectra of the: (a) AC and (b) AF 5.....	39
Figure 4-5- XP O 1s core level spectra of the: (a) AC and (b) AF 5	39
Figure 5-1. Effect of mixing rate on the copper recovery (0.5 M HCl, 1 g/L ferric concentration and at 80 °C).....	41
Figure 5-2. Copper recovery in the presence of AF 5 and AC at 80 and 90 °C and no catalyst at 90 °C (0.5 M HCl, 1.5 M Cl ⁻ , 5 g/L cupric ions, 5 g/L ferric ions, 0.1 L/min O ₂ , concentrate/catalyst=1:1).....	43
Figure 5-3. Effect of concentrate/ catalyst ratio on copper recovery (a) with AC (b) with AF 5 (5 g/L cupric ions, 5 g/L ferric ions, 0.1 L/min O ₂ , 90 °C).....	46
Figure 5-4. Effect of AC ratio on copper recovery at 80 and 90 °C (5 g/L cupric ions, 5 g/L ferric ions, 0.1 L/min O ₂)	47
Figure 5-5. Effect of surface area on final copper recovery after 96 h of leaching with AC and AF 5.....	48
Figure 5-6. Effect of ferric ion concentration on the copper recovery (a) without catalyst (80 °C, without catalyst) (b) with AF 5 catalyst (5 g/L cupric ions, concentrate to AF 5 1:1, 90 °C)	49
Figure 5-7. Effect of temperature on the copper recovery (5 g/L cupric ions, 5 g/L ferric ions oxygen flow rate 0.1 L/min) (a) without a catalyst (b) With AC (concentrate to AC 1:1) (c) With AF 5 (concentrate to AF 5 1:1)	51
Figure 5-8. Effect of oxygen sparging rate on copper recovery in the presence of: (a) AC (b) AF 5 (5 g/L cupric ions, 5 g/L ferric ions, concentrate to catalyst 1:1, 90 °C).....	53

Figure 5-9. Effect of sulfate addition on copper recovery (a) without catalyst (ferric ions 1 g/L, cupric ions 0 g/L, 80 °C) 1 g/L (b) with AC (5 g/L cupric ions, 5 g/L ferric ions, concentrate to AC 1:1, 80 °C)	55
Figure 5-10. Effect of cupric ion addition on copper recovery (a) with AC (b) with AF 5 (90°C, concentrate to catalyst =1:1, 5 g/L ferric ions)	56
Figure 5-11. Effect of pulp density on the copper recovery in the presence of AC (90°C, concentrate to AC=1:1).....	58
Figure 5-12. Effect of time on the leaching recovery (5 g/L ferric ions, 5 g/L cupric ions, 70°C, concentrate to AC=1:1).....	59
Figure 5-13. SEM images of enargite concentrate after 1 day of leaching in the presence of AC (a) powder (b) cross section	60
Figure 5-14. SEM and EDS analysis on an AF 5 bead cross section after two days of leaching (a) Back scatter image (b) EDS map for sulfur	60
Figure 6-1. Speciation of copper complexes during leaching experiment in the presence of AF 5 with 5 g/L initial ferric ions and 5 g/L initial cupric ions at 90 °C, (a) Simulated by Phreeqc software, (b) Simulated by OLI software	65
Figure 6-2. Speciation of iron complexes during leaching experiment in the presence of AF 5 with 5 g/L initial ferric ions and 5 g/L initial cupric ions at 90 °C, (a) Simulated by Phreeqc software, (b) Simulated by OLI software.....	66
Figure 6-3. The effect of temperature on the copper recovery during the enargite leaching processes (a) without a catalyst, (b) plot of SCM for product layer diffusion control process without catalyst, (c) with AC catalyst, (d) plot of SCM for product layer diffusion control process with AC catalyst, (e) with AF 5, and (f) plot of SCM for product layer diffusion control process with AF 5 catalyst.	71
Figure 6-4. The effect of temperature on the arsenic recovery during the enargite leaching process (10 g enargite concentrate, 5 g/L initial cupric and 5 g/L initial ferric) (a) without a catalyst, (b) plot of SCM for product layer diffusion control process without catalyst, (c) with AC catalyst, (d) plot of SCM for product layer diffusion control process with AC catalyst, (e) with AF 5, and (f) plot of SCM for product layer diffusion control process with AF 5 catalyst	74
Figure 6-5. Effect of particle size on arsenic recovery in the presence of AF 5	75
Figure 6-6. Plot of K_R versus $1/r_0$ and K_D versus $1/r_0^2$ (10 g concentrate, 1:1 concentrate to AF 5 ratio, 5 g/L initial cupric ions, 5 g/L initial ferric ions at 90 °C)	76
Figure 6-7. Effect of initial cupric concentration on arsenic recovery (10 g concentrate, 1:1 concentrate to AF 5, 5 g/L initial ferric ions at 90 °C)	77

Figure 6-8. Effect of initial ferric concentration on arsenic recovery (10 g concentrate, 1:1 concentrate to AF 5, 5 g/L initial cupric ions at 90 °C)	77
Figure 6-9. Chronoamperometric test at 80 °C: Current vs. time plot at different potentials.....	79
Figure 6-10. Chronoamperometric test at 60 °C: Current vs. time plot at different potentials.....	80
Figure 6-11. SEM cross section of leaching residue after 1 day of leaching.....	81
Figure 6-12. (a) SEM cross section of fresh AC (b) SEM cross section of fresh AC in higher magnification, (c) SEM cross section of utilized AC, (d) SEM cross section of utilized AC in higher magnification	82
Figure 6-13. (a) SEM cross section of fresh AF 5 (b) SEM cross section of fresh AF 5 in higher magnification, (c) SEM cross section of utilized AF 5, (d) SEM cross section of utilized AF 5 in higher magnification	83
Figure 6-14. SEM micrograph of leach residue after 1 day of leaching	84
Figure 7-1. Effect of temperature on the arsenic recovery in the absence of catalyst (0.5 M HCl, 5 g/L ferric ions, 5 g/L cupric ions, 1.5 M Cl ⁻)	88
Figure 7-2. Effect of temperature on arsenic recovery in presence of AF5 (0.5 M HCl, 5 g/L ferric ions, 5 g/L cupric ions, 1.5 M Cl ⁻ , concentrate:AF 5 ratio 1:1, 0.1 L/min oxygen sparging rate)	89
Figure 7-3. Effect of the AC addition on arsenic recovery (90 °C, 0.5 M HCl, 5 g/L ferric ions, 5 g/L cupric ions, 1.5 M Cl ⁻ , 0.1 L/min oxygen sparging rate)	91
Figure 7-4. Effect of the AF 5 addition on the arsenic recovery from the enargite concentrate (90 °C, 0.5 M HCl, 5 g/L ferric ions, 5 g/L cupric ions, 1.5 M Cl ⁻ , 0.1 L/min oxygen sparging rate).....	92
Figure 7-5. Effect of ferric ion dosage on the arsenic recovery in the presence of AF 5 (90° C, 0.5 M HCl, 5 g/L cupric ions, 1.5 M Cl ⁻ , concentrate:AF 5 ratio 1:1)	93
Figure 7-6. Effect of oxygen on arsenic recovery in the presence of AF 5 (90 °C, 0.5 M HCl, 5 g/L cupric ions, 1.5 M Cl ⁻ , concentrate:AF 5 ratio 1:1)	95
Figure 7-7. Effect of seed particle addition on arsenic recovery	96
Figure 7-8. Free acid titration results during leaching without catalyst, with AF 5 and without seed and with AF 5 with scorodite seed addition (all the leaching experiments were performed with 5 g/L ferric ions, 5 g/L cupric ions at 90 °C).....	97
Figure 7-9. Ferric/ferrous ion concentration in the presence of (a) AC at 90 °C, (b) AF 5 at 90 °C and (c) of AF 5 at 70 °C.....	100
Figure 7-10. Effect of initial ferric concentration on: (a) final iron dissolution and (b) ferric ion concentration.....	101
Figure 7-11. Effect of different AF5 ratios on ferric concentration.....	102

Figure 7-12. XRD patterns of the solid residue with 5 g/L ferric ions, 5 g/L cupric ions, concentrate: AF 5 1:1 at 90 °C (a) after 60 h of leaching (b) after 96 h of leaching	103
Figure 7-13. XRD patterns of solid residue with: (a) 5 g/L ferric ions, 5 g/L cupric ions, without catalyst (b) 5 g/L ferric ions , 5 g/L cupric ions and 200 g AC (c) 5g/L ferric ions, 5 g/L cupric ions and 25 g AF 5 (d) 2.5 g/L ferric ions, 5 g/L cupric ions and 50 g AF 5 (e) 10 g/L ferric ions, 5 g/L cupric ions and 50 g AF 5 (f) 5 g/L ferric ions, 0 g/L cupric ions and 50 g AF 5, (g) 5 g/L ferric ions, 5 g/L cupric ions and 50 g AF 5.....	104
Figure 7-14. TGA curve of final leaching residue on the final leaching residue with and without the seed and on the initial precipitation solid after 60 h of leaching in the nitrogen environment (90 °C with 5 g/L ferric ions, 5 g/L cupric ions and concentrate: AF 5 1:1).....	106
Figure 7-15. SEM micrograph of the precipitates obtained (a) after 50 hours of leaching (b) after 96 h of leaching (c) after 50 h of leaching in the presence of seed crystals (d) after 96 h of leaching in the presence of seed crystals (at ferric ion dosage of 5 g/L, in the presence of AF 5 at 90 °C).....	107
Figure 7-16. Optical microscopy micrograph of the precipitated scorodite	108
Figure 8-1. Oxygen, sulfur and nitrogen functional groups on the surface of CBC	112
Figure 8-2. DRIFT spectra of the treated AF 5 in the 4000-450 cm ⁻¹	114
Figure 8-3. XPS spectra of AF 5 with different pre-treatment	115
Figure 8-4. XPS spectra of oxygen 1s peak for different AF 5 treatments: (a) Water treated (b) Hydrochloric acid treated, (c) Sulfuric acid treated, (d) Nitric acid treated, (e) Raw data comparison....	117
Figure 8-5. XPS spectra of sulfur 2p peak for different AF 5 treatments: (a) Water treated (b) Hydrochloric acid treated, (c) Sulfuric acid treated, (d) Nitric acid treated, (e) Raw data comparison....	119
Figure 8-6. XPS spectra of carbon 1s peak for different AF 5 treatments (a) Water treated (b) Hydrochloric acid treated, (c) Sulfuric acid treated, (d) Nitric acid treated, (e) Raw data comparison....	121
Figure 8-7. XPS spectra of nitrogen 1s peak for nitric acid treated AF 5.....	123
Figure 8-8. (a) Copper adsorption values for different initial concentration of copper on AF 5, (b) iron adsorption values for different initial concentration of iron on AF 5 (0.5 M hydrochloric acid, 1 L solution, 1.5 M Cl ⁻ and 50 g AF 5 at 90 °C)	125
Figure 8-9. (a) Concentration of Fe(II) ions in the solution versus time, (b) concentration of Fe(III) ions in the solution versus time (0.5 M hydrochloric acid, 5 g/L initial cupric and ferric ion concentration, 0.1 L solution, 1.5 M Cl ⁻ and 5 g AF 5 at 90 °C)	126
Figure 8-10 . Oxidation of As versus time in the presence of the catalysts, 5 g/L iron and copper in chloride media with 2 g/L As(III) initial concentration at 80 °C.....	127
Figure 8-11. Effect of acid type and catalyst pretreatment on copper recovery	129
Figure 8-12. Effect of acid type and catalyst pretreatment on arsenic recovery	131

Figure 8-13. Effect of acid type and catalyst pretreatment on iron recovery (50 g enargite, concentrate to AF 5 ratio 1:1, 90 °C for 96 h)	132
Figure 8-14. XPS spectra of the leaching residue from hydrochloric acid experiment for (a) arsenic 3d, (b) iron 2p, (c) sulfur 2p.....	136
Figure 8-15. XPS spectra of the AF 5 used in leaching experiment for (a) arsenic 3d, (b) iron 2p, (c) sulfur 2p, (d) oxygen 1s	137
Figure 8-16. XPS spectra of nitrogen 1s peak for nitric acid treated AF 5 after 96 h of leaching.....	138

List of Tables

Table 2-1. Conventional copper minerals in copper extraction industry	4
Table 2-2. Hydrometallurgical processes for copper (Ghahreman, 2018).....	22
Table 3-1. Head assay of enargite sample.....	29
Table 3-2. XRD results for head concentrate.....	29
Table 4-1. Characterization and properties of AC and AF 5	36
Table 5-1. The copper recovery from solid and solution analysis (0.5 M HCl, 1.5 M Cl ⁻ , 5 g/L cupric ions, 5 g/L ferric ions, 0.1 L/min O ₂ , concentrate/catalyst=1:1).....	44
Table 5-2. Solution ORP values during the leaching without catalyst, AF 5 and AC (0.5 M HCl, 1.5 M Cl ⁻ , 5 g/L cupric ions, 5 g/L ferric ions, 0.1 L/min O ₂ , concentrate/catalyst=1:1)	44
Table 6-1. R square values and slope of the fitted lines of different controlling mechanisms in SCM.....	72
Table 6-2. Diffusivities of Cu ²⁺ at different temperatures	85
Table 7-1. Comparison between the arsenic precipitation recovery from solid and solution analysis	105
Table 8-1. Relative content of functional groups in O 1s peak.....	116
Table 8-2. Relative concentration of different groups in C 1s peak	122
Table 8-3. Sulfur content in AF 5 samples	123
Table 8-4. The free acid concentration in leaching solution.....	133
Table 8-5. Sulfur balance of the leaching experiments.....	134

List of Abbreviations

AC	Activated Carbon
ASL	Alkaline Sulfide Leaching
b	Stoichiometric coefficient
BFA	Basic Ferric Arsenate
BSE	Back Scatter Electron
CBC	Carbon Based Catalyst
CIL	Carbon in Leach
D	Diffusion coefficient (cm ² /s)
EDS	Energy Dispersive X-Ray Spectroscopy
FH	Ferrihydrate
FTIR	Fourier-Transform Infrared Spectroscopy
HTPOX	High Temperature Pressure Oxidation
ICP	Inductively Coupled Plasma
k _D	Kinetic parameter for product layer diffusion control
k _F	Kinetic parameter for liquid film diffusion control
k _R	Kinetic parameter for reaction control
M	Molar
MPAES	Microwave Plasma Atomic Emission Spectroscopy
MTPOX	Medium Temperature Pressure Oxidation
P ₈₀	80% of particles passing
PGM	Platinum Group Metals
PLS	Pregnant Leach Solution
<i>Q_d</i>	Activation energy for diffusion (kJ/mol)

R	Gas constant (J/mol.K)
r_0	Particle radius (m)
SCM	Shrinking Core Model
SE	Secondary Electron
SEM	Scanning Electron Microscope
SHE	Standard Hydrogen Electrode
t	Time (min)
T	Absolute temperature (K)
TGA	Thermogravimetric Analysis
tph	Tons Per Hour
X	Fraction of reacted particle
XPS	X-Ray Photoelectron Spectroscopy
XRD	X-Ray Diffraction
μm	Micrometer
$\rho_{Cu_3AsS_4}$	Molar density of enargite

Chapter 1

Introduction

1.1 General overview

Enargite (Cu_3AsS_4), the most refractory copper mineral, has recently gained attention due to the value of metals, such as copper and gold, present in the mineral and the significance of arsenic immobilization (Safarzadeh et al., 2012). Arsenic-bearing sulfide minerals, such as enargite, were traditionally treated using a roasting process in the past (Peacey et al., 2010; Safarzadeh et al., 2012). However, in the past decade strict environmental regulations have required pyrometallurgical methods treating arsenical minerals to decrease sulfur and arsenic emissions (Nazari et al., 2017).

Hydrometallurgical methods, on the other hand, can be more environmental friendly processes which are often capable of treating low grade ores and are less capital intensive. In addition, hydrometallurgical processes are able of produce a stable arsenical compound compared to that formed by the pyrometallurgical techniques. However, there are several common issues with the hydrometallurgical alternatives that make most of them impractical or commercially unappealing. Most of these processes suffer from one or more of the following challenges: low metal recovery, high acid generation, co-precipitation problems, corrosion, and high oxygen consumption due to sulfur oxidation.

A chloride-based process at ambient pressure is one of the most effective methods to leach copper-bearing sulfides (Lundström et al., 2005) owing to its higher copper dissolution rate, higher elemental sulfur generation, enhanced redox behavior, and smaller scale of the plant unit operations (Liddicoat and Dreisinger, 2007; Lundström, 2009; M S Safarzadeh et al., 2012).

1.2 Research objectives

The ultimate goal of this study is to develop an atmospheric hydrometallurgical leaching process for enargite treatment. To reach this goal, the enargite leaching process is investigated in chloride media with and without the addition of carbon-based catalysts (CBC): activated carbon (AC), and Lanxess Lewatit® AF 5 (abbreviated as AF 5), which is a novel carbon based catalyst. The objectives of the study are:

- To study the effect of different parameters and identify the effective factors on the CBC performance and leaching process
- To propose a comprehensive leaching reaction for enargite leaching in chloride media based on the thermodynamic calculations and solution simulation
- To investigate the behavior of arsenic during the leaching process and evaluate the effective factors on the in-situ precipitation of arsenic during the leaching process
- To improve the catalytic activity of AF 5 by chemical pre-treatments in the leaching process and boost the activity and performance of this catalyst

1.3 Thesis organization

In the second chapter, the literature pertaining to different recovery methods and background of this research will be discussed.

The experimental methods used in this study and the analytical methods will be explained in Chapter 3 and the catalysts characterizations will be discussed in Chapter 4.

Chapter 5 will discuss the dissolution of enargite in chloride media and investigate the effect of different parameters on the dissolution process. Moreover, single and synergistic effects of different parameters on copper dissolution rate will be presented. This chapter will be followed by a thermodynamic and kinetics study of the dissolution process in Chapter 6.

Chapter 7 is assigned to the arsenic fixation process, the characterization of the arsenical compound generated in the leach process, and the effective parameter on the precipitation process.

The characterization of the catalyst's functional groups, and their manipulation by the chemical pre-treatment of the catalysts, will be presented in Chapter 8. At the end, the conclusions and recommendations for future work will be presented in Chapter 9. Literature citations in this thesis are given in the Reference section.

Chapter 2

Literature review

There are several copper minerals which can be used as a source of copper in the copper extraction industry, as listed in Table 2-1. Enargite, one of the most refractory copper minerals, is the main contaminant for chalcopyrite concentrates. Chalcopyrite is the most abundant copper reserve in the world (representing about 70% of Cu resources). The depletion of copper resources and need for deeper mining operations for higher grade copper ores have led to exposure of more enargite veins in the ores, a major issue in copper mining and for the metallurgical industry (Safarzadeh et al., 2012).

Table 2-1. Conventional copper minerals in copper extraction industry

Mineral Name	Chemical Formula
Azurite	$2\text{CuCO}_3 \cdot \text{Cu}(\text{OH})_2$
Bornite	Cu_5FeS_4
Brochantite	$\text{CuSO}_4 \cdot 3\text{Cu}(\text{OH})_2$
Chalcocite	Cu_2S
Chalcopyrite	CuFeS_2
Chrysocolla	$\text{CuSiO}_3 \cdot 2\text{H}_2\text{O}$
Covellite	CuS
Cuprite	Cu_2O
Dioptase	$\text{CuSiO}_3 \cdot \text{H}_2\text{O}$
Enargite	Cu_3AsS_4
Malachite	$\text{CuCO}_3 \cdot \text{Cu}(\text{OH})_2$
Tennantite	$\text{Cu}_{12}\text{As}_4\text{S}_{13}$
Tenorite	CuO
Tetrahedrite	$\text{Cu}_{12}\text{Sb}_4\text{S}_{13}$

The refractoriness of copper minerals can be compared as follows:

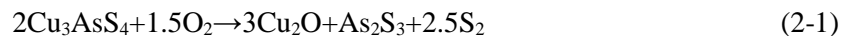
Chalcocite (Cu₂S) < Covellite (CuS) < Bornite (Cu₅FeS₄) < Chalcopyrite (CuFeS₂) < Enargite (Cu₃AsS₄)

Several treatment methods have been developed for copper sulfide minerals and enargite. The two major methods can be classified as either pyrometallurgical or hydrometallurgical, which will be explained later.

2.1 Enargite treatment processes

2.1.1 Pyrometallurgical methods (roasting)

Roasting is one of the commercially used processes for treating large quantities of enargite. This process is performed at 600-750 °C and its products are low arsenic calcine and arsenic trioxide dust or solution. The chemical reaction which takes place in the limited oxygen roasting process is described in Equation 2-1. The roasting reaction starts at about 525 °C, however the maximum arsenic removal rate can be achieved at 700-750 °C (Lattanzi et al., 2008; Peacey et al., 2010; Safarzadeh et al., 2012).



Usually the roasting process is carried out under oxidizing conditions to oxidize most of the elemental sulfur to SO₂. Arsenic sulfide, which is a volatile mineral, usually oxidizes to arsenic trioxide in hot cyclones to produce arsenic oxide as product, given that there is a market for it. Due to its toxicity, the market for arsenic trioxide has been very small in the past decades and thus, the arsenic in the roaster off gas is currently scrubbed into a weak acid solution. This solution is recovered and is often sent for arsenic immobilization. The calcine product of the roasting processes usually contains less than 0.5% As from an enargite concentrate (Lattanzi et al., 2008; Peacey et al., 2010; Safarzadeh et al., 2012).

Multiple-hearth and fluidized bed roasters often are used in commercial enargite roasting plants. A multiple hearth roaster was used in Barrick's El Indio Mine to treat enargite concentrate, containing

up to 9% As. Fluidized bed reactors have been used by Lepanto in the Philippines and by Boilen in Sweden to roast high arsenic copper concentrates (Peacey et al., 2010; Safarzadeh et al., 2012). The major draw backs of the roasting process are the lack of effective methods to decrease the scrubbing, arsenic fixation, and disposal costs. In the roasting treatment method for chalcopyrite and enargite concentrates, arsenic contamination is a severe concern for the off gasses and most of the smelters do not accept a copper concentrate with higher than 1 % As (Peacey et al., 2010; Safarzadeh et al., 2012).

2.2 Hydrometallurgical processes

In dealing with strict environmental regulations and penalties for processing of arsenic-bearing copper minerals via roasting or smelting, researchers have developed several hydrometallurgical processes for enargite treatment. However, the hydrometallurgical processes developed often lack a low capital cost and most require a separate process for arsenic immobilization. The hydrometallurgical processes for copper sulfide minerals can be classified into two main groups: atmospheric leaching methods and pressure leaching.

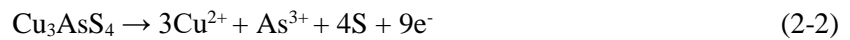
2.2.1 Atmospheric leaching

The atmospheric leaching processes that have been developed act as low capital and low operating cost methods, although the atmospheric processes lack efficiency and fast leaching kinetics in copper recovery (Padilla et al., 2010, 2008a; Riveros and Dutrizac, 2008; Ruiz et al., 2011). In order to enhance the leaching rate in atmospheric leaching processes, a variety of different lixivants, oxidants, and catalysts have been used for chalcopyrite and enargite leaching (Safarzadeh et al., 2012).

2.2.1.1 Ferric and cupric leaching

Ferric (Fe^{3+}) and oxygen are the main oxidants used in most atmospheric leaching processes, owing to their efficiency, availability, and low prices. More specifically, ferric can be generated during

the leach process from the iron containing minerals of the leach feed, such as pyrite or pyrrhotite. The U.S. Bureau of Mines' Reno Metallurgy Research Center studied ferric chloride leaching for chalcopyrite in 1969 which resulted in 99.9% of copper recovery after 2 h of leaching under optimum conditions, when fine grinding was applied (Haver and Wong, 1971; Wang, 2005). The average particle size in this study was 3.8 μm and the optimum temperature was found to be 106 $^{\circ}\text{C}$ (Haver and Wong, 1971; Wang, 2005). Dutrizac and MacDonald studied enargite leaching in a ferric sulfate solution, where 50% of the copper was leached after 7 days at 80 $^{\circ}\text{C}$. They concluded that leaching enargite in ferric sulfate media can be written as two half-cell reactions (as follows in Equation 2-2 and 2-3) and the schematic of this reaction is shown in Figure 2-1 (Dixon et al., 2008; Dutrizac and MacDonald, 1972):



Chloride media has some advantages over sulfate media including a higher dissolution rate of metals, smaller scale of operation, and the ability to form stable species with copper (Liddicoat and Dreisinger, 2007). Riveros and Dutrizac (Riveros and Dutrizac, 2008) reported 27% copper dissolution after 16 h leaching with 0.3 M FeCl_3 -0.3 M HCl media at 100 $^{\circ}\text{C}$ of an enargite sample (-23+15 μm). The other oxidant that has been used for copper sulfide mineral leaching is the cupric ion (Parker et al., 1981). It has been reported that for copper sulfide mineral leaching in ferric media, cupric/cuprous ions are more effective than ferric/ferrous ions. Cupric ions show a catalytic effect in the coexistence of ferric ions (Al-Harashsheh et al., 2008; Hiroyoshi et al., 2004; Lundström et al., 2009).

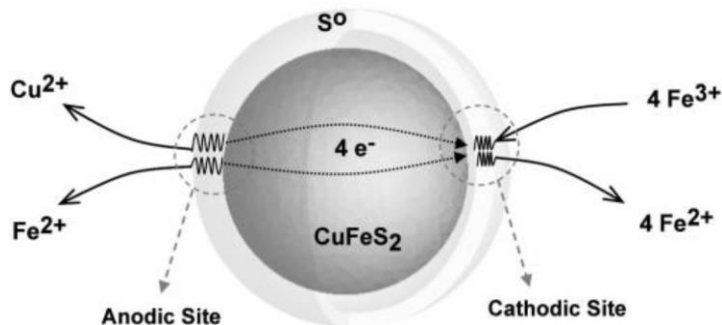
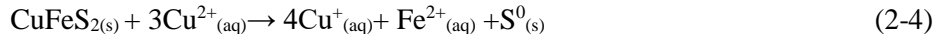


Figure 2-1. Schematic diagram of chalcopyrite electrochemical leaching in the presence of ferric ions (Dixon et al., 2008)

Cupric ions can also be used as an oxidant. Parker et al. (1981) stated that cupric/cuprous couples are more effective than ferric/ferrous couples in chloride media because their redox reaction is rapid and reversible. The “Hydrocopper process™” is one of the processes for copper sulfide leaching in chloride solution which is catalyzed by cupric ions. In this process, copper dissolves as cuprous ions in the presence of cupric ions (about 10 g/L) (Hyvärinen and Hämäläinen, 2005).



Cupric ions can have a synergistic effect in the presence of ferric ions and enhance the copper sulfide leaching rate (Al-Harabsheh et al., 2008; Hiroyoshi et al., 2004; Lundström et al., 2005). The copper sulfide leaching in chloride media is beneficial due to the improved redox behavior, higher reaction rate, and higher copper dissolution (Dutrillac, 1990; Liddicoat and Dreisinger, 2007).

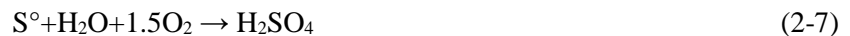
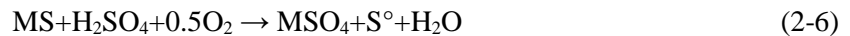
2.2.1.2 Albion process

The Albion Process was developed and patented in 1994 by MIM Holdings (now Glencore). This process is a combination of fine grinding of the sulfide minerals and oxidative atmospheric leaching. The ultrafine grinding causes a high degree of strain within the mineral lattice which leads to fractures on the grain boundaries and increases the lattice defects. Higher defect density and

fractures lower the required activation energy for the leaching process and make atmospheric leaching a viable option. Furthermore, ultrafine grinding of minerals to a P₈₀ of 10-12 µm prevents partially leached sulfide mineral surface passivation during leaching. Passivation in the sulfide minerals occurs by a coating of elemental sulfur or iron oxide on the surface of the mineral which hinders the leachate from diffusing into the mineral surface. The ultrafine ground particles will leach thoroughly before the passivating layer reaches its critical thickness (Aylmore, 2012; Hourn et al., 2012; Rohner et al., 2012; Technologies, 1991).

The oxidative leaching reaction of sulfide minerals to elemental sulfur or sulfate liberates heat which helps the process to be operated autothermally at elevated temperatures close to the boiling temperature (93-98 °C). The use of higher leaching temperature can increase the recovery. In this process, oxygen is also sparged by lances (HyperSparge™) into the leaching reactors to increase the oxygen solubility in the leach solution and to increase the leaching rate. The very first commercial Albion Copper Leaching Process was commercialized in December 2017 in Zambia (Stieper, 2018).

The reactions associated in the Albion Leaching Process are shown in Reactions 2-6 and 2-7 respectively.



During the leaching of copper, zinc, or nickel acidity is maintained between 5-15 g/L, so when the elemental sulfur oxidation happens, the acidity increases. However, in the copper sulfide oxidation case, Reaction 2-6 is the dominant reaction and a small portion of the elemental sulfur is oxidized through Reaction 2-7 (usually less than 15%). It should be mentioned that, through the neutral Albion Leach Process, the refractory gold concentrates are mostly oxidized at the neutral pH of 5.5. In the leaching process of As bearing refractory gold ores, a stable ferric arsenate product can form at the neutral pH, given that the arsenic is present as the As(V) species in the PLS. Therefore, after the leaching process, the slurry is neutralized to precipitate iron, arsenic, and other hazardous

elements. The elemental sulfur also is oxidized to sulfate and precipitated in the form of gypsum during this process. After solid/liquid separation, the pregnant leach solution is sent to the recovery stage and the solid products are sent for cyanide leaching to recover the precious metals. It should be mentioned that the precipitated iron, in the form goethite, is not affected by cyanide leaching.

The Albion Process patent (Bowen and Hourn, 2015) claims that in a treated concentrate, which included 12% chalcocite, 21% enargite, and 50% pyrite (19.5% Cu and 4% As), over 92% of copper was recovered in 10 hours. The concentrate was ground to $P_{80}=20\ \mu\text{m}$, and a test was performed at 90 °C and the leaching solution contained 30 g/L ferric ions, and 50 g/L sulfuric acid at a 10% pulp density. Oxygen was injected in the reactor during the test. It was reported that, if air was replaced by pure oxygen, 92% recovery was reached after 14 hours (Aylmore, 2012; Hourn et al., 2012; Rohner et al., 2012; Technologies, 1991). The commercial plant of Albion in Zambia claims 99% copper recovery from a chalcopyrite concentrate (Stieper, 2018).

The Albion Process was commercialized for two zinc plants in 2010 and 2011, a Pan Terra gold project in 2012, and a GPM gold project in Armenia in 2015. The Pan Terra gold project is treating 100 tph of tailing and has a production capacity of 65,000 ounces per annum of gold and 600,000 ounces per annum of silver. The feed to the project is high grade gold/silver pyritic CIL tailings from prior operation of the Rosario Mine in the Dominican Republic (Aylmore, 2012; Hourn et al., 2012; Rohner et al., 2012; Technologies, 1991; Voigt et al., 2015).

2.2.1.3 Galvanox process

Atmospheric leaching of enargite is a very slow process, regardless of the acid type. Enhancement of the leach reaction rate requires using a stronger oxidising agent, such as iodine, which is not practical due to its high operating cost. A variety of catalysts have been exploited in atmospheric leaching experiments. Dixon et al. (Dixon et al., 2008) studied galvanically-assisted atmospheric leaching of chalcopyrite, where pyrite acts as the catalyst of the process to prevent passivation on the chalcopyrite or other sulfide mineral surfaces. Pyrite, in this case, acts as the cathode and

provides available surface area for ferric ions reduction to ferrous. The schematic of galvanically-assisted leaching of chalcopyrite in the presence of pyrite is shown in Figure 2-2 (Dixon et al., 2008).

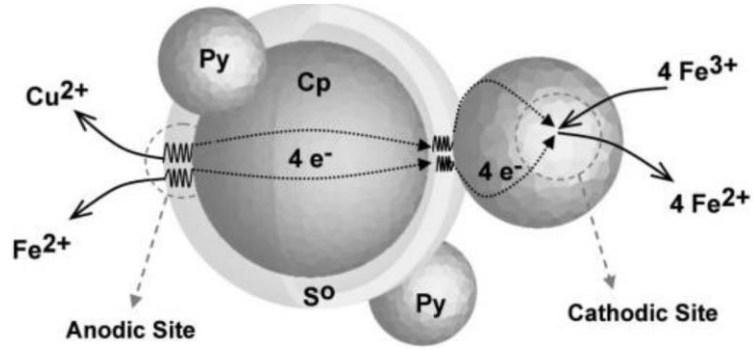


Figure 2-2. Schematic diagram of galvanically-assisted electrochemical leaching (Dixon et al., 2008)

This process was initially developed for chalcopyrite and then applied for copper leaching from other sulfide minerals, such as enargite. The potential of the leaching reactor was kept lower than 500 mV versus Ag/AgCl thus the pyrite oxidation can be maintained at a low level. The preferred potential range for this process is 460-500 mV; to maintain this potential the ferric addition must not exceed the stoichiometry of the leach reaction. The pyrite concentration should not decrease less than 9 g/L in the leach solution. The copper recovery of 98% was obtained at 80 °C after 4 h of leaching in the ferric sulfate solution with pyrite as catalyst (Dixon et al., 2008). In the presence of pyrite, the copper recovery increased from 30% after 55 h to 99% after 24 h of leaching enargite in the ferric sulfate solution. The effect of pyrite on the leaching results was observed progressively and completion was reached under 24 h in the solution with a pyrite to enargite ratio of 1:1 (Rivera-Vasquez and Dixon, 2015). It has been stated that enargite leaching in the presence of pyrite is not sensitive to the ferric concentration between 7 and 20 g/L (Rivera-Vasquez and Dixon, 2015). Acid concentration does not have a significant effect on the dissolution rate. Temperature was found to be the most important factor in leaching experiments. The most effective ratio of pyrite to

concentrate was determined at the Py:En ratio of 4:1 and higher. The copper recoveries after 48 h of leaching in the experiment with 60 g/L sulfuric acid, 580 mV potential and pyrite to enargite ratio of 3:1 at 90, 80, 65 and 50 °C were about 89, 87, 58 and 38% respectively (Rivera-Vasquez and Dixon, 2015). As expected, copper recovery was dependent on the enargite concentrate particle size. 89% and 99% of copper recovery was achieved after 40 and 48 h of leaching enargite concentrate with a P_{80} of 78 and 38 μm , respectively (Rivera-Vasquez and Dixon, 2015).

Arsenic was immobilized in the leach reactor as the ferric and arsenic co-precipitate as ferric arsenate. Copper can be recovered from the pregnant leach solution by a conventional solvent extraction process followed by electrowinning, and it has been claimed that gold recovery can be performed on the leaching residues at very modest levels of cyanidation, despite the presence of a high concentration of elemental sulfur in the residue (Dixon et al., 2008).

2.2.1.4 Silver assisted Galvanox process

The copper recovery kinetics by the Galvanox process showed very high dependence on the silver content of the catalyst pyrite. The addition of silver also has shown a positive effect on the leaching of copper sulfide minerals; it was shown that the silver addition can increase the recovery of the Galvanox process and enhance the catalytic properties of pyrite in the leaching process (Nazari et al., 2011). With the addition of 60 mg of silver per kg of copper the reaction rate increased significantly and copper extraction reached completion in 10 h. The best leaching results were achieved at a solution potential of 450 mV. The possibility of recycling the pyrite in the presence of silver was a positive side of this process. In a usual Galvanox process, recycling of pyrite decreases the efficiency of the catalytic effect but in the presence of silver, recycled pyrite acts the same as a fresh pyrite (Nazari et al., 2011).

The addition of silver has a positive effect on the leaching of copper sulfide minerals. Three different models have been proposed to explain the mechanism of this phenomenon (Córdoba et al., 2008a; Ghahremaninezhad et al., 2015; Hiroyoshi et al., 2002; Nazari et al., 2012). Hiroyoshi

et al. (Hiroyoshi et al., 2002) stated that chalcopyrite leaching is performed in a two-step reaction of reduction to Cu_2S and oxidation of Cu_2S . In this process, silver acts as a scavenger for the H_2S generated and improves the reaction rate of Ag_2S formation (Hiroyoshi et al., 2002). Nazari et al. (2012) proposed that the silver ions adsorb to the non-conductive elemental sulfur layer on the surface of chalcopyrite and mediate its conductivity to a range that the mineral can exchange electrons and dissolve via an electrochemical leaching reaction (Nazari et al., 2012). Ghahremaninezhad et al. (2015) proposed that the reaction of the passivating elemental sulfur layer on the surface of the chalcopyrite with silver creates sulfur vacancies and produces holes (the opposite of electrons) on the passive layer. It also promotes charge transfer through the passive layer. The vacancies on the elemental sulfur layer can improve the diffusion of copper from the bulk of the mineral into the leach solution, which causes leaching rate enhancement (Ghahremaninezhad et al., 2015).

Hiroyoshi et al. (2007) studied the effect of coexisting ions and the possible catalytic effect of these ions in the chalcopyrite leaching process at room temperature. It was found that the addition of Cd^{2+} , Zn^{2+} , Ni^{2+} , Co^{2+} and Mn^{2+} had no significant effect on the chalcopyrite leaching rate, however Pd^{2+} and Hg^+ addition oxidized Fe^{2+} to Fe^{3+} at potentials below 0.57 V. Regardless of the increase in the ferric concentration, copper recovery was reported as unaffected. Furthermore, the addition of Bi^{3+} ions enhanced the dissolution rate of chalcopyrite by increasing the critical potential (Hiroyoshi et al., 2007).

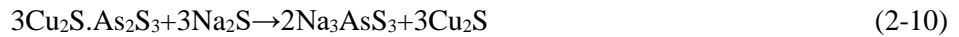
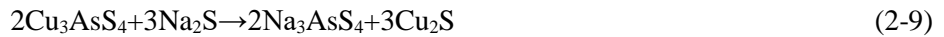
2.2.1.5 AC assisted leaching

The concept of catalytic leaching for enargite is not limited to the Galvanox process. AC can be used as a catalyst to leach sulfide minerals. Rivera-Vasquez and Dixon (2012) used AC as a catalyst in the enargite leaching process. In the presence of 100 g AC, the copper recovery increased from 58% after 35 h to 99% after 20 h of leaching enargite in the ferric sulfate solution at 80 °C. Different ratios of AC to enargite concentrate changed the kinetic path of the leaching process but led to the

same recovery value. The effect of oxidation reduction potential was also studied, which demonstrated that a higher copper recovery can be achieved at higher potentials among the tested ORP values of 450, 490, 515 and 530 mV. The reaction rate was faster when the ORP was under 530 mV. It has been reported that the addition of different AC types results in different copper recoveries, which have varied between 80% to 99% in the Dixon and Rivera Vasquez study (Dixon and Rivera-Vasquez, 2012).

2.2.1.6 Alkaline sulfide leaching

Alkaline sulfide leaching (ASL) of copper-arsenic concentrates can be performed in Na₂S-NaOH systems. The reaction of NaOH with NaSH can form Na₂S which will be used as the leaching reagent (Reaction 2-8). Sunshine Mining has used this process to treat tennantite for many years (Safarzadeh et al., 2012). In this process arsenical copper sulfide concentrates were converted to Cu₂S, which was sold to the refineries as a clean copper concentrate. The reactions for enargite and tennantite is shown in Reaction 2-9 and Reaction 2-10 (Safarzadeh et al., 2012).



Balaz et al. (2010) enhanced alkaline leaching of enargite and tennantite with a mechanical activation method and designed a process called MELT (Baláž et al., 2000a). The overall residence time of alkaline leaching was reduced from 120 min with 86% recovery to 10 min of leaching with 98% arsenic recovery (Baláž et al., 2000b; Baláž and Achimovičová, 2006).

2.2.2 Pressure oxidation process

The pressure leaching method is an efficient and rapid method which has been used in industry for the treatment of gold, zinc, and copper concentrates and, most recently, is being further developed by Codelco, Chile for treatment of enargite and chalcopyrite concentrates and roaster dusts (Padilla

et al., 2008a). This process is currently at the final Engineering Study step by Ecometales, and after approval the project will advance to the construction phase. The high operating cost associated with the development of autoclaves as well as neutralization of the acid discharge are the main disadvantages of this method.

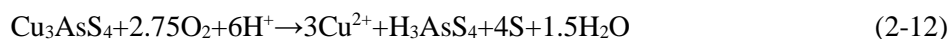
2.2.2.1 Ammonia pressure leaching

The ammonia leaching of enargite was performed at an oxygen overpressure between 34-344 kPa (5-50 psi). The reaction between the ammoniacal solution and enargite is shown in Reaction 2-11. The dissolution rates of arsenic and copper were slow in this process with 60% copper recovery after 24 h of leaching at 82 °C (Raghavan and Gajam, 1983).



2.2.2.2 Acidic pressure leaching

The Chemical Construction Company and Sherritt Gordon Mines Limited developed the first commercial process of continuous autoclave pressure leaching of sulfide ores in the early 1950's. This process was applied to Lepanti Mine enargite concentrates. Pressure leaching can be performed under different conditions. There are a variety of processes, based on their condition, which can be classified into two major categories based on their working temperatures. These are medium temperature pressure oxidation (MTPOX) which is carried out between 150-170 °C and high temperature pressure oxidation (HTPOX) which is carried out under oxygen overpressures up to 2000 kPa (290 psi) which is performed at above 180 °C, mostly about 220 °C. In the MTPOX process, most of the sulfides partially oxidize to elemental sulfur but the HTPOX will result in sulfate production due to the stronger oxidative condition. The reactions associated with the MTPOX and HTPOX processes are written in Reaction 2-12 and Reaction 2-13. Ferrous to ferric oxidation also happens in the case of oxygen overpressure which is shown in Reaction 2-14 (Dreisinger, 2014; Peacey et al., 2010; Ruiz et al., 2011; Safarzadeh et al., 2012).



SGS Lakefield developed an HTPOX process to treat El Indio enargite concentrate in 1993 and performed a bench scale HTPOX process for treating Codelco chalcopyrite-enargite concentrate in 1994. The El Indio bench scale tests were performed at temperatures between 200-220 °C and an oxygen overpressure of 1034 kPa (150 psi) and retention time between 60-180 min. The enargite concentrate contained 22.6% Cu, 18% Fe, 35.4% S and 8.6% As. The results of the El Indio enargite concentrate HTPOX showed 95% of Cu extraction with the oxidation rate of near completion. The copper recovery loss in this process is because of re-precipitation of copper as a mixed Fe-Cu-As-S-O compound. The gold recovery stage was followed by cyanidation of the post leaching residues. In silver containing concentrates, the silver content formed argento-jarosite which cannot be treated by cyanidation. In order to recover silver from argento-jarosite by cyanidation, a lime boil treatment is needed (Gupta, 2010; Peacey et al., 2010; Safarzadeh et al., 2012).

Freeport McMorran has been operating medium temperature (160 °C) and high temperature (220 °C) pressure oxidation of chalcopyrite in their Bagdad and Morenci operations in Arizona, although at some points the operations have been shut down (Ghahreman, 2018). Currently the Morenci operation is operating at 195 °C, particularly because the autoclave design temperature and pressure does not permit higher temperatures and pressures above 195 °C and 3240 kPa (470 psi). The current pressure oxidation process at Morenci operation is designated as Pressure Oxidation Lite process (Ghahreman, 2018).

Nadkarni and Kusik (1988) have studied the leaching of enargite in a batch autoclave at 225°C and 1034 kPa (150 psi) oxygen overpressure. The tests result showed 98% copper recovery with pyrite addition and 70% of copper extraction without pyrite addition (Nadkarni and Kusik, 1988).

Padilla et al. (2008) studied the effect of pyrite on pressure leaching of enargite. The leaching condition was 128 µm enargite particle size, 0.2 M sulfuric acid and 689 kPa (100 psi) of partial

pressure of oxygen at 200°C (Padilla et al., 2008b). Agitation rate was found to be an effective parameter on copper recovery and increasing the mixing rate up to 600 rpm can enhance the copper recovery. The sulfuric acid concentration in the range of 0.2-0.5 M did not change the dissolution rate of copper.

However, increasing the oxygen partial pressure from 303 to 1006 kPa (44 to 146 psi) enhanced the copper recovery. The copper dissolution rate was highly dependent on the operating temperature and recovery increased from 30% in 180 min at 160 °C to 100% in 140 min at 220 °C (Padilla et al., 2008a).

During the HTPOX process, a large portion of the arsenic forms scorodite ($\text{FeAsO}_4 \cdot 2\text{H}_2\text{O}$) or basic ferric arsenate. After the HTPOX process, the remaining As can be treated by a stabilization process in the autoclave to form scorodite. The whole HTPOX flowchart for enargite treatment is shown in Figure 2-3.

Pressure leaching is one of the most effective methods for refractory copper sulfide mineral treatment. It is rapid, efficient, flexible, and controllable. On the other hand, it needs a high operating cost including pressurizing, depressurizing, temperature control, neutralization of a large volume of the sulfuric acid generated in the autoclave, and a high oxygen consumption rate (Liddicoat and Dreisinger, 2007; Safarzadeh et al., 2012).

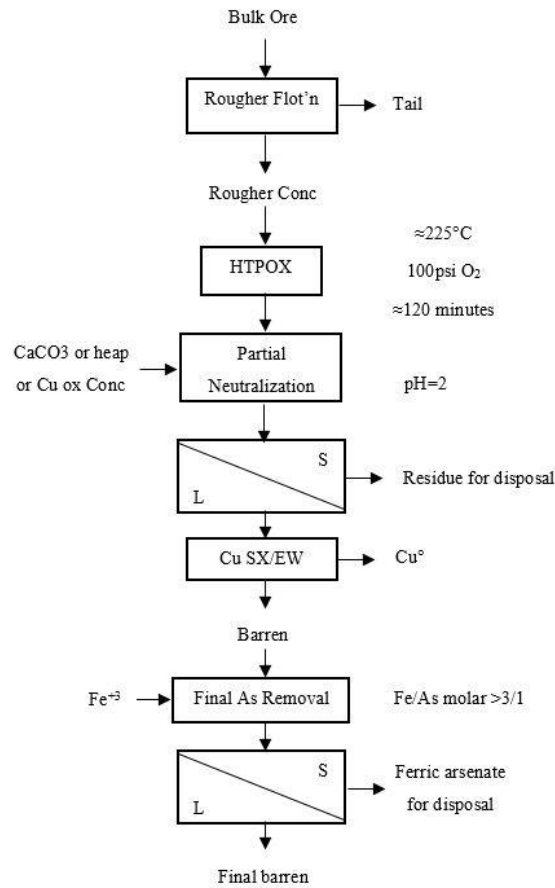


Figure 2-3. High temperature pressure oxidation flow sheet to treat copper arsenide minerals (Safarzadeh et al., 2012)

Several different types of pressure leaching processes were developed and demonstrated for copper sulfide treatment with minor differences which will be explained in the following paragraphs.

The Activox process was developed by Western Minerals Technology Ltd for the leaching of sulfide minerals (originally refractory gold concentrates). This process is a mix of ultrafine grinding (P_{80} around 10 μm) and a low temperature (100-110 °C), low pressure (1000 kPa (145 psi)) autoclave leaching process. The leach solution contains 48 g/t sulfuric acid to the feed concentrate and about 4 g/L chloride ions in the form of sodium chloride to enhance the leaching rate of the sulfides (Palmer and Johnson, 2005).

The CESL process was initially designed and developed by Cominco Ltd for copper sulfide concentrate treatment (Palmer and Johnson, 2005). During the CESL process, a light regrinding is applied on the after-flotation concentrate in order to increase the surface area and reduce the particle size to a P_{90} of 45 μm . Then, autoclave leaching is performed on the concentrate where the leach solution contains 5 to 20 g/L chloride, NaCl and acid. The leaching condition involves 1379 kPa (200 psi) pressure and a retention time of 60-90 mins at 150 °C, and yielded 98% of copper recovery and 99% of arsenic department (Barr et al., 2005b, 2005a; Bruce et al., 2010; Mayhew et al., 2010). The Dynatec process is a counter current atmospheric leaching treatment of sulfide minerals followed by oxidative pressure leaching at 150 °C using 25 kg of coal per ton of concentrate to collect elemental sulfur generated by leaching. A copper recovery of 98% was reported for this process when the feed was finely ground to 25 μm (Molnar and Verabaan, 2003; Wang, 2005).

2.2.3 Biological leaching of enargite

Bioleaching can potentially become one of the most cost-efficient methods to treat low grade enargite ores. Bio-hydrometallurgical processes are easy to operate and do not require complex technological hardware or highly trained operators. These methods are environmentally friendly due to the more stable wastes and non-hazardous off gases produced (Rawlings and Johnson, 2007). Bio-hydrometallurgical processes have their own disadvantages. Primarily the kinetics of bioleaching processes are usually slow which makes bioleaching processes a low pace process, thus requiring long retention time. Long retention time can be translated to the need for larger leaching reactors and larger volumes of wastes (Rawlings and Johnson, 2007).

When using the bioleaching process for the secondary copper sulfide minerals mesophiles are an appropriate choice. The suitable particle size for bioleaching of copper sulfide minerals is a P_{80} of 38 μm for non-refractory and a P_{80} of 25 μm for refractory minerals. Enargite is the most refractory mineral in bioleaching and the dissolution is slow when using mesophilic bacteria compared to

thermophilic bacteria (Escobar et al., 2000; Lattanzi et al., 2008; Takatsugi et al., 2011). Several bioleaching processes have been developed to treat enargite which will be discussed.

2.2.3.1 BioCOP process

The BioCOP process was designed and developed for high grade refractory sulfide minerals with high concentrations of arsenic and other hazardous elements by BHP Billiton and Codelco Chuquicamata in northern Chile (Batty and Rorke, 2006; Rawlings and Johnson, 2007). Thermophilic microorganisms are used in this process at temperatures up to 80 °C to treat copper sulfide concentrates. The thermophilic microorganisms include *Acidithiobacillus caldus* (formerly *Thiobacillus caldus*), *Acidimicrobium ferrooxidans*, *Sulfobacillus acidophilus*, *Sulfobacillus disulfidooxidans*, *Sulfobacillus thermosulfidooxidans*, *Ferroplasma acidarmanus*, *Thermoplasma acidophilum*, and *Alicyclobacillus acidocaldrius*. The operating condition of the BioCOP process is very similar to that of the other bioleaching oxidation procedures in the gold industry. The cell wall does not exist in thermophilic microorganisms as they only have a cell membrane. Therefore, thermophilic organisms are more delicate than mesophilic microorganisms and they are sensitive to shear. These microorganisms can only survive in very dilute slurries (2% solids) held at a low agitation rate. Pulp density is limited from 20% in mesophiles to 12.5% in the thermophiles process and the operating temperature is around 78 °C. Applying higher temperatures will result in lower saturated partial pressure of oxygen (1/3 of original level). However, the oxygen demand is higher due to the higher oxidation rate of the process. Hence, oxygen gas should be introduced into the leaching solution (Batty and Rorke, 2006; Rawlings and Johnson, 2007).

Using thermophile microorganisms at a high temperature has a considerable effect on the copper recovery. The comparison of copper dissolution using thermophile and mesophile microorganisms is shown in Figure 2-4. The copper dissolution rate is improved from 45% to 90% when mesophiles are replaced by thermophiles at higher temperatures (Batty and Rorke, 2006; Rawlings and Johnson, 2007).

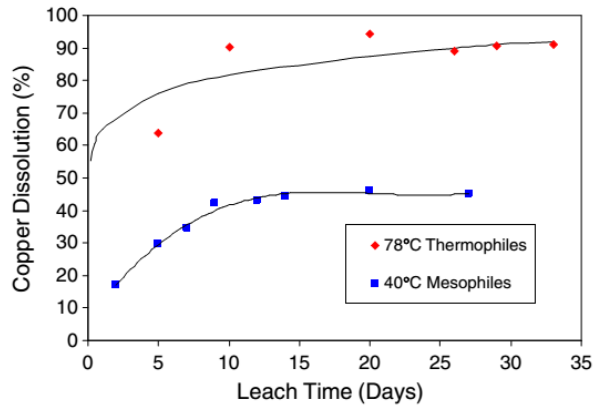


Figure 2-4. Copper dissolution rate for mesophiles and thermophiles of a chalcopyrite concentrate (Batty and Rorke, 2006)

2.2.3.2 The BacTech/Mintek process

The BacTech and Mintek process, which is a thermophile bacteria process at lower temperatures, was demonstrated for bioleaching of copper in Monterrey, Mexico (Wang, 2005). This 2.2 t/d demonstration plant used a series of countercurrent leach reactors and the operating condition of pH 0.5-2.5 and a retention time of 30 days at 25-55 °C. Carbon dioxide and nutrients were also added to the leaching solution. The copper recovery of 96.4% was achieved for this process during this demonstration from a variety of copper concentrate (Safarzadeh et al., 2012; Wang, 2005).

2.2.3.3 The GEOCOAT process

This process was developed by GeoBiotics for chalcopyrite leaching. In this process, a slurry made of concentrated copper sulfide minerals was coated on to the surface of crushed and screened support rock and was stacked for the biooxidation process on a lined pad. The biooxidation process is a bio-assisted heap leach with mesophilic, moderate, or thermophilic bacteria. The leach solution contains sulfuric acid and nutrients. The 94% copper recovery was achieved after 90 days of leaching with this method (Harvey et al., 2002, 1999; Safarzadeh et al., 2012).

Several hydrometallurgical processes have been developed for copper sulfide mineral treatment. To have a better understanding of the processes and understand the differences between the processes, they are presented in Table 2-2. The current status of the processes with respect to commercialization is shown in the status column of the table.

Table 2-2. Hydrometallurgical processes for copper (Ghahreman, 2018)

Process	Status	Temp (°C)	Pressure (kpa) (psi)	Ultrafine Grind	Chloride	Surfactant	Special
Activox	D	110	1000 (145)	Yes	No	No	
Albion	P	85	100 (14)	Yes	No	No	
Biotech/Mintek Low T Bioleach	P	35	100 (14)	Yes	No	No	
BIOCOP™	C	80	100 (14)	No	No	No	Thermophiles
Buenaventura	P	90	100 (14)	No	No	No	Special Carbon catalyst
Carrapanteena	P	N/A	N/A	No	Yes	N/A	
CESL	C	150	1378 (200)	No	Yes	Yes	
Cobre Las Cruces	C	90	100 (14)	No	No	No	Chalcocite
Dynatec	P	150	1213 (176)	No	No	Yes	Coal + Recycle
FLSmith®	P	80	100 (14)	Yes	No	No	Inter-stage grinding
Freeport McMoran HTPOX	C	220	3240 (470)	No	No	No	
Freeport McMoran Lite	C	195	3240 (470)	No	No	No	
Freeport McMoran MTPOX	C	160	323	Yes	No	Yes	
Galvanox	P	80	100 (14)	No	No	No	Galvanic
Mt. Gordon	C	90	806 (117)	No	No	No	Chalcocite
Outotec	P	105	100 (14)	No	Yes	No	
Sepon Copper	C	80-Cu 220- FeS ₂	100 (14) 3240 (470)	No	No	No	Chalcocite
Total Pressure Oxidation	C	225	3240 (470)	No	No	No	

2.3 Activated carbon (AC) properties and catalytic mechanism

Generally AC refers to a group of carbon based materials with different adsorption and catalytic properties. This group of materials is identified by their properties, but not by chemical formula or physical structure. The unique properties of most carbon based catalysts, including AC, such as their chemical inertness, high porosity, and high surface area, make them an interesting group of catalysts. The mechanism of the catalytic effect of AC in the sulfide leaching process is not completely known yet. There are two major theories for this effect (Ghanad, 2011).

The first theory is that any conductive material with a higher rest potential than the ore can act as a galvanic couple. AC is a good choice to select as a galvanic couple for enargite. Enargite acts as the electron donating anode and dissolves, whereas AC is the cathode and accelerates the enargite leaching by providing extra surface area for ferric ion reduction. The galvanic leaching of enargite in the presence of AC is shown schematically in Figure 2-5. This picture describes the mechanism of the galvanic leaching process and the act of AC as the catalyst (Ghanad, 2011).

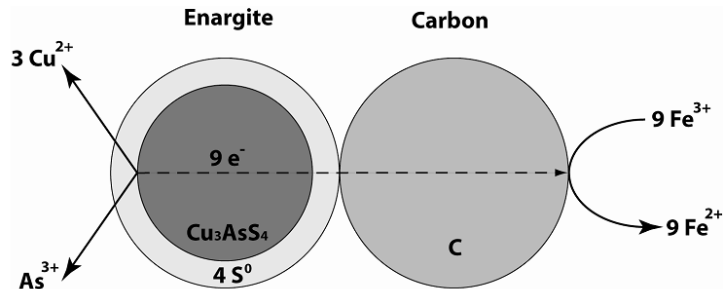


Figure 2-5. Galvanic interactions between enargite and AC particles (Ghanad, 2011)

The second theory describes that AC generates hydrogen peroxide in the presence of oxygen. Ahumada et al. (2002) noted that some of the AC types can make H_2O_2 and HO_2^- in the presence of oxygen and this phenomenon can be explained by the availability of chromene and quinone groups on the surface of the AC. In the presence of oxygen on the carbon surface, the re-oxidation process can occur due to the presence of the functional groups. This study has shown that the

existence of oxygen on the carbon surface helps the oxidation of Fe(II) to Fe(III). Oxidation of Fe(II) in the presence of oxygen can be written as the following reactions (Ahumada et al., 2002).



It has also been shown that the oxidation kinetics of 50 ppm Fe(II) with nitrogen sparging was negligible, but the value of Fe(III) increased from 5 ppm to 50 ppm within two hours in the presence of oxygen (Ahumada et al., 2002). The oxidation properties of AC are not limited to iron oxidation and the oxidation of other species in the leaching solution should also be considered. Radzinski (2017) reported that 16 mg/L of hydrogen peroxide was detected in 100 ml of 1 M sulfuric acid solution with 0.2 L/min oxygen sparging rate in the presence of 40 g AC after an hour, and even a small amount of hydrogen peroxide was detected in the test without any sparged oxygen. Arsenic (III) was fully oxidized in the batch tests with 10% of AC after 24 hours and oxidation was reported as negligible without AC (Radzinski, 2017).

The other important phenomenon to consider when utilizing AC is the surface adsorption of this porous catalyst. Radzinski (2017) found that about 50% of arsenic was adsorbed to the AC surface at 10% pulp density (Radzinski, 2017). Yu et al. (2016) studied adsorption capacity of AC at pH 5 and 25 °C and reported that AC showed an adsorption capacity of 42 mg/g for As(V) and 32 mg/g for As(III) and after around 30 min adoption steady state was reached (Yu et al., 2016). Park et al. (Park et al., 2007) studied the effect of oxygen and nitrogen enriched AC for the removal of Cu(II) ions. They found that by increasing pH from 1.5 to 6 Cu(II) adsorption increased. Adsorption of Cu(II) ions at about pH 1.5 was reported as less than 1 mg/g. The best adsorption results were achieved using nitric acid treated AC. Nitric acid treatment increases acidity of AC 4 times, increases lactone groups 12 times, and increases oxygen containing functional groups enormously (Park et al., 2007).

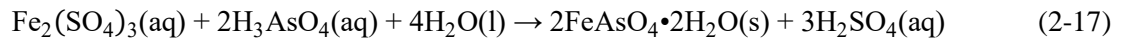
Arsenic is a major contaminant in copper sulfide minerals and enargite can be noted as the major arsenic bearing copper mineral present in chalcopyrite concentrates. Enargite leaching in

atmospheric conditions results in low copper recovery and arsenic fixation after the leaching. Roasting is no longer a sustainable treatment method due to the arsenic release into the environment and strict environmental rules and regulations.

2.4 Arsenic remediation

It should be mentioned that besides the copper recovery, another key challenge in the atmospheric enargite leaching is the arsenic remediation. The arsenic fixation is frequently implemented through the hydrometallurgical processes which are grouped into: lime neutralization, sulfide precipitation, co-precipitation of arsenic using ferric ions, scorodite precipitation, and encapsulation technology (Nazari et al., 2017). Lime neutralization is a simple and relatively cost-effective technique in which arsenic is immobilized in the form of calcium arsenate and/or calcium arsenite at pH 11-12. However, arsenic-calcium residues exhibit poor long-term stability and none of them pass the toxicity characteristic leaching procedure (TCLP) test (Nazari et al., 2017; Swash and Monhemius, 1994). The co-precipitation of arsenic with ferric ions is the best demonstrated available technology by the U.S. Environmental Protection Agency (EPA) (U.S. Environmental Protection Agency, 1992). In this technique, arsenic co-precipitates with the ferric ions to form As(V)-ferrihydrite (FH) residue at an Fe:As ratio > 3:1. The main drawbacks associated with this method are the availability of iron (in some cases iron is not readily available in the plant site) and the large volume of the arsenical FH sludge with low filterability. In addition, the FH phase is subjected to physical and chemical changes over time and will transform to alpha goethite (α -FeOOH), which consequently leads to arsenic release to the environment (Filippou and Demopoulos, 1997; Robins, 1987). Scorodite ($\text{FeAsO}_4 \cdot 2\text{H}_2\text{O}$) is a crystalline ferric arsenate, which has driven much attention due to its low arsenic solubility, high arsenic content (25-30 wt%), low iron requirements (Fe:As molar ratio of 1-1.5:1), and promising settling and filtration properties (Filippou and Demopoulos, 1997; Robins, 1987).

Scorodite precipitates could be formed through different methods and mechanisms, which are markedly dependent on the experimental conditions, such as pressure and temperature. Dutrizac and Jambor (1988) were the first to generate scorodite precipitates by means of a high temperature pressure oxidation (HTPOX) technique in which the temperature and oxygen pressure were 150-230 °C and 2000 kPa (290 psi), respectively. The experiments were carried out in an autoclave at pH 0.7 where the dosage of Fe(NO₃)₃ and pentavalent arsenic ions were set at 0.3 M and 25 g/L, respectively (Dutrizac and Jambor, 1988). HTPOX is frequently employed in gold ore pre-treatment processes to not only liberate gold minerals from the refractory sulfidic minerals structure, but also immobilize arsenic in the form of scorodite. The reaction occurring in the HTPOX process is shown in Equation 2-17. In spite of the high efficiency of HTPOX in the scorodite formation, the capital cost associated with this process is significantly high (Filippou and Demopoulos, 1997; Nazari et al., 2017).



An alternative method to generate scorodite precipitates at ambient pressure was initially implemented by Dutrizac and Jambor (1987). They reported that crystalline scorodite precipitated at 97 °C in a chloride solution (Dutrizac and Jambor, 1987). Demopoulos et al. (1995) probed the atmospheric scorodite crystallization through a slow stepwise neutralization (up to pH 1.1) in a chloride solution. A series of scorodite precipitation experiments was performed at different chloride concentrations (1-6 M) and at a temperature ranging from 80 °C to 95 °C (Demopoulos et al., 1995). It was illustrated that the crystalline scorodite precipitated only at 95 °C from 2 g/L As(V)-bearing solution in the absence of a seed. However, the addition of a 2 g/L seed decreased the precipitation temperature to 80 °C (Demopoulos et al., 1995). Atmospheric scorodite precipitation through a supersaturation-controlled process was studied in a sulfate solution containing As(V) and Fe(III) (Droppert, 1996). The crystallization of scorodite was reported at 95 °C in the presence of a 50 g/L scorodite seed. The scorodite precipitation in the sulfate media requires a higher seed dosage than that of chloride media, which is due to the greater stability of

supersaturated sulfate solutions (Droppert, 1996). Debekaussen et al. (2001) also investigated the As(III) immobilization in the form of scorodite precipitates in a sulfate media. In this study, the dissolution of trioxide arsenic was performed in a 0.5 M sulfuric acid solution at 95 °C, which was followed by the oxidation of As(III) to As(V) using hydrogen peroxide (Debekaussen et al., 2001). The crystalline scorodite residues were eventually formed by the stepwise pH adjustment, the addition of ferric sulfate, and a scorodite seed. Catano et al. (2009) conducted several experiments in continuous reactors to crystallize the As(III) present in the dilute industrial solutions (0.1-1.1 g/L) as scorodite precipitates. It was shown that hydrogen peroxide was an effective oxidant at room temperature. In addition, the increase in the surface area of the seed enhanced As removal (Caetano et al., 2009).

In the hydrometallurgical processing of arsenic, hydrogen peroxide in 30% stoichiometric excess can function as an effective oxidizing agent (Debekaussen et al., 2001). Hydrogen peroxide is a costly reagent which can account for over 20% of the arsenic immobilization process operating cost (Filippou and Demopoulos, 1997). Furthermore, the difficulty associated with the pH adjustment is another drawback for the application of hydrogen peroxide, as the oxidation efficiency is sensitive to pH change (Debekaussen et al., 2001).

Fujita et al. (2008) studied the effect of Cu salt addition and air/oxygen sparging on the scorodite precipitation process. The ORP value increased to nearly 400 mV after 2 h in the presence of oxygen, whereas, the maximum ORP value obtained in the presence of air after 7 h was 380 mV (Fujita et al., 2008). Increasing the copper concentration up to 20 g/L did not exhibit an obvious effect on the scorodite yield and precipitation. It was also shown that the generated scorodite precipitates were fine and poorly crystalline when the arsenic concentration was <10 g/L (Fujita et al., 2008). Fujita et al. (2009) reported that the pH significantly influenced the properties of scorodite precipitates. An increase in the solution pH above 1.2 led to both finer scorodite particles and an increase in dissolved arsenic concentration. This might be due to the formation of jarosite precipitates, which adversely affects the properties of the scorodite particles (Fujita et al., 2009).

The favorable pH range for the formation of the stable scorodite precipitates was 0.3-1 (Fujita et al., 2009).

Chapter 3

Materials and experimental methods

3.1 Materials

Flotation enargite concentrate containing 24.4% copper, 39.0% sulfur, 20.1% iron and 8.5% arsenic was used as raw material in the kinetics experiments. The head assay (ICP analysis) of the enargite sample is shown in Table 3-1. The results of Rietveld X-Ray Diffraction (XRD) analysis confirm that the concentrate includes 45.6% of enargite and 43.0% of pyrite. XRD results are presented in Table 3-2.

Table 3-1. Head assay of enargite sample

Element	Copper	Iron	Arsenic	Sulfur	Zinc	Silver
Composition	wt%					ppm
	24.4	20.1	8.5	39.0	0.7	99

Table 3-2. XRD results for head concentrate

Mineral	Chemical Formula	Mass %
Enargite	Cu_3AsS_4	45.6
Pyrite	FeS_2	43.0
Sphalerite Iron	$(\text{Zn}, \text{Fe})\text{S}$	2.6
Quartz	SiO_2	2.5
Chalcopyrite	CuFeS_2	2.4
Tennantite	$(\text{Cu}, \text{Fe})_{12}\text{As}_4\text{S}_{13}$	1.4
Bornite	Cu_5FeS_4	0.8
Arsenopyrite	FeAsS	0.6
Galena	PbS	0.6
Covellite	CuS	0.5
Total		100.0

In leaching experiments, hydrated cupric chloride (Acros Organics, 99%) was used as a source of cupric ions, hexahydrate ferric chloride (sigma Aldrich, 98%) as a source of ferric ions and sodium chloride (Fisher chemicals, 99%) as a source of chloride ions in the solution. In the experiments with sulfate addition or sulfuric acid, proper proportions of ferric sulfate pentahydrate ($\text{Fe}_2(\text{SO}_4)_3 \cdot 5\text{H}_2\text{O}$, Acros Organics, 97%) and cupric sulfate pentahydrate ($\text{CuSO}_4 \cdot 5\text{H}_2\text{O}$, Fisher chemicals, 98%) were added to have a required sulfate concentration in the initial leach solution. Additionally, granular coconut shell based AC and AF 5 (Lewatit®) were used in the experiments as the leaching catalysts.

3.2 Leaching experiments

Atmospheric leaching experiments were systematically carried out in a 2 L glass reactor surrounded by a jacketed heater in order to control the temperature. The central port of the reactor lid was fitted with an overhead mechanical stirrer with a dual blade glass impeller to ensure proper mixing of the solution. A reflux condenser was also fitted to the reactor lid preventing excessive evaporation of the solution at high temperature. The reactor was sealed during the experiments to eliminate solution loss. A temperature control probe and oxygen sparger were also inserted into the reactor through reactor lid ports. Oxygen sparging was controlled using an oxygen flow meter. The ORP and pH of the leaching slurry were recorded during the experiments using Eh and pH probes.

In order to carry out the enargite leaching tests, 1 L of solution containing 0.5 M HCl and hexahydrate ferric chloride, hydrated cupric chloride, and sodium chloride were added into the test reactor. The sulfuric acid leaching experiments were performed by using 1 L of 1 M H_2SO_4 solution with hydrated ferric sulfate. 50 g of enargite concentrate was then added to the solution in all of the experiments except for the pulp density experiments. Most of the experiments were performed for 96 h and some were conducted for 72 h.

15 mL samples were drawn from the solution using a syringe at 1, 3, 6, 12, 24, 36, 48, 60, 72, 84 and 96 h. The solution loss was compensated for by the addition of 15 ml of solution (average

concentration of acid ferric, cupric). The samples were then centrifuged at 6000 rpm for 10 min and filtered using 0.45 μm syringe filters to separate the insoluble particles from the liquid phases. The filtrates were analyzed by Agilent 4200 microwave plasma- atomic emission spectrometry (MP-AES) to measure the concentration of copper and iron. The leach solution was pressure filtered after 96 h. The residue was washed twice using 1 L of 10% hydrochloric acid. The concentration of wash-water was, thereafter, analyzed by MP-AES to quantify the concentration of copper and iron. The arsenic concentration for selected samples was analyzed by ICP-OES.

The low pulp density kinetics experiments were performed by using 10 g of enargite concentrate in 1 L of solution. At low pulp density tests samples were taken at 0.5, 1, 2, 3 and 4 h. The reason for carrying out the low pulp density experiments was to study the leaching kinetics in a more controlled environment while minimizing the change in the solution concentration. The arsenic dissolution was selected as the indicator of the enargite leaching process in the low pulp density experiments, particularly because the copper extracted into the leach solution was insignificant in comparison to the background copper concentration of the starting solution and this might have resulted in a significant error in our copper extraction results. An enargite concentrate with the particle size range of 40-53 μm was utilized for low pulp density leaching experiments.

Free acid titration and ferric/ferrous titration were also performed on the samples in order to measure the free acid and ferric/ferrous concentrations during the leaching. Free acid titration was performed on the kinetics samples using 5 mL of the solution and addition 10 mL of 3.4% oxalate to avoid interference of ferric hydrolysis during titration. The titration was performed with 0.5 M NaOH solution by a 916-Ti Touch Metrohm auto-titrator. Ferric-ferrous titration was conducted on the filtered solution using a 1 g/L KMnO_4 solution. 2 mL of the kinetic sample was added to 10 mL of deionized water and 1.2 mL of phosphoric acid in a 50 mL beaker. A burette was used to add drops of the KMnO_4 solution until discoloration was viewed in the beaker. When discoloration was achieved the amount of KMnO_4 consumed was recorded and the ferrous concentration could be calculated. The leach solution was pressure filtered after 96 hours. The residue and catalyst were

washed twice using 1 L of 10% hydrochloric acid and dried in a vacuum oven at 40 °C for a week. The mineralogy of the solid residue was examined using XRD.

The AF 5 catalyst pre-treatment was performed by stirring the AF 5 in 1 L of 1 M solution of the specific acids, including nitric, hydrochloric and sulfuric acids, for 24 h at room temperature. The treatment was followed by a washing stage including two times mixing the catalyst with 1 L DI water for 10 minutes and solid-liquid separation.

3.3 Oxidation and absorption

In order to carry out the oxidation and adsorption tests, 100 mL of solution containing 0.5 M HCl, 20 ml of arsenic solution with 10 g/L As(III) and hexahydrate ferric chloride, hydrated cupric chloride and sodium chloride were added into the test reactor. The concentrations of cupric and ferric were adjusted to 5 g/L in the experiments and the concentration of chloride was adjusted to 1.5 M. Then, 5g dry AF 5 was added to the tests as a catalyst. Each test was carried out for 6 h. 5 mL samples were drawn from the solution using a syringe at 0, 20, 60, 200, 300, and 360 min. The experimental setup for absorption and oxidation experiments is shown in Figure 3-1.

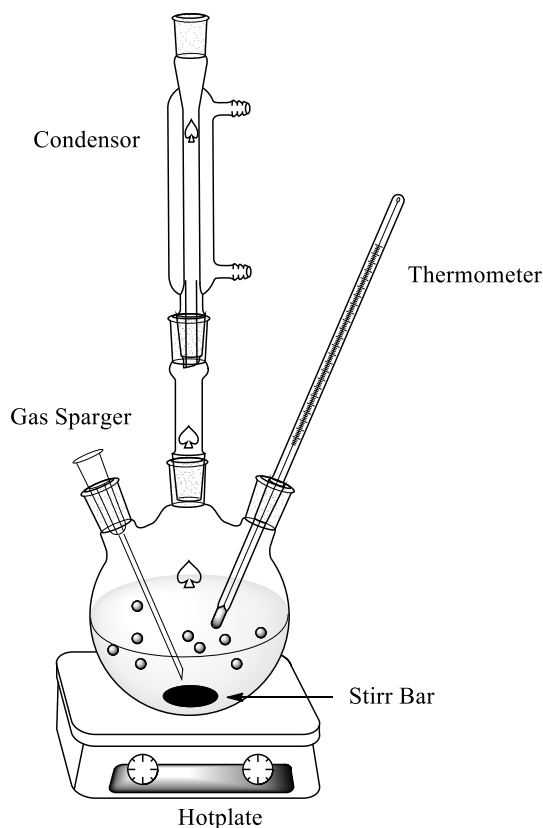


Figure 3-1. Absorption and oxidation experimental setup

3.4 Solid analysis

Brunauer-Emmett-Teller (BET) surface area and Barrett-Joyner-Halenda (BJH) pore size analysis was conducted by a Tristar 3000 surface area and pore size analyzer. Degasification process was performed for 2 h at 300 °C under nitrogen and the nitrogen adsorption for surface area measurement was performed at 77.35 K for 55 points. Scanning electron microscopy (SEM) and energy-dispersive X-ray spectroscopy (EDS) analysis were conducted by a NOVA NANOSEM 450 on the post leaching residue and catalyst for characterization purposes. All the samples were coated by carbon prior to the SEM analysis.

Identification and characterization of crystalline material including raw material and solid products were studied by X-ray Diffraction (XRD). Samples were prepared as the randomly oriented mounts of packed powder, spiked with corundum (10% wt.) to enable quantitative model analysis. Samples

were analyzed using a PANalytical X'Pert Pro diffractometer at 40 kV and 45 mA using Fe-filtered Co K α with scanning range 2θ of 5-110°. The semi-quantification and identification of crystalline phases were performed using Rietveld Refinements of the randomly oriented powder with Highscore Plus 4.5.

XPS analysis was conducted by a ThermoFisher Scientific K-Alpha XPS spectrometer with a monochromated Al K α X-ray source excitation (1486.6 eV). The system actually uses a microfocused X-ray spot, ranging in size from 30 to 400 μm , and the analyses in this study were done with a 400 μm spot. The analysis chamber vacuum was in the range of $\sim 10^{-9}$ mbar. The survey spectrum was typically acquired in a high pass energy (200 eV), low point-density (1 point/eV) scanned mode. Regional spectra, used to determine relative atomic composition as well as for determination of chemical information, were acquired in a low pass energy (50 eV), high point-density (0.1 eV spacing) scanned mode. The energy scale of the instrument was established using sputter-cleaned Au, Cu and Ag. Accepted binding energy (BE) values for the Au 4f (Au 4f_{7/2} = 84.0 eV), Cu 2p (Cu 2p_{3/2} = 932.67 eV) and Ag 3d (Ag 3d_{5/2} = 368.26 eV) transitions were used to establish absolute energy scale and linearity. After acquiring XP-spectra, XPS Peak 4.1 software was used for fitting XPS peaks.

Carbon and sulfur content analysis was performed on the catalysts and residue samples using an ELTRA CS-2000 induction furnace. Thermogravimetric Analysis (TGA) was performed on solid samples using a Netzsch STA 449 F3 Jupiter model with a heating rate of 5 °C/min under nitrogen atmosphere.

3.5 Electrochemical experiments

Electrochemical experiments were performed by a GSTAT302N potentiostat (Metrohm) controlled by Nova software (Version 2.0). All the experiments were carried out in a jacketed three-electrode electrochemical cell and the temperature was controlled by a Cole-Parmer Polystat water bath. The enargite carbon paste electrode was prepared by mixing 12 g of enargite concentrate, 3 g of graphite

(Aldrich grade, $< 20\mu\text{m}$) and 4g of silicone oil (Aldrich, Viscosity 100 kcSt). The well mixed paste was placed in a 50 ml plastic syringe and contact was made by an immersed copper wire in the paste. The surface area of the sample was 0.20 cm^2 and the surface area was renewed for each experiment. All the experiments were carried out in a three electrode electrolytic cell with an enargite carbon paste electrode as the working electrode, a graphite electrode as the counter electrode and a glass body Ag/AgCl electrode as the reference electrode. The reference electrode (Metrohm Ag) was filled with 3 M KCl electrolyte and showed 0.210 V vs. SHE at 25 °C.

Chapter 4

Catalyst characterization

Two types of carbon-based catalysts (CBC) were used in the experiments: (1) a granular coconut shell AC, and (2) Lewatit® AF 5, a new microporous carbon-based material in the form of small spherical beads, which has superior mechanical properties than conventional AC. The attrition rate of AF 5 has consistently been 10-fold less than that of AC. The optical microscope images of the surface of the fresh AC and AF 5 are presented in Figure 4-1, showing the different morphologies of the two catalysts. AC has a surface with visible porosities, while AF 5 is a spherical bead with a semi-vitreous surface. The surface area and particle size parameters of the two catalysts are presented in Table 4-1. The results of BET analysis of the two catalysts are shown in Figure 4-2. The distribution of width range, which is presented in Figure 4-2, confirms that AC contains about 64% of pores with width less than 5 nm; this value for AF 5 is equal to 71%. The smaller width range of AF 5 than AC is one of the major differences between the two catalysts.

Table 4-1. Characterization and properties of AC and AF 5

	AC	AF 5
Size range (mm)	1.7-3.35 Granular	0.3-0.8 Spherical
Surface area (m ² /g)	921	1154
Pore volume (cm ³ /g)	0.4373	0.4563

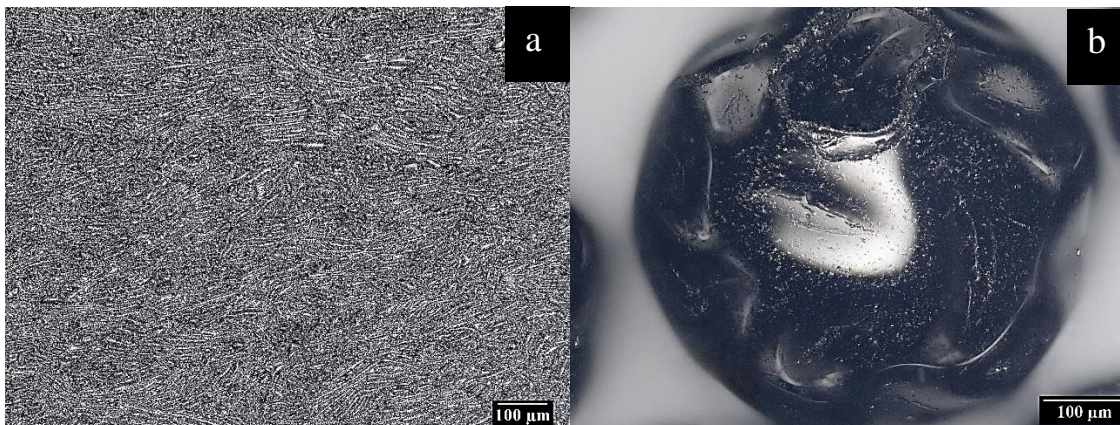


Figure 4-1. Optical microscope image of catalysts (a) AC, (b) AF 5

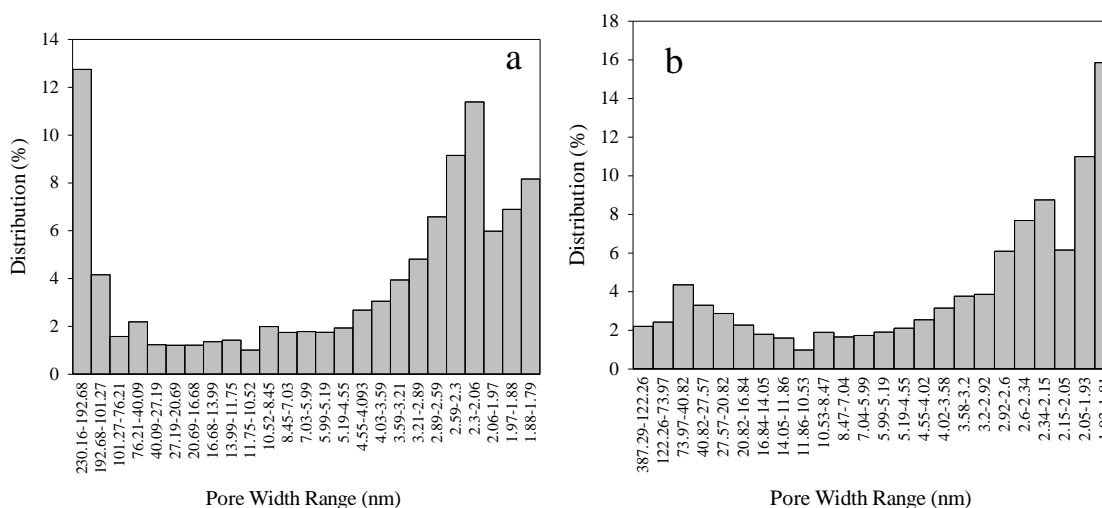


Figure 4-2. Pore volume distribution based on different pore width range (a) AC, (b) AF 5

The qualitative adsorption behaviors of the two catalysts were studied by the adsorption isotherm graphs (Martin-Gullon and Menendez-Diaz, 2006). The nitrogen adsorption isotherms of AC and AF 5 are presented in Figure 4-3. The fast increase in the adsorption at lower relative pressure and a knee to plateau relates to a narrow microporosity for AC. In the case of AF 5, the knee becomes more open up to 0.2 relative pressure which indicates the wider range of microporosity, in comparison to that of AC. In relative pressure, in the range of 0.2 to 0.7, the positive slope of the plateau is related to the presence of the mesopores in the two catalysts. The higher adsorption

capacity of AF 5 and higher micropore ratio can be seen in the more open isotherm knee of the adsorption graph compared to AC (Martin-Gullon and Menendez-Diaz, 2006).

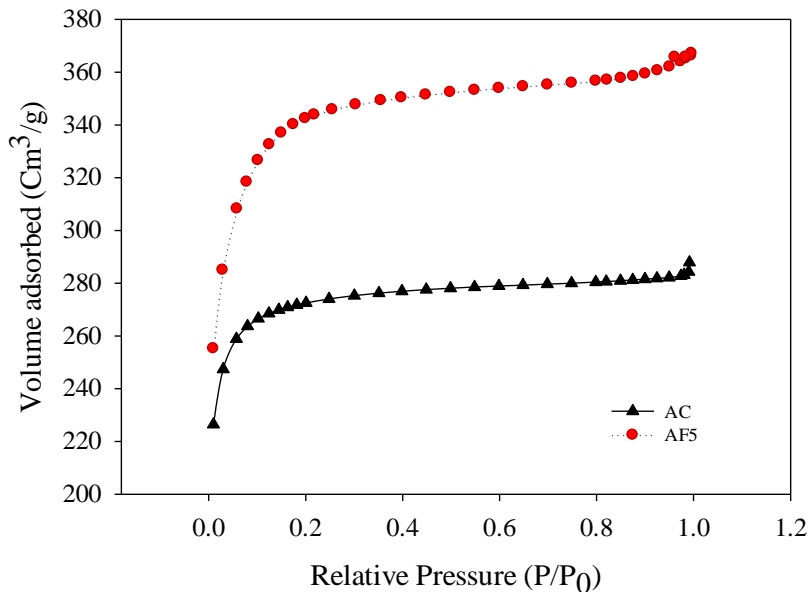


Figure 4-3. Nitrogen adsorption isotherm for AC and AF 5

The XPS analysis of the two catalysts supported the presence of 3 main groups of carbon, oxygen and nitrogen on the surfaces of AC and AF 5. The XPS method is often used to identify the functionalities on the surfaces of the CBC (Figueiredo and Pereira, 2010; Hulicova-Jurcakova et al., 2009; Kundu et al., 2008; Puziy et al., 2008; Zhou et al., 2007). The carbon and oxygen groups on the surface of the catalysts are shown in Figure 4-4 and Figure 4-5, respectively. The identification of oxygen functional groups by C1s is more practical due to the lower binding energy signals of the electronegative elements such as oxygen. Graphitic carbon is one of the major peaks for both AC and AF 5, which ranges from 284.6 to 285.1 eV (Figueiredo and Pereira, 2010; Kundu et al., 2008; Puziy et al., 2008), and which is connected to peak 2 and 3 in AC and peak 1 in AF 5 (Figure 4-4). Carboxylic acids or esters are the other significant groups which can be found in the range of 289.3 to 290.0 eV (Figueiredo and Pereira, 2010; Puziy et al., 2008) which are shown as peak 4 in AC (Figure 4-4a) and as peak 3 in AF 5 (Figure 4-4). The phenol group and maybe the

carbonyl group is indicated by a peak at 292.84 eV (Hulicova-Jurcakova et al., 2009; Zhou et al., 2007), presented by peak 2 in Figure 4-4b. It should be noted that the oxygen functionalities on the surfaces of the two catalysts are very similar, with slight differences in the availability of carbonyl groups on the surface of AF 5 (Bandosz and Ania, 2006; Biniak et al., 1997).

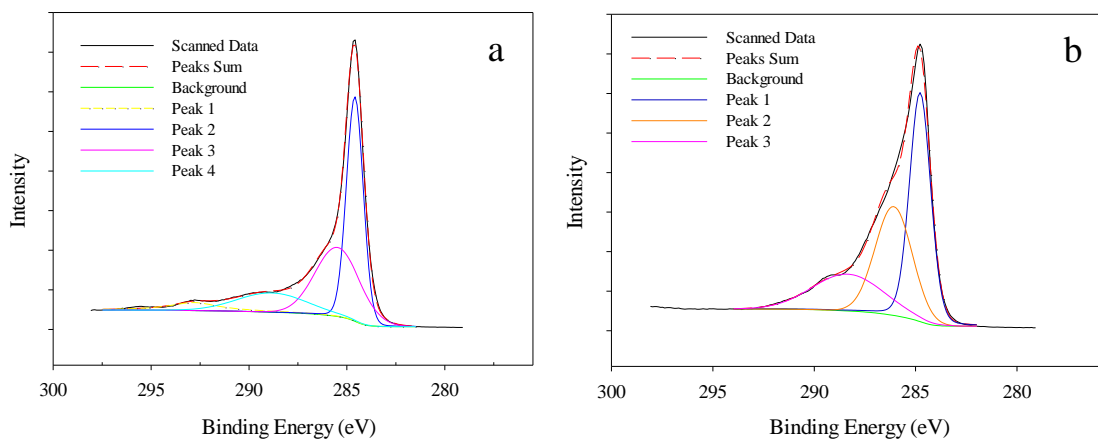


Figure 4-4. XP C1s core level spectra of the: (a) AC and (b) AF 5

The oxygen 1s analysis of Figure 4-5 proved the presence of C-OH and/or C-O-C groups between 532.4 to 533.1 eV as peak 1 in AF 5 and peaks 2 and 3 in AC (Puziy et al., 2008; Zhou et al., 2007). Chemisorbed oxygen and/or water at 535.05 eV is peak 2 in AF 5 (Hulicova-Jurcakova et al., 2009; Puziy et al., 2008) and sulfur esters or carboxylic acids are found at 534 eV (Figueiredo and Pereira, 2010; Hulicova-Jurcakova et al., 2009), labelled as peak 3 in AF 5 (Biniak et al., 1997).

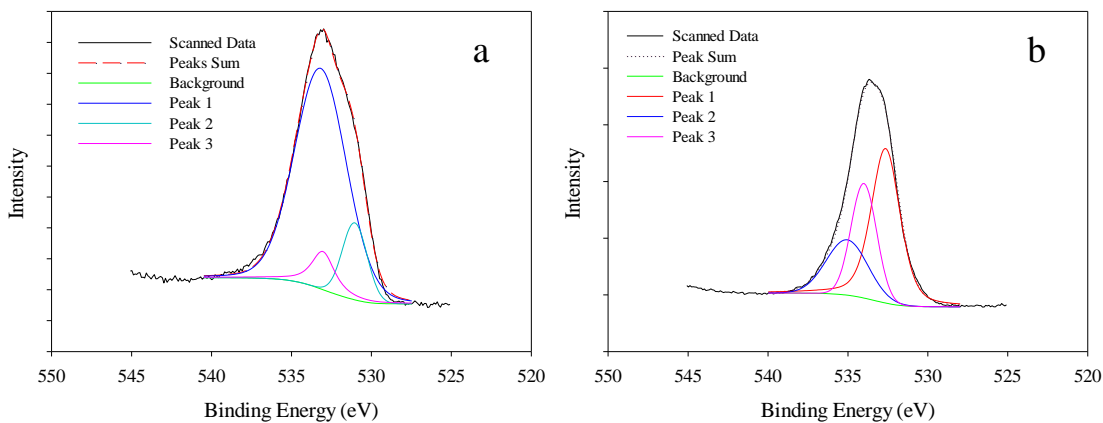


Figure 4-5- XP O 1s core level spectra of the: (a) AC and (b) AF 5

Chapter 5

Lanxess Lewatit® AF 5 and AC catalysis of enargite leaching in chloride media; A parameters study

5.1 Introduction

Previous studies have shown that one of the most effective media for the atmospheric leaching of enargite is a ferric-cupric chloride media. However, the recovery of this method cannot compete with industrial processes such as high pressure–high temperature autoclave leaching. The aim of the study in this chapter is to investigate the effect of different parameters on the copper recovery of enargite leaching without a catalyst, with AC, and with a novel CBC, Lanxess Lewatit® AF 5.

5.2 Results and discussion

5.2.1 Effect of mixing rate

The first set of experiments was performed with three different mixing rates of 800, 1000 and 1200 rpm. A 0.5 M hydrochloric acid leaching solution was used in the experiments and it contained 1 g/L of ferric ions without a catalyst. All of the experiments were conducted at 80 °C for 72 h. The optimum mixing rate for a process development depends both on the shape of the reactor and the slurry characteristics such as volume, density and viscosity etc. The effect of mixing rate in leaching experiments is shown in Figure 5-1. It was observed that different mixing rates of 800, 1000 and 1200 rpm did not have a significant effect on the copper recovery. The copper recoveries of 48% to 52% were achieved at different mixing rates. An agitation rate of 800 rpm was selected for the rest of the experiments of this study, in order to minimize the attrition rate of AC and AF 5. Elsewhere, Dixon and Rivera-Vasquez (Dixon and Rivera-Vasquez, 2012) have applied a mixing rate of 750 rpm for AC assisted leaching of sulfides, which is very close to the selected mixing rate in the present study.

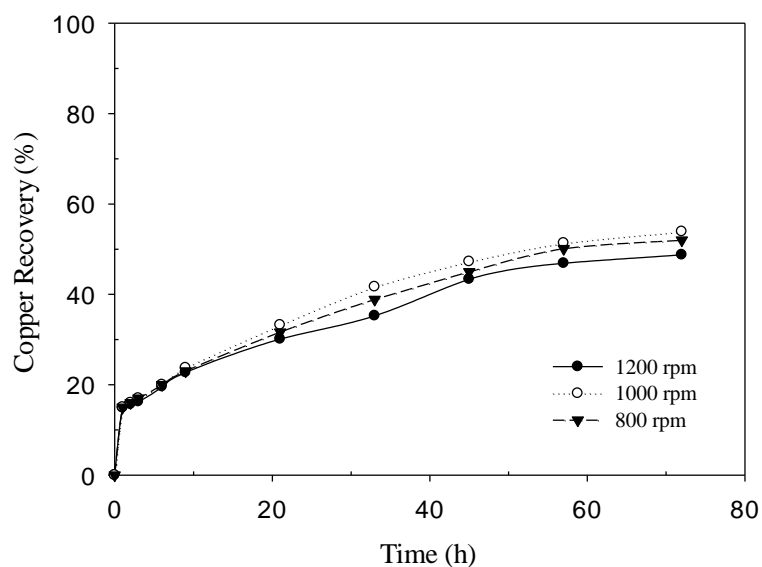


Figure 5-1. Effect of mixing rate on the copper recovery (0.5 M HCl, 1 g/L ferric concentration and at 80 °C)

5.2.2 Effect of catalysts

Without the use of a catalyst the dissolution rate of enargite is slow (Figure 5-1). In order to investigate the effect of carbon-based catalysts on the enargite dissolution rate, two types of CBC were studied: AC and AF 5. The CBC are believed to play two important roles in the enargite leaching reaction: (1) oxidizes ferrous to ferric (oxidant regeneration); and (2) oxidize the enargite directly by in-situ hydrogen peroxide production. The oxidation of ferrous ions by carbon-based catalysts is shown to occur by the in-situ formation of hydrogen peroxide generated via reactions with the carbon surface (Ahumada et al., 2002).

Equation 2-15 shows the oxidation occurring on the surface of catalysts by a quinone or other oxidant groups. It generates hydrogen peroxide, which subsequently oxidizes ferrous ions (Equation 2-16) (Ahumada et al., 2002). The quinone group is not the only oxygen containing functional group on the surface of the catalysts. Carboxylic acid, anhydrides, hydroxyls, lactol groups, lactone groups, phenol groups, and oxygen functional groups' concentrations can be increased by oxidation in gas or liquid phases (Bandosz and Ania, 2006; Figueiredo et al., 1999).

Figure 5-2 presents the effect of the two catalysts on the copper recovery, and compares those to the test with no catalyst addition at 90 °C. In addition, the effectiveness of the two catalysts at different temperatures of 80 and 90 °C are presented in this figure. In Figure 5-2 copper recoveries of the experiments with AF 5, AC and without a catalyst were compared for 96 h of leaching in 1.5 M chloride media with the addition of 5 g/L ferric and 5 g/L copper at 90 °C. Based on the recovery graphs, both catalysts played an effective role in the enargite leaching experiments. The copper recovery increased from about 65% in the experiment without a catalyst to 92 and 96% in the experiments with AC and AF 5 respectively. AC and AF 5 are carbon based catalysts and have similar structures, however, different ACs have different properties and they can have different effects on the copper sulfide leaching process (Dixon and Rivera-Vasquez, 2012). The difference between the copper recovery in the presence of AC and AF 5 is due to the different properties of these two catalysts.

The AC beads used in the experiments varied between 1.7-3.35 mm in size, and the AF 5 beads were spherical with diameters between 0.35-0.80 mm. The catalyst's effectiveness on enhancing the reaction rate is believed to be correlated to its available surface area to catalyze the reaction of interest. BET analysis was performed to measure the surface area of the two catalysts of this study. The AF 5 catalyst had a surface area of 1154 m²/g and pore volume of 0.4563 cm³/g, while AC had a surface area of 921 m²/g and pore volume of 0.4373 cm³/g. The 25% higher surface area of AF 5 compared to the AC is one of the reasons for its higher catalytic activity. Differences in the surface functional groups of various catalysts can also cause different behavior in the copper leaching process. The other reason for better copper recovery with AF 5 is likely connected to the higher affinity of elemental sulfur to AF 5. EDS analysis on the catalysts revealed the collection of sulfur on AF 5 beads, which is shown in the SEM study. Sulfur adsorption on the AF 5 catalyst beads can increase reaction kinetics and expedite the leaching process.

All the copper recovery results utilizing each catalyst from 60 °C to 90 °C were compared, however, only 80 °C and 90 °C results are demonstrated in Figure 5-2. Overall, the experimental trend was

as expected and AF 5 showed a higher dissolution rate. Leaching experiments with AF 5 were faster for the first 10 h of the leaching experiments. The recoveries were relatively the same for both AC and AF 5 up to 40 h of leaching. After 40 h the copper recovery for leaching experiments in the presence of AF 5 began to deviate from AC tests by a slight increase. The similar recovery trend proves that the catalytic effect of the two catalysts are independent for temperatures above 60 °C. It also shows that the mechanism for the entire catalytic reaction for both catalysts is similar. The catalytic mechanism can be written as the generation of hydrogen peroxide, which causes regeneration of the oxidants (Cowan et al., 2017; Radzinski, 2017). It is worth mentioning that the hydrogen peroxide can also effectively oxidize enargite via a direct hydrogen peroxide–enargite reaction.

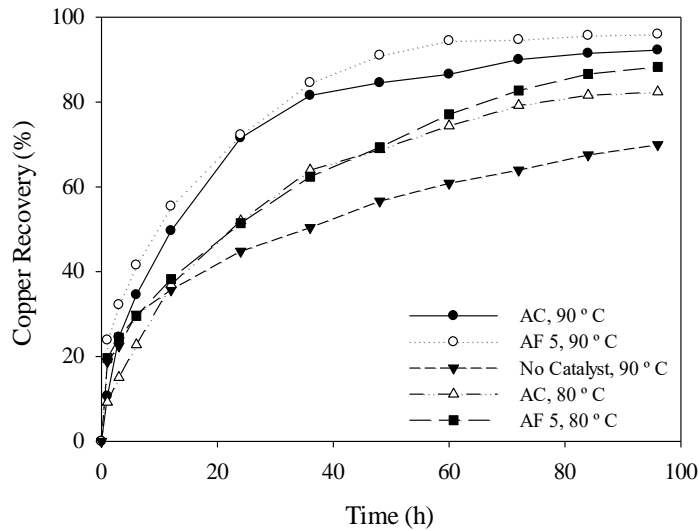


Figure 5-2. Copper recovery in the presence of AF 5 and AC at 80 and 90 °C and no catalyst at 90 °C (0.5 M HCl, 1.5 M Cl⁻, 5 g/L cupric ions, 5 g/L ferric ions, 0.1 L/min O₂, concentrate/catalyst=1:1)

The results of copper recovery from the leach solution and solid residues (via digestion of the residues and its chemical analysis) are compared in Table 5-1. The recovery calculated from the residues was slightly higher in all of the experiments, although the differences are in acceptable range of less than 3%.

Table 5-1. The copper recovery from solid and solution analysis (0.5 M HCl, 1.5 M Cl⁻, 5 g/L cupric ions, 5 g/L ferric ions, 0.1 L/min O₂, concentrate/catalyst=1:1)

Test conditions	Cu Recovery (%)	
	Solutions	Solid residues
AC, 90 °C	92	94
AF 5, 90 °C	96	97
AC, 80 °C	82	85
AF 5, 80 °C	88	90
No Catalyst, 90 °C	70	71

The measured solution ORP values versus time in different leaching conditions are presented in Table 5-2. The initial ORP value of solution was 625 mV because of the high concentrations of ferric and cupric in the initial test solution. After the initial contact of the solution with the catalyst, the reduction of ferric and cupric ions occurs, which decreases the ORP value. This phenomenon is not observed in the experiments without catalyst. The ferric and cupric reduction in the presence of AC catalysts have been reported previously by Bandosz and Ania (Bandosz and Ania, 2006).

Table 5-2. Solution ORP values during the leaching without catalyst, AF 5 and AC (0.5 M HCl, 1.5 M Cl⁻, 5 g/L cupric ions, 5 g/L ferric ions, 0.1 L/min O₂, concentrate/catalyst=1:1)

ORP vs. Ag/AgCl (mV)			
Time	AF5	AC	No Catalyst
Before Catalyst Addition	625	627	619
0	527	550	598
1	522	532	574
3	532	542	562
6	538	552	558
12	545	554	548
24	551	566	542
36	555	574	543
48	554	583	545
60	532	588	549
72	534	576	548
84	532	572	550
96	528	570	552

Furthermore, in the first 20 h of the leaching experiments, the reduction of the oxidants is higher because the dissolution rate of concentrate is also higher which consumes oxidants. The ORP drop in the presence of AF 5 was more substantial compared to the AC catalyst. After the first hour of the tests (Table 5-2), the ORP starts to increase in the two tests with the catalysts, which suggests that the oxidants are being regenerated. In the presence of catalyst, the ORP values experience a decrease on the third or fourth day of the leaching experiment, due to ferric precipitation as scorodite.

5.2.3 Effect of concentrate:catalyst mass ratio

In order to examine the effect of the catalyst concentration on the copper recovery, a series of leaching experiments were performed with different concentrate to catalyst ratios. First, the effect of five different ratios of concentrate to AC were tested in the leaching experiments. The copper recovery results are presented in Figure 5-3(a). The general trend of the leaching results confirms that the AC addition increased the enargite dissolution rate. The experiments with higher concentrate to AC ratios of 1:2 and 1:4 showed a close copper recovery of about 98% and 99%. This suggests that adding more AC than concentrate to AC ratio of 1:2 does not have a significant effect on the copper recovery. In contrast, decreasing the concentrate to AC ratio to 1:1, 2:1 and 4:1 diminished the copper recoveries to 92, 89 and 82% respectively. In general, it was found that the addition of a higher ratio of AC to concentrate would expedite the dissolution kinetics of enargite, which is in agreement with the results of the Dixon and Rivera-Vasquez study (Dixon and Rivera-Vasquez, 2012). Their study (Dixon and Rivera-Vasquez, 2012) found that the addition of the different ratios of concentrate to AC enhances the kinetics of the leach process. The concentrate to AC ratio was found to be one of the most influential parameters in the leaching experiments. Three different concentrate to AF 5 ratios of 1:2, 1:1 and 2:1 were examined and the results are depicted in Figure 5-3(b). The final recoveries in different ratios were generally higher and in a closer range compared to the AC assisted leaching experiments. However, the overall trend of

copper recovery for both catalysts was similar. The best copper recoveries were obtained in the experiments with concentrate to AF 5 ratios of 1:2 and 1:1 resulting in the copper recovery values of about 99% and 96%, respectively. The lowest copper recovery of 91% was attained for a concentrate to AF 5 ratio of 2:1. Copper recoveries for these two ratios were close and near completion and, therefore, the 1:2 ratio was the highest ratio examined in the leaching tests. Raising the concentrate to AF 5 ratios higher than 1:1 did not result in a considerable change in the copper recovery values leading to the conclusion that the optimum amount of catalyst for oxidation is around 1:1 to 1:2.

In summary, higher ratios of both AC and AF 5 resulted in higher copper recoveries. The AF 5 catalyst showed higher oxidation and dissolution values for the concentrate to catalysts ratios of 1:1 and 1:2. Similar copper recovery values were obtained for the concentrate to AC ratios of 1:2 and 1:4. These results showed that the catalytic effect of AF 5 is better than AC during enargite leaching.

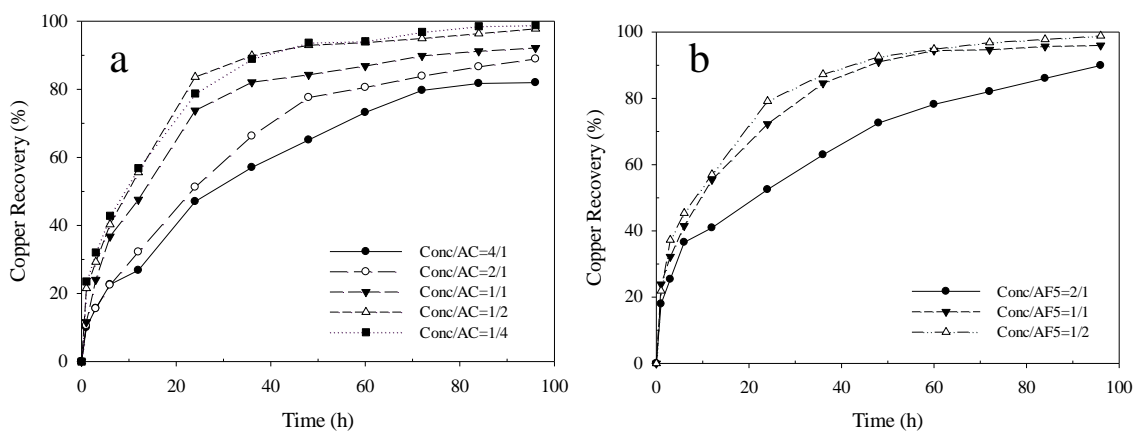


Figure 5-3. Effect of concentrate/ catalyst ratio on copper recovery (a) with AC (b) with AF 5 (5 g/L cupric ions, 5 g/L ferric ions, 0.1 L/min O₂, 90 °C)

Figure 5-4 illustrates the copper recovery with respect to variation of the concentrate to AC ratio and temperature. It is clear from Figure 5-4 that copper recovery increases to near complete recovery in 80 h by increasing the temperature to 90 °C and the concentrate:AC ratio to 1:1.

Nonetheless, the experiment at a lower temperature of 80 °C and concentrate:AC ratio of 4:1 resulted in copper recovery of only 70% at the 96 h mark.

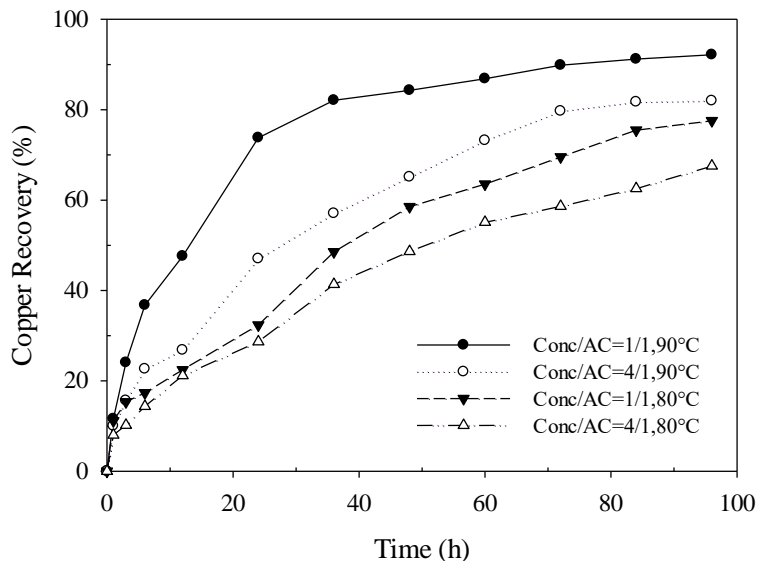


Figure 5-4. Effect of AC ratio on copper recovery at 80 and 90 °C (5 g/L cupric ions, 5 g/L ferric ions, 0.1 L/min O₂)

In order to confirm the effect of catalyst to concentrate mass ratio and the type of catalyst on the copper recovery, the copper recoveries after 96 h of the experiment with AC and AF 5 were graphed versus the surface area of catalysts. The surface areas of the catalysts were calculated using the data from BET experiments. This graph is shown in Figure 5-5. The copper recovery follows a close relation with the catalyst surface area, whereby increasing the surface area causes the dissolution rate increases, as well. The overall copper recovery with both catalysts is very similar; when normalizing the copper recovery with respect to the catalyst's surface area, however, the recovery is slightly higher with AF 5.

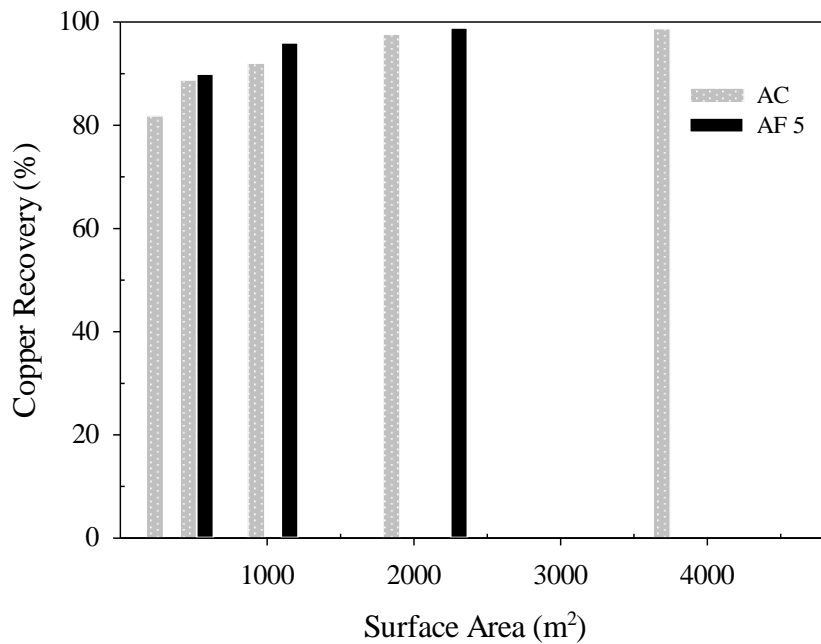


Figure 5-5. Effect of surface area on final copper recovery after 96 h of leaching with AC and AF 5

5.2.4 Effect of initial ferric ion concentration

To study the effect of ferric ion concentration on the copper recovery, four leaching experiments with ferric ion concentrations of 0.1, 1, 5 and 10 g/L were conducted without a catalyst, and the results are presented in Figure 5-6a. In general, the copper recovery did not change significantly with different ferric ion concentrations. The experiments with higher concentrations of ferric ions showed slightly higher copper recoveries at the early stage of leaching (around 40 h), followed by the reaction slowing down. The copper recovery value for the initial ferric ion addition of 5 and 10 g/L was 45%. The copper recovery value for the two tests with the initial ferric ion concentrations of 0.1 and 1 g/L were 52%. The oxidation reaction of ferrous to ferric is very slow, regardless of constant oxygen gas addition to the leach slurry.

Different initial ferric ion additions of 0, 5, 7.5 and 10 g/L were tested on the copper recovery of enargite leaching in the presence of AF 5 and the results are presented in Figure 5-6b. One of the experiments was conducted at an oxygen sparging rate of 1 L/min in order to investigate the

possible relation of oxygen sparging rate and initial ferric concentration on the leaching rate. However, the experimental results showed either no relation between these two parameters or a negligible effect in the examined range. The higher initial ferric ion concentration resulted in higher copper recovery, where the copper recovery value varied between 94-96%. When the leaching experiment was performed in the presence of a catalyst and oxygen was sparged during the tests, the initial ferric ion concentration did not have a significant effect on the overall copper recovery.

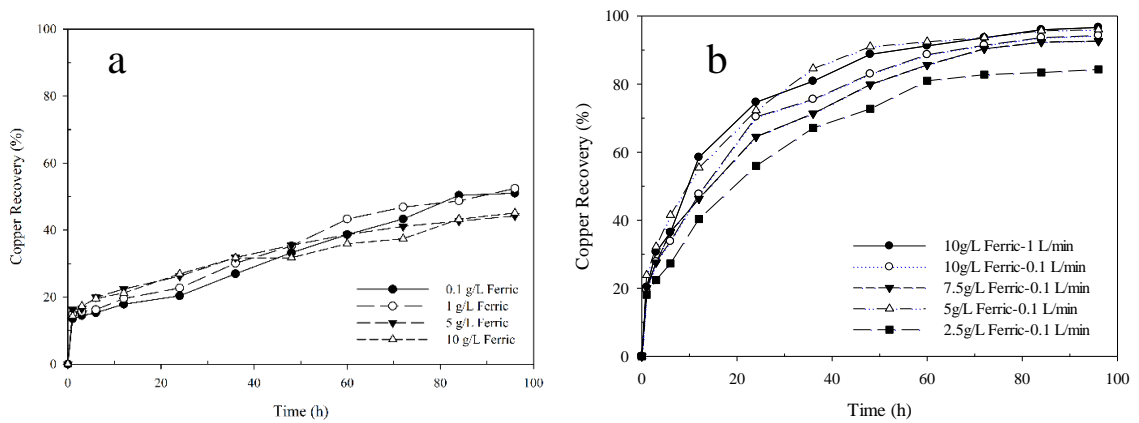


Figure 5-6. Effect of ferric ion concentration on the copper recovery (a) without catalyst (80 °C, without catalyst) (b) with AF 5 catalyst (5 g/L cupric ions, concentrate to AF 5 1:1, 90 °C)

5.2.5 Effect of temperature

Although any potential atmospheric leaching process for copper sulfides will be an autothermal process, meaning that the heat of the sulfide oxidation reaction will provide the heat needed to reach the process design temperature, nonetheless it is understood that the leach process temperature is one of the most important factors in defining the reaction kinetics. Thermodynamics and kinetics parameters of most reactions are dependent on temperature. To evaluate the effect of temperature on enargite leaching without a catalyst, four experiments were performed at 60, 70, 80 and 90 °C and the results are depicted in Figure 5-7(a). As expected higher temperature conditions resulted in the best outcomes. The copper recovery of 70%, 50%, 32% and 30% were achieved after 96 h of leaching at 90, 80, 70 and 60 °C respectively. The temperature dependence of copper

sulfide dissolution in hydrochloric acid media is also stated in Padilla et al. (Padilla et al., 2005a). In their experiments, arsenic dissolution was used as the indicator of overall leaching rates. In the study by Padilla et al. (2005) the arsenic recovery increased from 1% at 80 °C to 6% at 100 °C after 7 h of leaching (Padilla et al., 2005a). A higher diffusion rate at elevated temperatures is believed to be the reason for recovery enhancement in copper sulfide mineral leaching. The diffusion of reactant and dissolved metal ions through the metal deficient layer or the product layer has been increased effectively at higher temperatures (Dutrizac, 1989; Ghahremaninezhad et al., 2012).

The same set of experiments in Figure 5-7(a) was carried out in the presence of AC and AF 5 to determine the effect of temperature on copper dissolution and the results are shown in Figure 5-7(b) and Figure 5-7(c) respectively. The best leaching rates were accomplished at the elevated temperatures, where the leaching trends were faster. Both AC and AF 5 followed the same leaching recovery but, generally, AF 5 showed a higher dissolution rate. Copper dissolutions of 92, 86 and 82% in the presence of AC and 96, 91 and 88% in the presence of AF 5 were achieved at 90, 85 and 80 °C. The leaching results followed the same trend as was reported by Rivera-Vasquez and Dixon (Rivera-Vasquez and Dixon, 2015). Although the differences between the results of the current study and those of the study by Rivera-Vasquez and Dixon (Rivera-Vasquez and Dixon, 2015) were: i) a Py/En ratio of 3:1 is applied in the Rivera-Vasquez and Dixon study, and ii) a chloride media is used in this study, whereas a sulfate solution was used in the Rivera-Vasquez and Dixon study. As shown in in Figure 5-7(b) and Figure 5-7(c), the effect of temperature is consistently positive on copper recovery, such that, as the temperature increases, the overall copper recovery and leach kinetics increase. AF 5 was found to be a better catalyst at higher temperatures, however, at temperatures below 70 °C AC was shown to be a better catalyst for enargite leaching. Further research is needed to clarify the reason for the above differences in the catalytic behavior of AC vs AF 5.

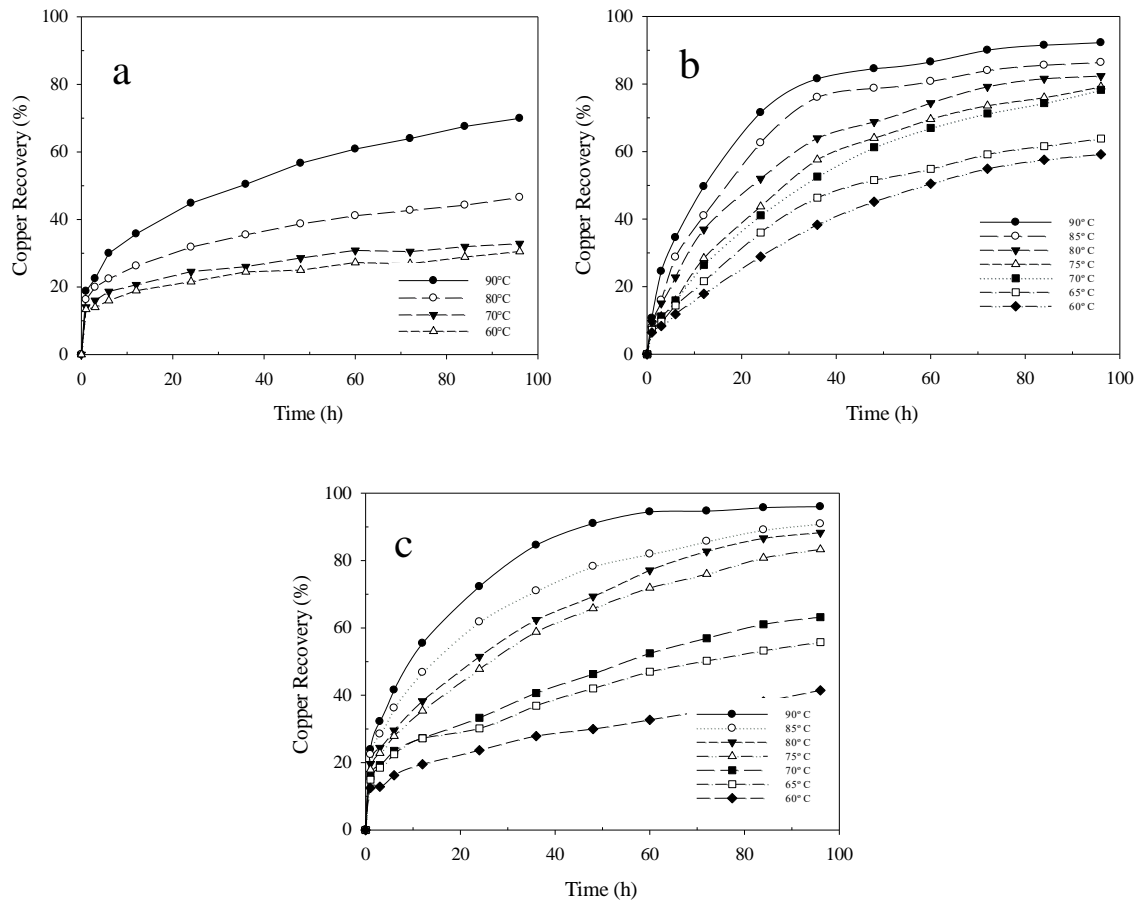


Figure 5-7. Effect of temperature on the copper recovery (5 g/L cupric ions, 5 g/L ferric ions oxygen flow rate 0.1 L/min) (a) without a catalyst (b) With AC (concentrate to AC 1:1) (c) With AF 5 (concentrate to AF 5 1:1)

5.2.6 Effect of oxygen addition

It is widely believed that the role of oxygen in the leaching processes is twofold: (1) oxygen can cause direct oxidation of ferrous to ferric ions, and regenerate the oxidant of the sulfide minerals, i.e ferric. The direct oxidation of ferrous to ferric is a very slow process, and can be catalyzed by CBC. (2) Oxygen is an indispensable element in the catalytic reaction of CBC. Without oxygen, the catalytic oxidation reactions will stop and catalysts will lose the ability to generate hydrogen peroxide. The oxygen sparging causes the regeneration of surface oxygen groups on the surface of the two catalysts and increases the catalytic activity of carbon-based catalysts. No catalytic effect

can be seen in the case of N₂ sparging (Ahumada et al., 2002). The effect of oxygen sparging rate was studied as one of the parameters in leaching experiments.

The effect of oxygen sparging rate was studied in AC assisted leaching tests conducted at 90 °C with five different oxygen sparging rates of 0.1, 0.2, 0.3, 0.5 and 1.0 L/min, and the results are shown in Figure 5-8(a). The addition of 0.1, 0.2, 0.3 and 0.5 L/min oxygen did not have a substantial effect on the copper recovery. However, the addition of 1.0 L/min oxygen in the leaching reactor increased the leaching rate and achieved complete copper recovery in less than 40 h. The same experiments as above were performed with AF 5 catalyst on two different oxygen sparging flow rates of 0.1 and 1.0 L/min, as shown in Figure 5-8(a), and one experiment with an argon sparging rate of 0.1 L/min, shown in Figure 5-8(b). The leaching kinetics of enargite with AC and AF 5 catalysts with different oxygen addition flow rates showed that the experiments are only slightly sensitive to the oxygen addition rate. The better copper recovery with AC might be connected to its larger porosity diameters vs. AF 5 (shown with BET experiments). BET analysis showed that the AC structure has 19.6% macropores, 65.4% mesopores and 15.1% micropores, whereas the AF 5 structure has 7.8% macropores, 65.3% mesopores and 26.9% micropores, confirming that AF 5 has a higher distribution of smaller porosities in its structure.

In the experiment where oxygen was replaced with argon, Figure 5-8(b), the copper dissolution rate increased to 13% in the first hour of the experiment, followed by a slight decrease because of adsorption, and stayed constant to the end of the experiment. This experiment shows that the effectiveness of the catalysts for copper leaching depends significantly on oxygen addition. The initial 13% Cu dissolution can be justified by leaching of less refractory copper sulfide minerals in the concentrate and availability of ferric ions, cupric ions and dissolved oxygen in the first few hours of the experiment to leach a proportion of the concentrate.

Increasing the oxygen sparging rate in the leaching experiments without catalyst did not have a significant effect on copper recovery because the dissolution of gases, in this case oxygen, is always

limited. The concentration of dissolved oxygen in chloride media at 35 °C was reported to be less than 1 ppm (Akilan and Nicol, 2016).

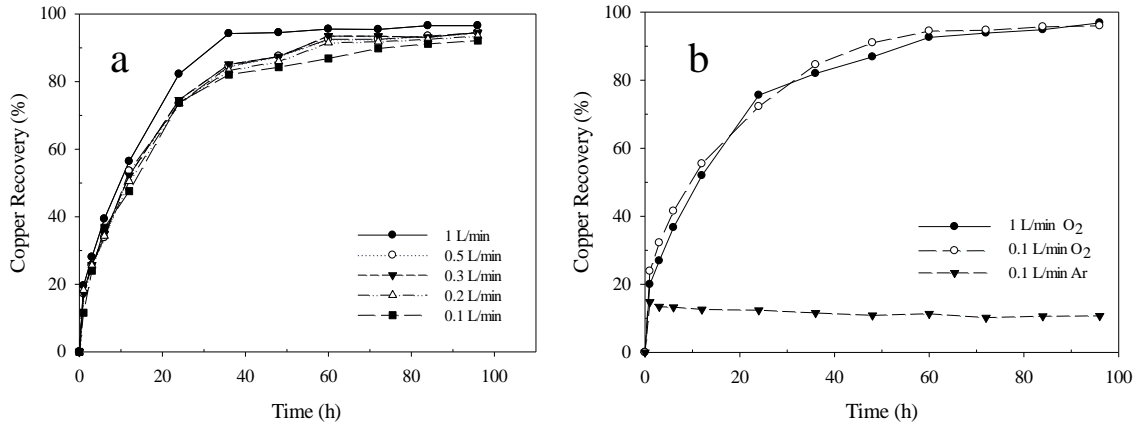


Figure 5-8. Effect of oxygen sparging rate on copper recovery in the presence of: (a) AC (b) AF 5 (5 g/L cupric ions, 5 g/L ferric ions, concentrate to catalyst 1:1, 90 °C)

5.2.7 Effect of sulfate addition

To probe the effect of sulfate addition on the copper recovery several leaching experiments were performed without a catalyst and in the presence of AC (Figure 5-9(a) and Figure 5-9(b) respectively). The leaching experiments without a catalyst were conducted at 80 °C and the highest copper recovery was achieved in the experiment with 1 g/L sulfate ion addition. Generally, the addition of different sulfate ions did not make a significant change in the leaching results. Padilla et al. (Padilla et al., 2005b) studied the effect of sulfate ions on enargite dissolution and noted that in the presence of sulfate ions enargite dissolution rate was increased. They reported that the addition of sulfate ions, in the form of sulfuric acid from 0.15 M to 0.25 M increased the As dissolution rate from 3.5 % to 6 % (As dissolution rate was chosen as an indicator for overall recovery). It was mentioned that the addition of sulfate ions from 0.25 M to 0.3 M did not make any changes in the As dissolution rate. Based on the leaching results, the addition of up to 1 g/L of sulfate ions expedited the leaching experiments, however, higher concentrations of sulfate decelerated the process. The 4% increase in the leaching rate, resulted from adding sulfate ions,

was consistent with the results of Padilla et al. (Padilla et al., 2005b) and Dutrizac and Macdonald (Dutrizac and MacDonald, 1972). The decrease in the copper dissolution by the addition of sulfate concentrations higher than 0.3 M is believed to be related to the oxygen solubility decrease (Narita et al., 1983; Padilla et al., 2005b). Nonetheless it has been shown that the oxygen solubility does not change substantially by the addition of 1-15 g/L sulfate in chloride containing solutions at high temperatures such as 80 °C (Tromans, 1998a, 1998b). The reduction of copper recovery with higher levels of sulfate addition might be due to the different bonding of sulfate ions in the solution or formation of a passive layer on the surface of the particles.

The experiments in the presence of AC were carried out at 80 °C, with 5 g/L of cupric ions and two different levels of sulfate ions: 0 and 4 g/L. One experiment was performed with the initial ferric to ferrous ion ratio of 1:1 with a total of 5 g/L iron ions in the solution. No significant effect of sulfate ions in the final copper recovery was observed in the presence of AC. The sulfate ions were added in two forms of sulfuric acid and ferric sulfate with varying overall ferric ions, however the same results were achieved. This experiment verified that not only does sulfate addition change the results but also, in this range, changing the acid concentration does not substantially affect the outcome. These results are in agreement with the Rivera-Vasquez and Dixon study (Rivera-Vasquez and Dixon, 2015). The addition of iron in the form of ferric and ferrous ions also did not affect the leaching rate significantly. Most ferrous ions will oxidize to ferric in the presence of AC within 24 h of the leaching experiments. The addition of more ferrous or the initial ferrous amount will not make a considerable change in the leaching process. Therefore, the total iron content can be considered to be a more important factor than the initial ferric ions. To reiterate, the addition of sulfate was not an influential factor for the leaching experiments and has no significant effect on the catalyst's performance.

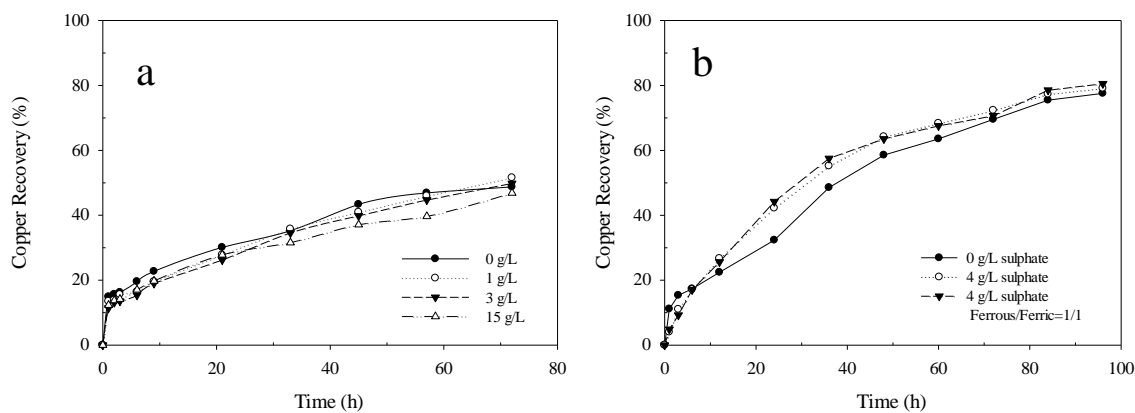


Figure 5-9. Effect of sulfate addition on copper recovery (a) without catalyst (ferric ions 1 g/L, cupric ions 0 g/L, 80 °C) 1 g/L (b) with AC (5 g/L cupric ions, 5 g/L ferric ions, concentrate to AC 1:1, 80 °C)

5.2.8 Effect of cupric addition

During the atmospheric leaching of copper sulfides, cupric ions act as an oxidant and are known to be more effective than ferric ions (Parker et al., 1981). In higher concentrations of chloride media, i.e. higher than 5 M chloride, cupric ions are believed to induce the ferric ion generation as shown in Equation 2-5 (Miki and Nicol, 2008). However, regeneration of cupric and ferric ions by dissolved oxygen is required for the process (Miki and Nicol, 2008).

The regeneration of ferric by cupric ions is unlikely in the present study, because the concentration of chloride ions is 1.5 M, which is lower than the minimum suggested chloride concentration required for ferric regeneration by cupric ions, i.e. 5 M (Miki and Nicol, 2008). The effect of cupric ion addition was examined in the leaching processes without a catalyst, with AC and with AF 5. Figure 5-10(a) shows the effect of cupric ions on the copper recovery in the presence of AC. Similar to the experiments without a catalyst, cupric ions have a catalytic effect in the presence of a catalyst. The copper recovery increased in this condition from 87% to 92% in the presence of 5 g/L initial cupric addition. Addition of cupric ions enhanced the rate of copper leaching significantly in the experiments with no catalyst. The improvement of the process is the result of the improved redox potential of the leaching solution (i.e. a mixed potential of ferric/ferrous ion and cupric/cuprous ion

couples and stabilisation of cupric and cuprous ions through complexation with chloride ions) (Dutrizac, 1992; Liddicoat and Dreisinger, 2007).

Figure 5-10(b) shows the effect of cupric ions on copper recovery on leaching experiments in the presence of AF 5. In this set of experiments, five different levels of cupric ion concentrations of 0, 2.5, 5, 7.5 and 10 g/L were tested at 90 °C. The enhancement of copper recovery in the presence of cupric ions is considerable, as the copper recovery had changed from 88% with no cupric addition to 96% with 5 g/L cupric addition. The copper recovery amplified to 99% in the presence of 10 g/L cupric. The copper recovery for the leaching experiments with over 5 g/L cupric ion addition was close to completion after 96 hours of leaching. The same results were reported by Yévenes et al. (2010) who showed in chalcopyrite chloride leaching process, the addition of cupric ions improved the leaching rate, but different concentrations of cupric did not enhance the dissolution rate in the optimum potential range (Yévenes et al., 2010). The effect of addition of cupric ions in the leach solution without ferric ion addition was investigated in an experiment with 5 g/L cupric ions and no ferric ions added to the initial leach solution. The results of this experiment are presented in Figure 5-6. The results showed that the main oxidant for the enargite leaching is cupric ions and the copper dissolution rate is sensitive to the initial cupric concentration.

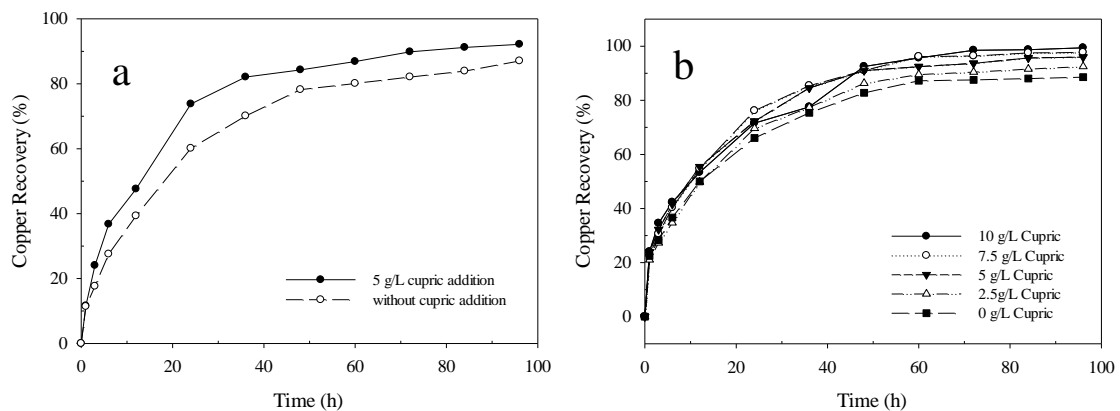


Figure 5-10. Effect of cupric ion addition on copper recovery (a) with AC (b) with AF 5 (90°C, concentrate to catalyst =1:1, 5 g/L ferric ions)

5.2.9 Effect of pulp density

Pulp density is an important parameter for further process development (Martinez-Gomez et al., 2016; Parada et al., 2014). Higher pulp densities usually lead to a smaller scale operation and a lower capital cost. In our studies, most of the leaching experiments were performed at 100 g solids/L pulp density. Two initial experiments were performed with 10 g/L and 50 g/L pulp density without a catalyst, which led to a higher recovery in a higher pulp density condition. The addition of a catalyst considerably increased the pulp density, rendering the comparison between the experiments with and without a catalyst meaningless. To examine the effect of pulp density in the presence of a catalyst, three experiments with 50, 100 and 200 g/L pulp density were conducted. Figure 5-11 demonstrates the results of these studies. The copper recoveries for 50 and 100 g/L pulp density were identical but 6% improvement was observed in the test with 200 g/L pulp density. Dixon and Rivera-Vasquez (Dixon and Rivera-Vasquez, 2012) reported that the leaching kinetic was faster for the experiments with 40 g concentrate and 40 g AC than for the experiment with 20 g concentrate and 20 g AC, stating that the higher kinetics in the high pulp density experiment is due to the higher interaction of AC and enargite particles and more stable ORP values. The higher pulp density test reached about 97% recovery after 20 h and the lower pulp density test was completed after 45 h of leaching (Dixon and Rivera-Vasquez, 2012). The effect of pulp density with both types of catalysts was similar, therefore only the results of the experiments with AC are presented.

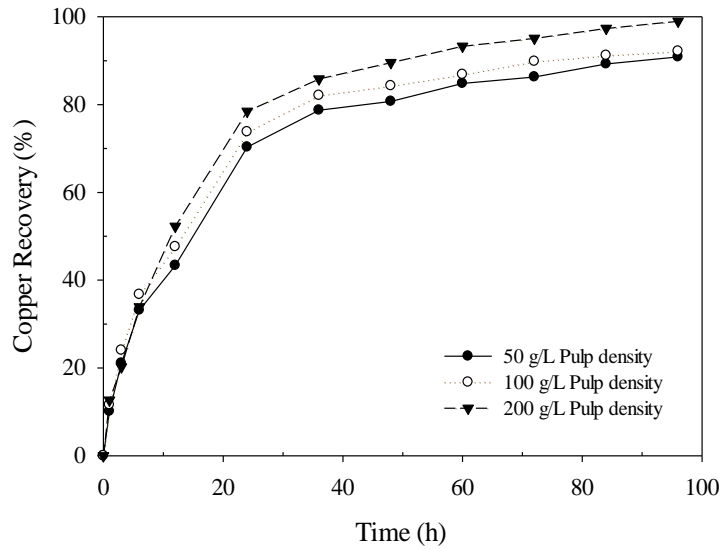


Figure 5-11. Effect of pulp density on the copper recovery in the presence of AC (90°C, concentrate to AC=1:1)

5.2.10 Effect of retention time

Long leaching residence time for a process is not desirable, because it has a direct impact on the capital cost of the plant development. To develop an idea on the effect of retention time on the leaching experiments, a leaching test was carried out for 7 days at 70 °C, and the results of the test are shown in Figure 5-12. The results indicate that copper continuously dissolves during the 7 days of the experiment, reaching 97% copper recovery after 7 days.

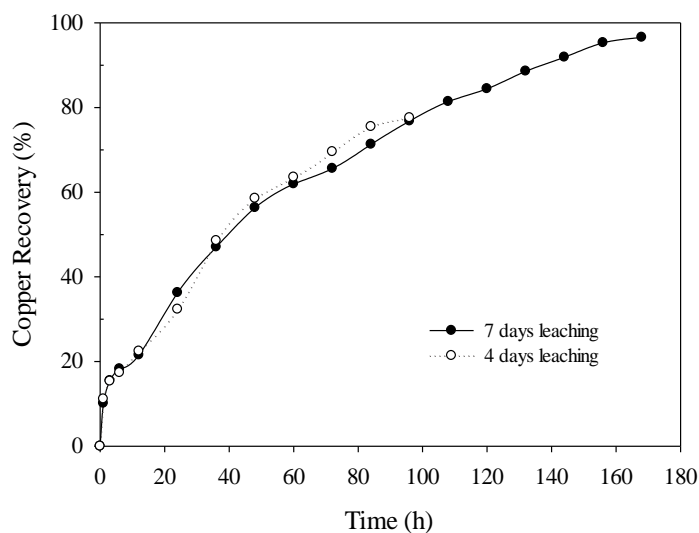


Figure 5-12. Effect of time on the leaching recovery (5 g/L ferric ions, 5 g/L cupric ions, 70°C, concentrate to AC=1:1)

5.2.11 SEM study

In order to study the effect of the leaching process on the surface of the concentrate, a SEM study was performed on the leaching particles after 1 day of leaching in the presence of the catalyst. The SEM images are presented in Figure 5-13. EDS analysis was used to characterize the particles which confirmed the generation of elemental sulfur as the product of the leaching reaction. No sulfur accumulation was observed on the surface of the particles. Small elemental sulfur particles were deposited onto the pyrite and enargite particle surfaces but most of those particles were in the form of an isolated particle. After 3 days of leaching most of the enargite particles were leached to completion, and sulfur accumulation was more visible.

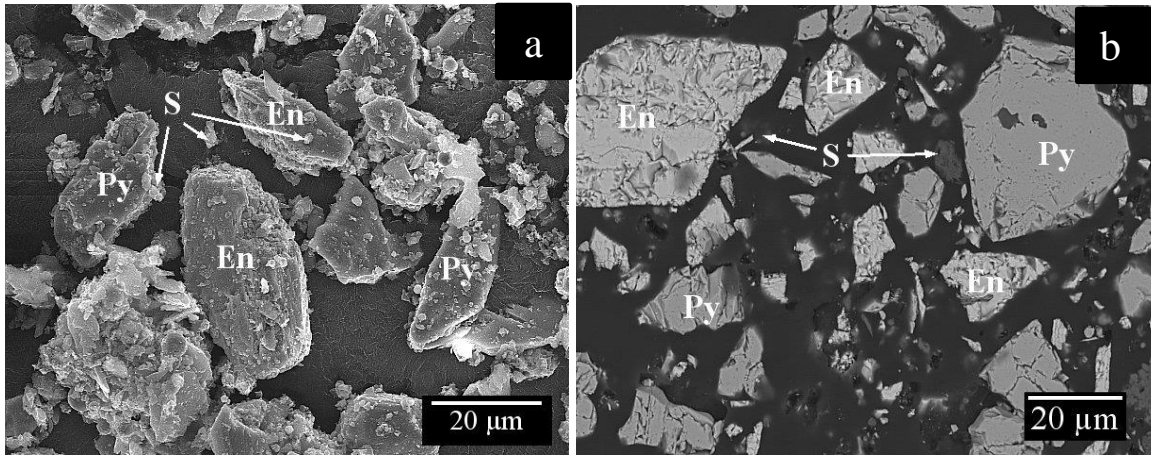


Figure 5-13. SEM images of enargite concentrate after 1 day of leaching in the presence of AC (a) powder (b) cross section

The SEM and EDS analysis of the cross section of an AF 5 bead after two days of leaching is presented in Figure 5-14(a) and Figure 5-14(b), respectively. The EDS map of Figure 5-14(b) shows that the elemental sulfur formed during the leach reaction is adsorbed and has diffused into the AF 5 bead. This phenomenon was not observed with AC.

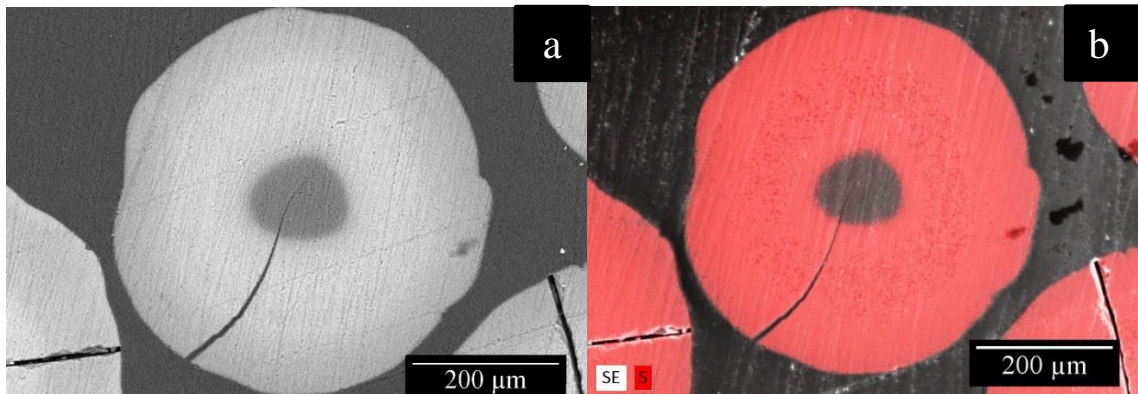


Figure 5-14. SEM and EDS analysis on an AF 5 bead cross section after two days of leaching (a) Back scatter image (b) EDS map for sulfur

5.3 Conclusions

This study has focused on the chloride leaching of enargite with and without a catalyst in the presence of ferric and cuprous ions. Both catalysts enhanced the process rate effectively. The copper recovery increased from 69% in the experiment without a catalyst to 92% and 96% in the presence of AC and AF 5 respectively. The difference in the catalytic effect of these two catalysts

is due to their different surface properties and surface areas. The ratio of concentrate to catalyst was found to be an effective parameter and the best results were achieved with the ratio higher than 1:2 for AC and higher than 1:1 for AF 5.

The higher ferric concentrations increase the copper recovery in the presence of a catalyst. Copper recovery of 94 to 96% was achieved with the addition of 0 to 10 g/L ferric ion concentration. As expected, the copper dissolution rate was found to be dependent on the temperature. Similarly, increasing the temperature significantly influenced the copper recovery regardless of any catalyst present. However, the addition of sulfate ions and acid did not change the copper recovery with or without a catalyst. Moreover, the addition of 5 g/L of cupric ions expedited the reaction rate and increased the copper recovery from 88% to 96%. The best copper recovery results were achieved in the experiments with 5 to 10 g/L cupric addition. An increase in the pulp density from 5 to 20% amplified the copper dissolution from 90 to 99%.

Chapter 6

The kinetics of enargite dissolution in chloride media in the presence of AC and AF 5 catalysts

6.1 Introduction

Most of the reported results on enargite concentrate leaching kinetics in the literature are in catalyst free media. Padilla et al. (2005) studied the process of enargite leaching in $\text{H}_2\text{SO}_4\text{-NaCl-O}_2$ media and achieved 7% arsenic dissolution in 7 h of leaching at 100 °C. The leach lixiviant in their study contained 0.25 M sulfuric acid and 1.5 M sodium chloride while the oxygen sparging rate was 0.3 L/min. The shrinking core model was used as the kinetic model and the kinetic controlling step was believed to be surface reaction. Padilla et al. (2005) stated that the elemental sulfur produced during the 7 h leach does not generate a passive layer on the surface of enargite particles. The calculated activation energy from the Arrhenius plot was 55.6 kJ/mol for enargite leaching (Padilla et al., 2005a). In another study, Padilla et al., (2008) performed oxidative pressure leaching of enargite in $\text{H}_2\text{SO}_4\text{-O}_2$ and reported a complete copper recovery. The calculated activation energy of enargite leaching was 69 kJ/mol at the temperature range between 160 °C to 220 °C (Padilla et al., 2008b). Dutrizac and MacDonald (1972) have treated enargite leaching in an aqueous ferric sulfate solution at temperatures ranging between 60 to 95 °C. The reported copper dissolution rate was slow with only 50% of the copper dissolved after seven days of leaching in an experiment with 0.1 M ferric sulfate and 0.1 M sulfuric acid at 80-85 °C. Based on their experiments, enargite dissolution obeys a linear trend in the temperature range of 60 to 95 °C and the activation energy was calculated as 55.64 kJ/mol (Dutrizac and MacDonald, 1972). Herreros et al. (2002) treated enargite in a mixed solution of hypochlorite and hydrochloric acid. It is believed that the generated chlorine from the reagent reaction improves enargite leaching kinetics. The kinetic studies showed that the reaction was controlled by mass transport in the initial stage (< 30 seconds) and the following stage was

controlled by diffusion through the product layer. The apparent activation energies for the first stage and second stage of the reaction were 14.8 kJ/mol and 20.9 kJ/mol, respectively. The shrinking core model was used in this study to investigate the kinetics of the process.

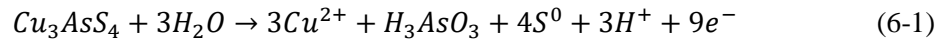
Very limited studies have investigated the effect of carbon-based catalysts on enargite leaching kinetics and efficiency. Dixon and Rivera-vasquez, (2012) presented a new method to treat enargite using AC in ferric sulfate media under atmospheric conditions. Complete copper recovery was achieved at 80 °C, after 20 hours of leaching (Dixon and Rivera-Vasquez, 2012). Kinetic data were not reported in this patent.

This chapter provides important kinetic information for enargite leaching with and without the two catalysts, AC and AF 5. The shrinking core model was used for modeling the process.

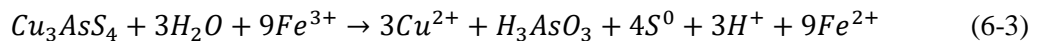
6.2 Results and discussion

6.2.1 Thermodynamic of enargite dissolution

The equation for the oxidative atmospheric leaching of enargite in acidic ferric sulfate solutions can be written as the combination of the following two half-cell reactions represented by Reaction 6-1 and Reaction 6-2.



The standard free energy values for Equation 6-1 and Equation 6-2 at 25 °C are calculated as 445.64 kJ/mol and -667.8 kJ/mol, respectively (Dean, 1999; Henke, 2009; Padilla et al., 2005b; Safarzadeh et al., 2012; Wagman et al., 1982). When these two electrochemical equations are combined, as in Reaction 6-3, the total standard free energy of the reaction will be -222.16 kJ/mol which shows the feasibility of the reaction (Dean, 1999; Henke, 2009; Wagman et al., 1982).



It is believed that in chloride media, Cu^{2+}/Cu^+ couples are the main oxidant of the sulfide minerals rather than Fe^{3+}/Fe^{2+} couples, due to the formation of stronger copper chloride complexes in the

chloride media (McDonald et al., 1984; Winand, 1991). In order to determine the dominant species of the dissolved ions in the leach solutions of the current study the speciation of the complexes within the leaching experiment was quantified with PHREEQC 3.3.7.11094 and OLI Studio 9.5 software. Complexes present in the chloride solution are a function of the activity of the solution, and species which are highly related to acidity, chloride concentration, and other compounds (Lundström et al., 2007). This simulation was performed on the experimental data from an enargite leaching experiment with initial 5 g/L ferric ions, 5 g/L cupric ions, 0.5 M HCl and 1.5 M of total Cl^- ions in the solution at 90 °C in the presence of AF 5. The cupric and cuprous ions are stable in different complexes in chloride solutions. The likely cupric complexes in the chloride leach media are $[\text{CuCl}]^+$, $[\text{CuCl}_2]$, $[\text{Cu}]^{2+}$, $[\text{CuCl}_3]^-$, $[\text{CuCl}_4]^{2-}$, $[\text{CuOH}]^+$, $[\text{Cu}_2(\text{OH})_2]^{2+}$, $[\text{Cu}(\text{OH})_2]$, $[\text{Cu}(\text{OH})_3]^-$, and $[\text{Cu}_2(\text{OH})_4]^{2-}$ and the complexes for cuprous are $[\text{CuCl}_3]^{2-}$, $[\text{CuCl}_2]^-$, and $[\text{Cu}]^+$ (Christov, 2001). Figure 6-1 shows the concentration of the different copper complexes available in the leaching experiment in the presence of AF 5 calculated with (a) Phreeqc software and (b) OLI software. The most dominant cupric species was $[\text{CuCl}]^+$ complex which accounted for 70% of the total cupric ions in the solution. The remaining cupric ions are mostly in the form of $[\text{CuCl}_2]$ and $[\text{Cu}]^{2+}$. The cupric complexes speciation results obtained from the two softwares were both in an acceptable range with only a slight difference between the findings. The cuprous speciation was only calculated by Phreeqc software, particularly because the $[\text{CuCl}_3]^{2-}$ species was not available in the OLI software species database. The Phreeqc software determined that the $[\text{CuCl}_3]^{2-}$ complex is the most abundant cuprous complex (more than 93%), and the rest of the cuprous ions are in the form of $[\text{CuCl}_2]^-$. The copper speciation results calculated by the software are presented in Figure 6-1.

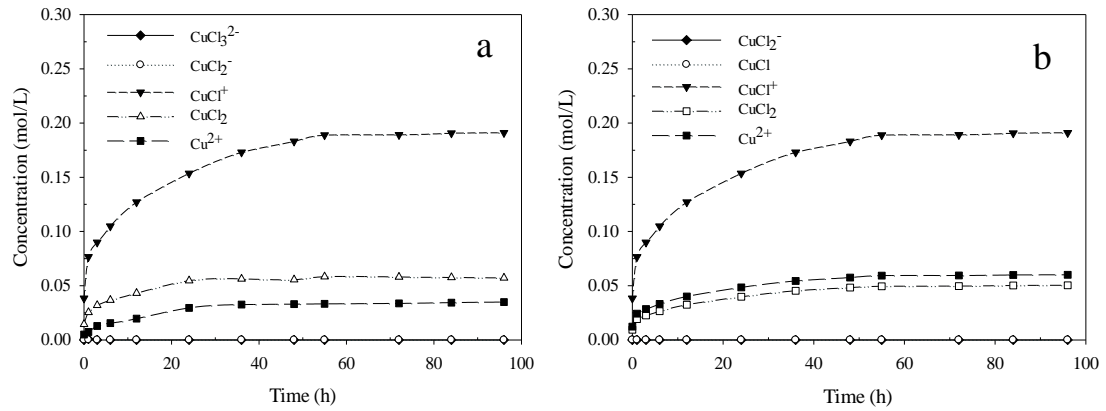


Figure 6-1. Speciation of copper complexes during leaching experiment in the presence of AF 5 with 5 g/L initial ferric ions and 5 g/L initial cupric ions at 90 °C, (a) Simulated by Phreeqc software, (b) Simulated by OLI software

A similar simulation process was performed to calculate the speciation of iron species in the chloride leach solution. Various ferric complexes of $[\text{Fe}^{+2}]$, $[\text{FeCl}^+]$, $[\text{FeOH}^+]$, $[\text{Fe}(\text{OH})_2]$, and $[\text{Fe}(\text{OH})_3^-]$ and ferrous complexes of $[\text{FeCl}^{+2}]$, $[\text{FeCl}_2^+]$, $[\text{Fe}^{+3}]$, $[\text{FeOH}^{+2}]$, $[\text{FeCl}_3]$, $[\text{Fe}_2(\text{OH})_2^+]$, $[\text{Fe}(\text{OH})_3]$, $[\text{Fe}_3(\text{OH})_4^-]$, and $[\text{Fe}(\text{OH})_4^-]$ were considered in the calculations. The simulation results of the two softwares are shown in Figure 6-2. Based on the simulations, most of the ferrous ions are in the form of free ferrous (more than 80%). The OLI software suggested that free ferric ions are the dominant ferric species, however $[\text{FeCl}^{2+}]$ was identified as the most abundant ferric ion species by Phreeqc. The increase in the overall iron content is due to the dissolution of pyrite and the decrease at the 36th hour is related to the co-precipitation of ferric and arsenic species.

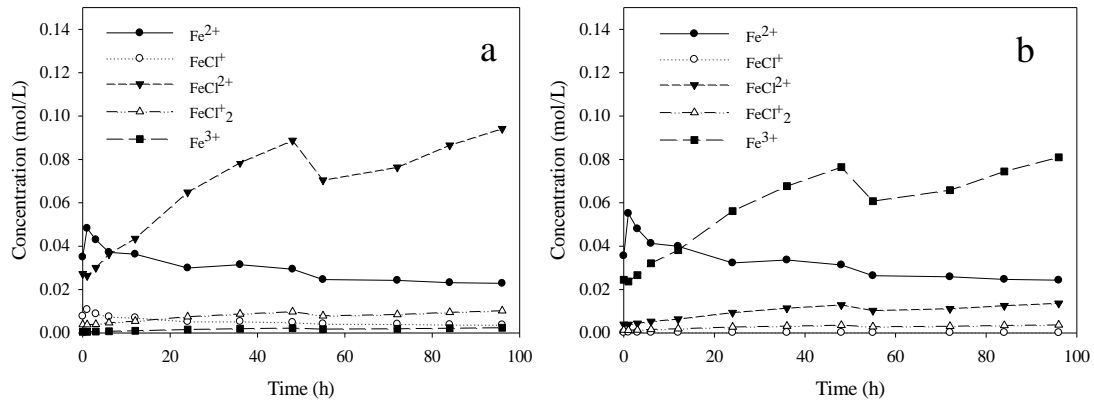
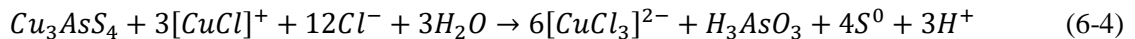


Figure 6-2. Speciation of iron complexes during leaching experiment in the presence of AF 5 with 5 g/L initial ferric ions and 5 g/L initial cupric ions at 90 °C, (a) Simulated by Phreeqc software, (b) Simulated by OLI software

Thus, in an oxidative acidic chloride media, a general enargite dissolution reaction can be suggested by Equation (6-4). Based on the simulation of the leaching solution with Phreeqc software, the CuCl^+ and CuCl_3^{2-} are expected to be the two dominant species of Cu^{2+} and Cu^+ , respectively. The similar reaction was suggested for chalcopyrite dissolution in chloride solutions by Wilson and Fisher (Wilson and Fisher, 1981).



The standard free energy value for this reaction is calculated as -226.7 kJ/mol, which shows that Equation 6-4 is a spontaneous reaction (Dean, 1999; Henke, 2009; Wagman et al., 1982).

6.2.2 Leaching kinetic model

Kinetic studies can fill the gap between the leaching experiments and fundamentals, potentially leading the way to understanding the reason behind the slow leaching rates of the refractory sulfide minerals. In this part, the comparison between the kinetic models of the enargite leaching processes, with and without the catalysts, are presented to reveal the enargite leaching process mechanism. A Shrinking Core Model (SCM) was selected as the model for this study, particularly because of a good compatibility with the solid-liquid reactions including leaching processes (Gbor and Jia, 2004; Safari et al., 2009). The SCM assumes that a leaching process consists of three mechanisms. The

leaching process will be either liquid film diffusion controlled, solid product diffusion controlled, or reaction controlled depending on which mechanism is rate determining (Levenspiel, 1999). The simplified equation for the liquid film diffusion control mechanism is written in Equation 6-5.

$$k_F \cdot t = X \quad (6-5)$$

Where k_F is the kinetic parameter for liquid film diffusion control, X represents the fraction of the reacted particle, and t is time in minutes (Levenspiel, 1999).

The oxidation of sulfide minerals will often generate a solid elemental sulfur product layer or other passivating layers, such as metal-deficient passive films on the surface of the mineral particle (Córdoba et al., 2008b, 2008c; Dutrizac, 1989; Ghahremaninezhad et al., 2012). In such instances, the progress of the leaching process can be controlled by the diffusion through the solid product layer. The equation for such process is (Levenspiel, 1999):

$$k_D \cdot t = 1 - 3(1 - X)^{\frac{2}{3}} + 2(1 - X) \quad (6-6)$$

where:

$$k_D = \frac{6bD_{Cu^{2+}}[Cu^{2+}]}{\rho_{Cu_3AsS_4} \cdot r_0^2} \quad (6-7)$$

k_D is the kinetic parameter for product layer diffusion control, and b is the stoichiometric coefficient which is equal to 3 in this case, based on the suggested reaction. $\rho_{Cu_3AsS_4}$ is the molar density of enargite and r_0 is the particle radius (m). Lastly, the leaching rate of sulfide minerals can also be controlled by the chemical reactions. The rate equation for chemical reaction control can be written as Equation 6-8 (Levenspiel, 1999).

$$k_R \cdot t = 1 - (1 - X)^{\frac{1}{3}} \quad (6-8)$$

where

$$k_R = \frac{bk_s[Cu^{2+}]^n}{\rho_{Cu_3AsS_4} \cdot r_0} \quad (6-9)$$

k_R is the kinetic parameter for reaction control, k_s is the chemical reaction rate constant and n is the order reaction for Cu^{2+} ions.

6.2.3 High pulp density leaching

The kinetics study of enargite leaching was performed in three sets without a catalyst, with AC, and with AF 5. These experiments were performed with high pulp density in order to have a close to reality situation.

6.2.3.1 Enargite leaching without a catalyst

Leaching experiments were conducted at 60, 70, 80 and 90 °C to study the leaching rate of copper in chloride media. The effect of temperature on the copper recovery, in tests without the application of catalysts, is shown in Figure 6-3a. After the leaching experiments, the experimental data was analyzed and fit to the different shrinking core kinetic model. The leaching process, as shown in Figure 6-3a, is slow at lower temperatures and the rate increases with increasing temperature. Leaching experiments at 60 and 70 °C showed about 30% and 32% copper recovery after 96 h. The copper recoveries at 60 and 70 °C are very close, within 2%, and the leaching rate plateaus after 5 h of leaching. By increasing the temperature to 80 °C and then to 90 °C, the copper recovery was increased to approximately 50% and 70%, respectively.

The R squared values found after applying the diffusion through the liquid film model, Table 7-1, range between 0.32 and 0.38 for the various temperatures, presenting a poor correlation between the model and the experimental data. Fitted lines of diffusion through the product layer controlling mechanism, Figure 6-3b, showed very good compatibility to the linear equation at higher temperature leaching experiments of 80 °C and 90 °C with R squared values of 0.90 and 0.98, respectively. However, at 60 and 70 °C, R squared values are lower at 0.77 and 0.74, respectively. Diffusion through a solid product layer is one of the conventional kinetic controlling mechanisms for leaching sulfide minerals, which often is connected to the formation of an elemental sulfur layer and/or a metal deficient sulfide layer on the surface of a partially leached mineral particle (Córdoba et al., 2008b; Dutrizac, 1989; Ghahremaninezhad et al., 2012). Finally, the linear correlation, represented by the R-square values, of the kinetic data modeled by the reaction control mechanism

as shown in Table 6-1 is being poor, 0.66 at 90 °C, suggesting that this mechanism is not a good fit for the process.

The comparison of the R^2 values for the different temperature conditions confirms that the diffusion through the solid product layer is the kinetic controlling mechanism and the slowest step during the enargite leaching process under the conditions of the present study.

6.2.3.2 Enargite leaching with AC

The effect of temperature on enargite leaching efficiency at 60, 65, 70, 75, 80, 85 and 90 °C, and in the presence of AC, is shown in Figure 6-3c. It can be seen that the temperature has a drastic effect on enargite leaching rate and efficiency. The initial copper recovery, during the first 30 h of leaching, is steep and approximately 70% of copper is leached during this time. After 30 h of leaching, the copper recovery decreases and finally reaches 92% at the end of the 90 °C experiment. Final recovery and reaction rate is highly dependent on temperature. The temperature dependency of the leaching process can be seen from the copper recovery data, as changing the temperature from 90 °C to 85 °C results in a decrease of copper recovery from 92% to 86%. The comparison of Figure 6-3a and 6-3c is a good indicator of the effectiveness of AC as a copper leaching catalyst. The kinetics of the leaching process in the presence of AC are determined using the same procedure used for leaching without a catalyst. In the diffusion through the product layer, values of R square are very low for higher temperatures and they are closer to one at lower temperatures. AC is a very effective leaching catalyst, whilst the diffusion through the product layer appears to be the controlling step of the process, still. This has been confirmed by the good modeling fit of Figure 6-3d. R square values for different temperatures are very close to one and the model is in good agreement with the experimental data.

6.2.3.3 Enargite leaching with AF 5

In order to see the effect of AF 5 catalyst on enargite leaching with chloride media, another set of experiments was conducted using AF 5 as a catalyst. AF 5 assisted leaching experiments were

carried out at 60, 65, 70, 75, 80, 85, and 90 °C in order to generate detailed plots and better understand the kinetics of the enargite leaching process. Copper recovery results of the leaching experiments in the presence of AF 5 are illustrated in Figure 6-3e. Based on the results presented in Figure 6-3e, the copper dissolution rate increases in the presence of AF 5 and the higher leaching efficiencies were achieved, in comparison to the leaching tests without a catalyst or with the use of AC. At 90 °C, copper recovery reaches a maximum after approximately 60 h of leaching and remains steady through to the end of the experiment (96 h), with overall copper recovery of 96%. At lower temperatures, such as 85 °C, copper leaching efficiency decreased to only 91%. The copper recovery drops to only 41% at 60 °C, which shows the significance of temperature as a leach parameter.

After collecting the experimental data (presented in Table 6-1) for the AF 5 assisted leaching tests, kinetic calculations and model fittings were conducted. Assuming that the diffusion through product layer is the controlling step, the R square values were calculated. Each value is close to 1 for all the temperatures tested, which confirms that the model is a good representation of the leaching process. The R square values for the kinetic models are presented in Figure 6-3f. From the chemical analysis of the leaching residues and AF 5 it was confirmed that most of the generated elemental sulfur in the tests with AF 5 are accumulated on the AF 5 beads, and negligible elemental sulfur is left in the residue.

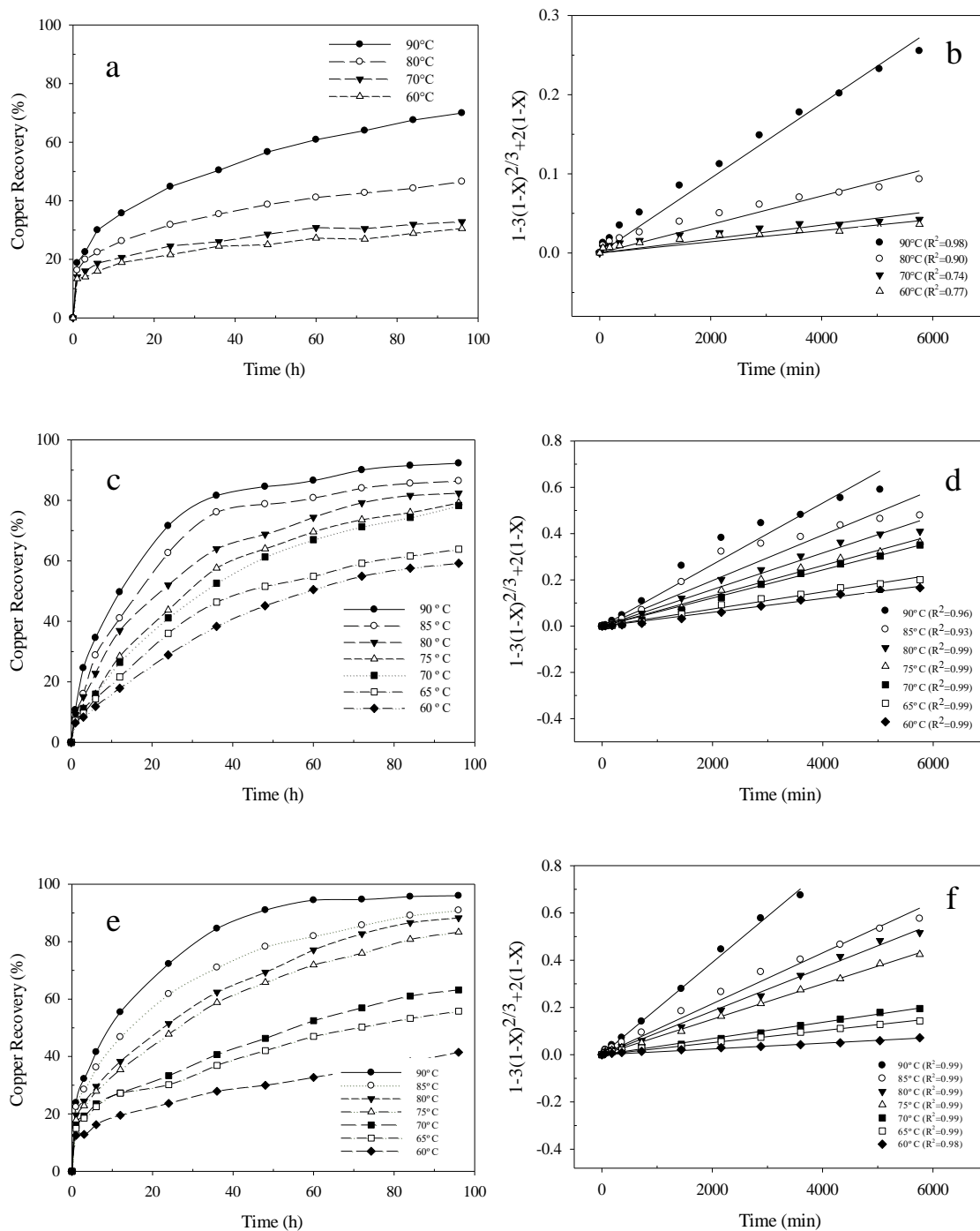


Figure 6-3. The effect of temperature on the copper recovery during the enargite leaching processes (a) without a catalyst, (b) plot of SCM for product layer diffusion control process without catalyst, (c) with AC catalyst, (d) plot of SCM for product layer diffusion control process with AC catalyst, (e) with AF 5, and (f) plot of SCM for product layer diffusion control process with AF 5 catalyst.

Table 6-1. R square values and slope of the fitted lines of different controlling mechanisms in SCM

T (°C)		Without catalyst			With AC			With AF 5		
		Liquid film	Product layer	Reaction control	Liquid film	Product layer	Reaction control	Liquid film	Product layer	Reaction control
90	Slope (x10 ⁻⁵)	21.2	4.7	6.8	20	10	10	30	20	20
	R ²	0.38	0.98	0.66	0.45	0.99	0.78	0.49	0.99	0.88
85	Slope (x10 ⁻⁵)				20	9.8	10	20	10	10
	R ²				0.57	0.99	0.79	0.4	0.99	0.81
80	Slope (x10 ⁻⁵)	12.2	1.8	4.0	20	7.9	9.2	20	9.2	10
	R ²	0.34	0.92	0.27	0.68	0.99	0.87	0.61	0.99	0.89
75	Slope (x10 ⁻⁵)				20	6.5	8.2	20	7.5	8.9
	R ²				0.79	0.99	0.91	0.62	0.99	0.87
70	Slope (x10 ⁻⁵)	7.4	0.9	2.7	20	6.1	7.8	10	3.4	5.6
	R ²	0.35	0.74	0.16	0.82	0.99	0.93	0.59	0.99	0.78
65	Slope (x10 ⁻⁵)				10	3.7	5.9	10	2.5	4.8
	R ²				0.79	0.99	0.88	0.48	0.99	0.82
60	Slope (x10 ⁻⁵)	6.7	0.7	2.48	10	3.0	5.2	8.54	1.2	3.2
	R ²	0.32	0.77	0.15	0.86	0.99	0.92	0.42	0.99	0.57

6.2.4 Low pulp density leach tests

Similar leaching experiments were performed with 10 g enargite concentrate at four different temperatures of 60, 70, 80, and 90 °C without catalyst, with AC, and with AF 5. The leaching results are shown in Figure 6-4. Similar to the copper behavior, the arsenic dissolution rate was increased at elevated temperatures. The arsenic recovery increased from 3.9% after 4 h of leaching without catalyst at 60 °C to 10.7% at 90 °C. This increase was even more significant when a catalyst was used. By increasing the temperature from 60 to 90 °C the arsenic dissolution rate improved from 4.2 % to 12.2 % in the presence of AC and from 4.7 to 13.4 % in the presence of AF 5. Comparing the catalysts, AF 5 appeared more effective than AC for copper dissolution. After applying the kinetic models on the experimental data at different temperatures the diffusion, through the product layer was found to be the main kinetics controlling mechanism in enargite leaching, as it resulted in R^2 values close to 1.

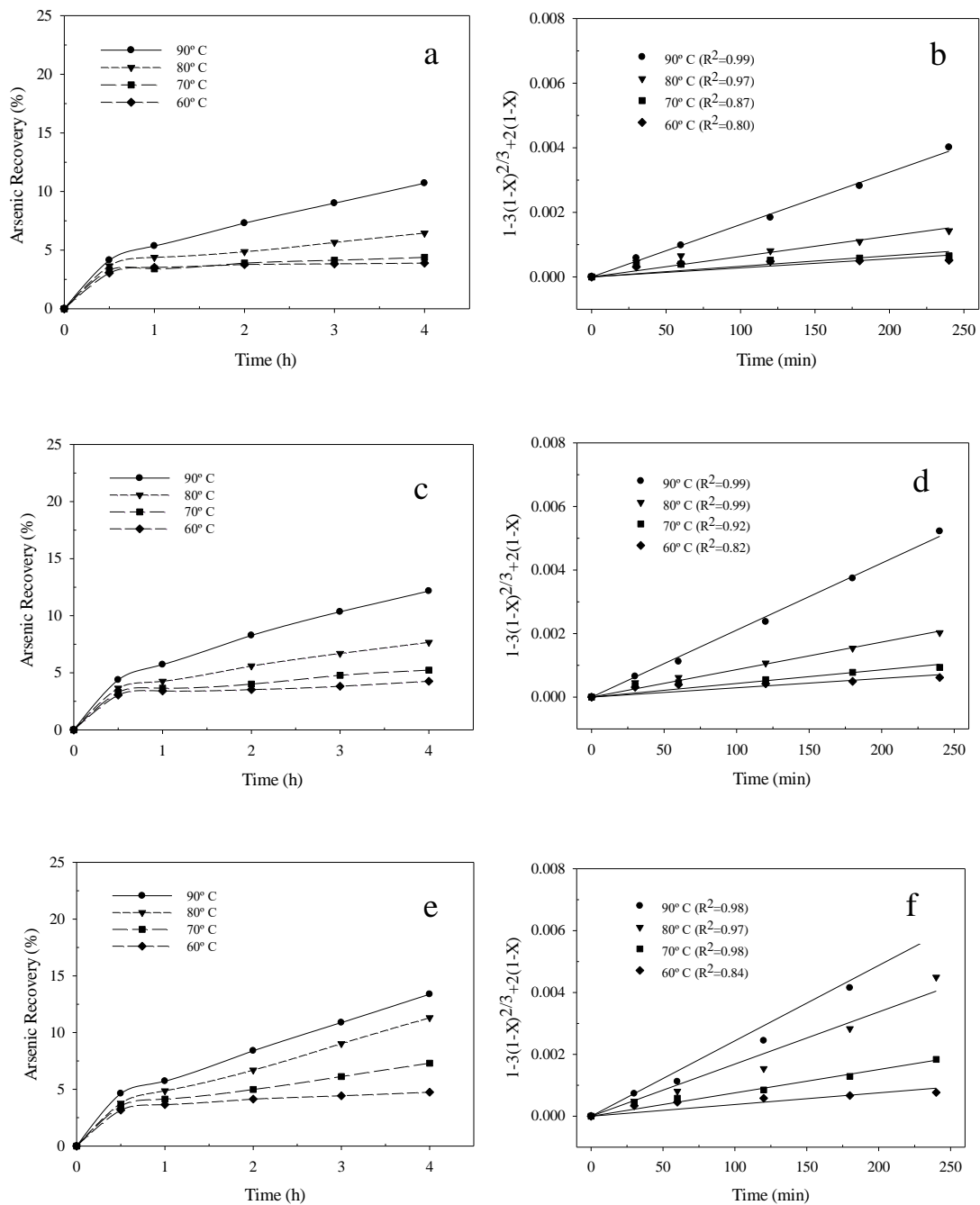


Figure 6-4. The effect of temperature on the arsenic recovery during the enargite leaching process (10 g enargite concentrate, 5 g/L initial cupric and 5 g/L initial ferric) (a) without a catalyst, (b) plot of SCM for product layer diffusion control process without catalyst, (c) with AC catalyst, (d) plot of SCM for product layer diffusion control process with AC catalyst, (e) with AF 5, and (f) plot of SCM for product layer diffusion control process with AF 5 catalyst

6.2.4.1 Effect of particle size

In order to examine the chosen kinetics model and study the effect of enargite particle size on leaching rate, low pulp density leaching experiments were performed in the presence of AF 5 at 90 °C with 5 g/L initial cupric and ferric ions with concentrate particle sizes in three ranges of 53-75 µm, 44-53 µm and 37-44 µm. As shown in Figure 6-5, the arsenic dissolution rate has increased by decreasing the particle size. The arsenic dissolution rate increased from 11.8% to 13% after 4 h when the particle size decreased from 53-75 to 37-44 µm, respectively.

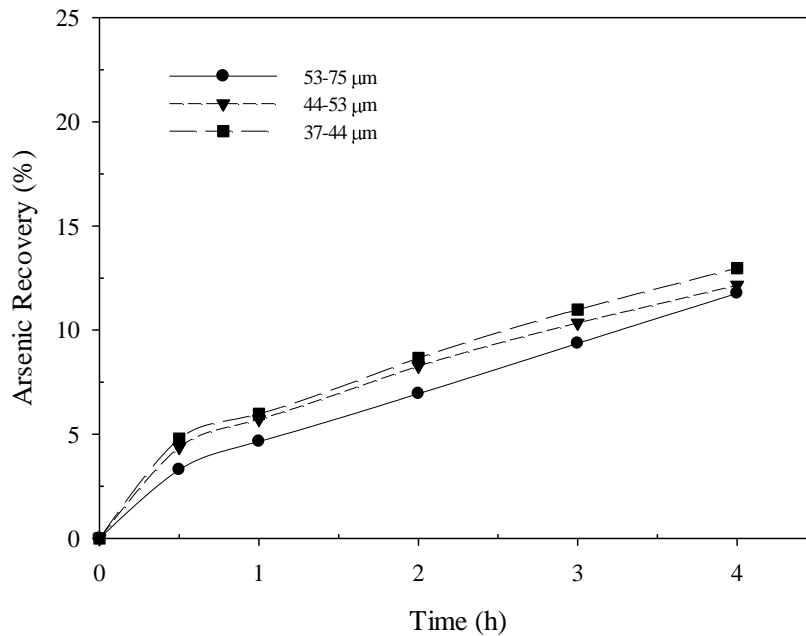


Figure 6-5. Effect of particle size on arsenic recovery in the presence of AF 5

The model constant for diffusion through the product layer, or K_D in the SCM model, is a function of the particle size of the concentrate, $1/r_0^2$ (r_0 is the initial particles radius), and the model constant for the reaction control, or K_R , is dependent on $1/r_0$ (Levenspiel, 1999; Souza et al., 2007). The dependency of the rate constants to the particle size, or K_R versus $1/r_0$ and K_D versus $1/r_0^2$ is shown in Figure 6-6, which displays the linear relationship of K_D versus $1/r_0^2$, with R^2 of 0.99. This confirms that the dominant kinetics model is indeed the diffusion through the product layer.

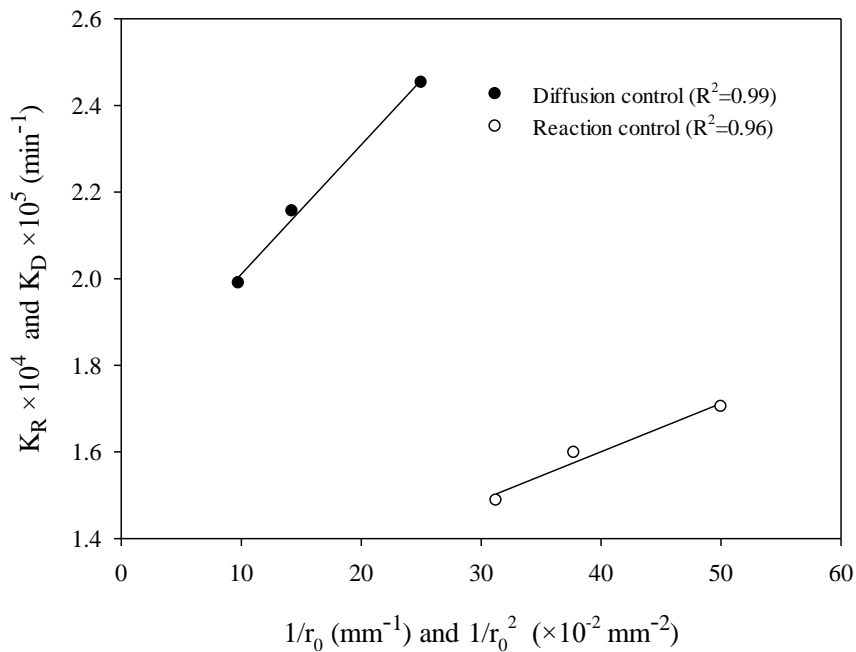


Figure 6-6. Plot of K_R versus $1/r_0$ and K_D versus $1/r_0^2$ (10 g concentrate, 1:1 concentrate to AF 5 ratio, 5 g/L initial cupric ions, 5 g/L initial ferric ions at 90 °C)

6.2.4.2 Effect of initial cupric and ferric ions

In order to study the reaction pathway and the effect of oxidant, three initial concentration levels of 0, 5 and 10 g/L for cupric and ferric ions were examined and compared to the arsenic recovery. All the experiments were performed in the presence of AF 5 at 90 °C. In these experiments, the changes in the cupric and ferric ion concentrations were minimal based on the experiment conditions. The effect of cupric ion concentration is depicted in Figure 6-7 and the effect of ferric ion concentration is shown in Figure 6-8. The increase in the cupric concentration has a profound effect on the enargite dissolution rate. By increasing the initial cupric ion concentration from 0 to 10 g/L, the arsenic recovery increased from 10.1 to 13.4% after 4 h of leaching. On the contrary, by increasing the initial ferric ion concentration the dissolution rate did not experience a significant change. The effectiveness of cupric ions confirms again that the enargite dissolution happens based

on the reaction of Equation 6-4 and ferric ions do not have a significant effect on the mechanism of the reaction.

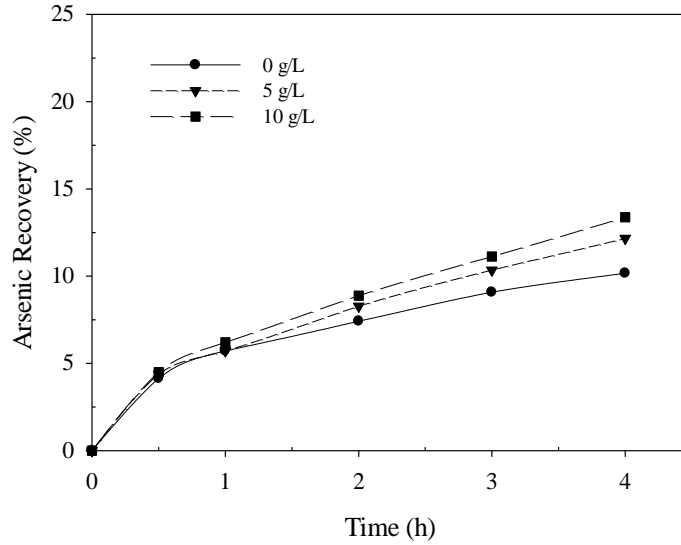


Figure 6-7. Effect of initial cupric concentration on arsenic recovery (10 g concentrate, 1:1 concentrate to AF 5, 5 g/L initial ferric ions at 90 °C)

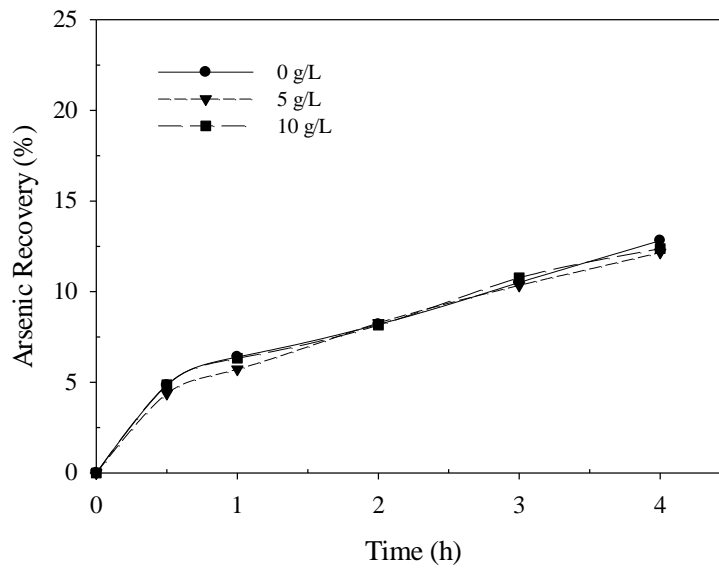


Figure 6-8. Effect of initial ferric concentration on arsenic recovery (10 g concentrate, 1:1 concentrate to AF 5, 5 g/L initial cupric ions at 90 °C)

6.2.5 Chronoamperometry experiments

The leach mechanism study of the previous section showed that the enargite leaching process is controlled by the diffusion of the species through a solid film on the surface of partially leached enargite particles. Rivera-Vasquez and Dixon (2015) have previously shown the formation of an elemental sulfur layer on the partially leached minerals' surfaces. The sulfur layer formed during the catalytic leaching of enargite was shown to have a highly porous morphology (Rivera-Vasquez and Dixon, 2015). The porous morphology of the elemental sulfur is not considered a barrier for the diffusion of the liquid phase, meaning that the porous sulfur layer cannot be a passivating film. The chronoamperometry tests were conducted to better understand the nature of the passive film on the surface of the partially leached enargite particles. In chronoamperometry experiments, the potential of the working electrode was varied from a level that no Faradaic reaction occurs to a higher potential level (Wang, 2006). Then, the diffusion process on the surface of the enargite minerals were studied by monitoring the current versus time (Figure 6-9). Assuming that a passivating layer covers the surface of the mineral at anodic potentials, the mass transfer process should then occur via diffusion through the surface layer at a fixed potential. The current density of the enargite electrode was monitored to determine the passivation process of the electrode. In this set of experiments, an enargite carbon paste electrode was used as the working electrode in a chloride solution. The first set of experiments was performed at 80 °C to investigate the effect of different potentials on the passive layer at a higher temperature and a second set was carried out at 60 °C to study the passive layer at a lower temperature. The chronoamperometry tests were carried out at 80 °C and at potentials 400, 450, 500 and 550 mV which is shown in Figure 6-9. The passivation of the surface starts immediately after the experiments began, and near-complete passivation of the surfaces was achieved in less than 100 s in all experiments. The registered steady state current densities for different potentials of Figure 6-9 are very close to zero, representing a complete passivation of the electrode surfaces. The current versus time plots of Figure 6-9 in fact relates to the gradient of the diffused species from the surface of the working electrode (Wang,

2006). Along with the application of the potential to the electrode, copper and arsenic on the surface of the electrode leach into the solution, however, a passivating film, likely a metal deficient surface layer, covers the partially-leached mineral surfaces. The gradual increase in the product layer thickness reduces the current density as shown in Figure 6-9. This process is referred to as “passivation”. The formation of a metal-deficient passivating layer has been studied in detail by Ghahremaninezhad et al. (Ghahremaninezhad et al., 2012). It has been shown that a thin passive film on the surface of chalcopyrite has a very low ionic conductivity, which impedes the mass transfer rate. The calculated thickness of the passive film for chalcopyrite is 1- 1.5 nm and other researchers have calculated it to be in the range of 2-3 nm (Biegler, 1977; Biegler and Horne, 1985; Ghahremaninezhad et al., 2012).

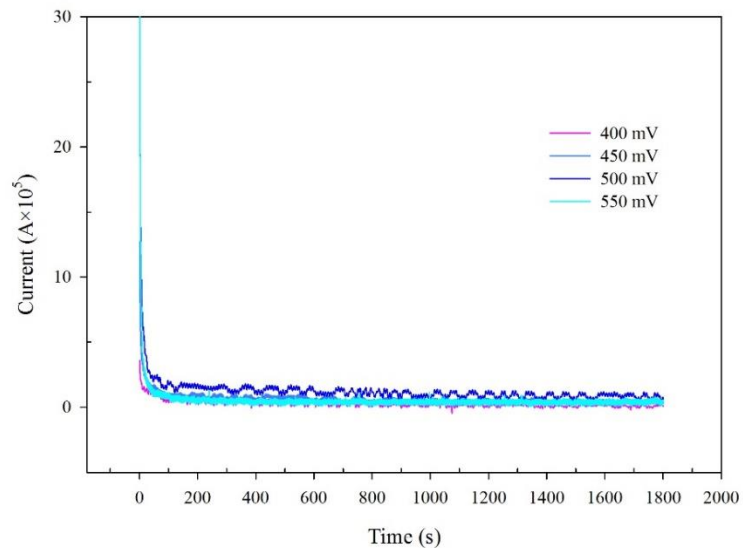


Figure 6-9. Chronoamperometric test at 80 °C: Current vs. time plot at different potentials

Another chronoamperometry set of tests was performed at 60 °C and plotted in Figure 6-10. This set of tests shows similar results to the 80 °C tests and that passivation is also occurring at a lower temperature. The current density reaches a steady state in less than 100 seconds and values are very close to zero again. This validates the concept that diffusion through the product layer is the main controlling mechanism for the leaching of enargite with and without different catalysts. The passive

film which forms on the partially leached mineral is a diffusion barrier, and controls the diffusion of oxidized copper species from the boundary of mineral-passive film into the boundary of passive film-solution. The mechanism observed via the electrochemical experiments agrees well with those of the leaching kinetic modeling, as both methods show that solid-state diffusion is controlling the leaching process of enargite. The leaching kinetic study also confirmed that the diffusion of Cu^{2+} ion through the passive film is the controlling step.

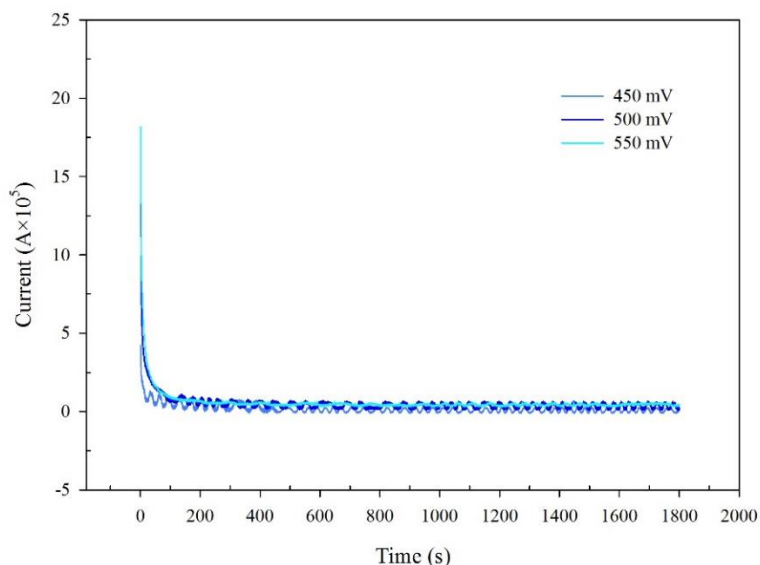


Figure 6-10. Chronoamperometric test at 60 °C: Current vs. time plot at different potentials

6.2.6 SEM analysis

In order to achieve a better understanding of the morphology of the product layer or the passive layer, SEM with EDS analysis was performed on the post-leaching residues and the catalyst surfaces. SEM analysis was performed on a solid sample of residue after one day of leaching as shown in Figure 6-11. Enargite, pyrite, and elemental sulfur particles were determined by EDS analysis and were marked in the picture. As shown in Figure 6-11, enargite particles do not have an apparent coating on their surfaces. EDS analysis also confirmed that there was no elemental sulfur layer generated on the surfaces of the leached enargite particles as a passivating layer. EDS

analysis further identified small sulfur particles being generated and present as separate particles in the leach residue.

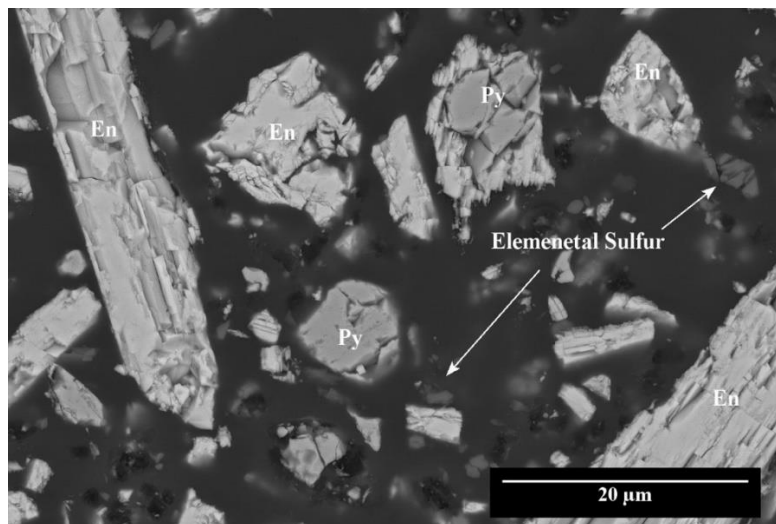


Figure 6-11. SEM cross section of leaching residue after 1 day of leaching.

Cross sections of a fresh and a post-leaching AC are shown in Figure 6-12. Figure 6-12 (a) shows the porous surface of the AC with high surface area making AC a very good catalyst. As it is illustrated in Figure 6-12 (a), fresh AC shows no trace of elemental sulfur in the SEM micrograph nor was elemental sulfur detected in EDS analysis. Figure 6-12 (b) presents Figure 6-12 (a) with a higher magnification. An image of a post-leaching AC is shown in Figure 6-12 (c). In this picture, AC is similar to that shown in Figure 6-12 (a), however small sulfur particles can be observed in its pores. Figure 6-12 (d) presents Figure 6-12 (c) with a higher magnification, showing fine particles of elemental sulfur formed in the pores of AC.

Cross sections of a fresh and a post-leaching AF 5 are presented in Figure 6-13. Figure 6-13 (a) shows the surface of fresh AF 5. Unlike the AC, no porosity can be seen on the AF 5 surface, which is due to the small size of AF 5 porosities. The AF 5 porosities are about 8 nm in diameter. Figure 6-13 (b) presents Figure 6-13 (a) with a higher magnification. As it is illustrated in Figure 6-13 (b), fresh AF 5 has a very smooth surface and no elemental sulfur can be detected on the surface with EDS analysis.

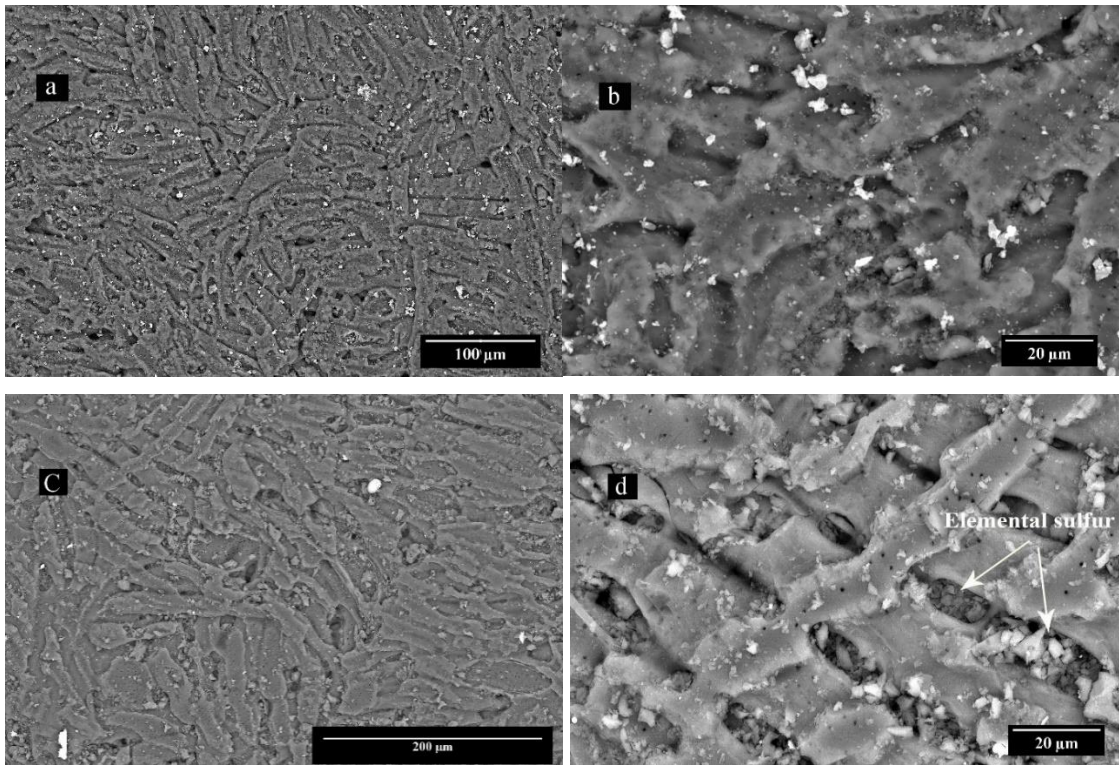


Figure 6-12. (a) SEM cross section of fresh AC (b) SEM cross section of fresh AC in higher magnification, (c) SEM cross section of utilized AC, (d) SEM cross section of utilized AC in higher magnification

A micrograph of a post-leaching AF 5 sample is shown in Figure 6-13 (c). The surface of the used AF 5 appears slightly rougher than that of fresh AF 5, due to the sulfur accumulation. As it is illustrated in Figure 6-13 (d) in higher magnification, growth and adsorption of sulfur is clearly visible. The sulfur adsorption has changed the morphology of the AF 5 surface. In addition, sulfur particle morphology on AF 5 is different than that on AC surfaces of Figure 6-12 (d). Sulfur analysis also proved that most of the generated elemental sulfur in the leach tests with AF 5 is collected on the surface of AF 5 and not in the residue.

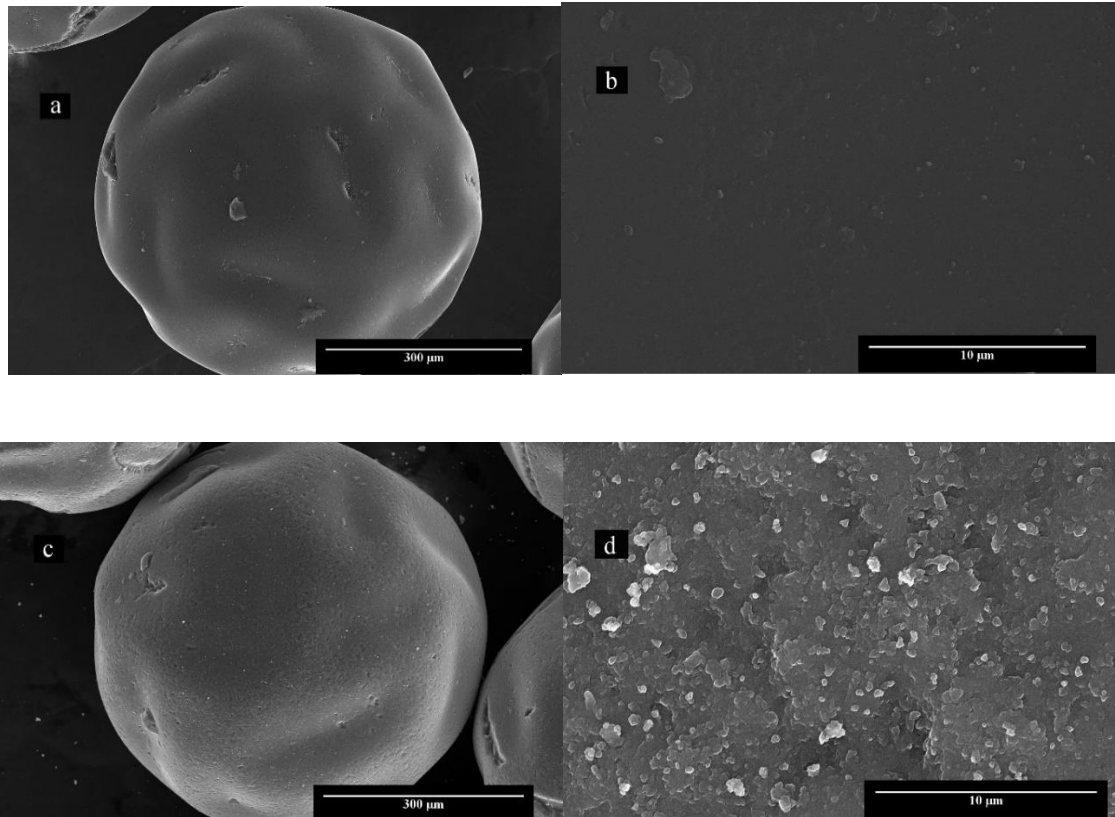


Figure 6-13. (a) SEM cross section of fresh AF 5 (b) SEM cross section of fresh AF 5 in higher magnification, (c) SEM cross section of utilized AF 5, (d) SEM cross section of utilized AF 5 in higher magnification

The SEM micrograph of a leach residue after leaching with AC is shown in Figure 6-14. In this image the elemental sulfur particles are visible on the surface of the enargite and pyrite particles. From the SEM and EDS study it appears that the elemental sulfur does not necessarily form a layer around the partially leached mineral particles, which agrees with the observations of Lundström (Lundström, 2009).

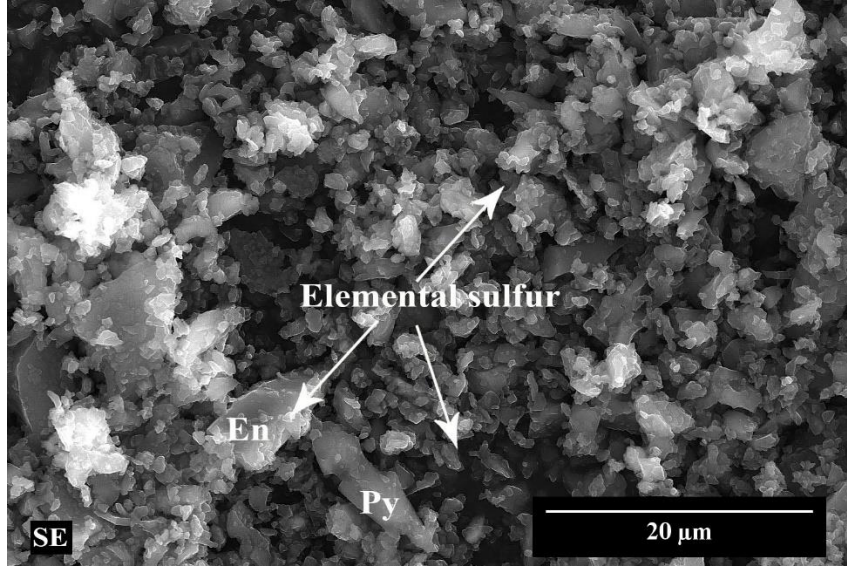


Figure 6-14. SEM micrograph of leach residue after 1 day of leaching

6.2.7 Effect of diffusivities

As shown in the leaching experiments, temperature is an important parameter in controlling the leaching kinetics of enargite. Assuming that the nature of passive film on the mineral surface is a metal deficient film, and the leaching is controlled via the diffusion of Cu^{2+} through this film, then increasing the leaching temperature increases the cation diffusion rate through the passivating film and, thus, increases the leaching rate. The effect of temperature on the solid state diffusion can be stated by Fick's equation which is shown in Equation 6-10 (Callister and Rethwisch, 2007).

$$D = D_0 \exp\left(-\frac{Q_d}{RT}\right) \quad (6-10)$$

In this equation D_0 is the temperature independent diffusion coefficient, D is the diffusion coefficient, Q_d is the activation energy for diffusion, R is the gas constant and T is absolute temperature in K. From Fick's equation, the effect of temperature on the diffusion coefficient can be written as Equation 6-11

$$Q_d = -2.3R \left[\frac{\log D_1 - \log D_2}{\frac{1}{T_1} - \frac{1}{T_2}} \right] \quad (6-11)$$

where D_1 and D_2 are diffusion coefficients corresponding to T_1 and T_2 . According to the Herreros et al. study (Herreros et al., 2002), the activation energy of enargite leaching in chloride media under diffusion control is 14.8 kJ/mol. Thus, increasing the leaching temperature from 60 °C to 90 °C would give a D_{90}/D_{60} ratio of 1.56; this value shows that the diffusion through the metal deficient layer can potentially be enhanced by an increase in temperature.

Solid state diffusion occurs within the passivating film. The diffusivity of reagent inside the solid particle is usually much slower than the diffusivity of the same ion in the solution. When a leaching process is controlled by the diffusion through the product layer, then the term k_D in Equation 6-7 relates to the diffusivity of the cations via the passive film. When porosity of the solid particles is being considered, Equation 6-7 can be re-written as Equation 6-12. This model is called the random pore or grain models (Bhatia and Perlmutter, 1981; Georgiou and Papangelakis, 1998).

$$1 - 3(1 - X)^{\frac{2}{3}} + 2(1 - X) = \frac{6bD_{Cu^{2+}}[Cu^{2+}]}{\rho_{Cu_3AsS_4} r_0^2 (1 - \varepsilon)} \quad (6-12)$$

The term ε is the porosity of the solid which is equal to 0.09, $\rho_{Cu_3AsS_4}$ is equal to 0.058 M and b is 3 based on Equation 6-7. The effective diffusivity of the Cu^{2+} in the enargite particles can be calculated from the linear regression of Figure 6-3 b, d and f and Equation 6-12. The calculated effective diffusivities of Cu^{2+} are shown in Table 6-2. The small value of the $D_{Cu^{2+}}$ is related to the fact that the diffusion through a solid phase, i.e. passive film, is a slow process.

Table 6-2. Diffusivities of Cu^{2+} at different temperatures

Temperature (°C)	$D_{Cu^{2+}}$ (cm^2/s)		
	Without Catalyst	With AC	With AF 5
90	2.4×10^{-11}	6.2×10^{-11}	8.2×10^{-11}
80	1.1×10^{-11}	3.8×10^{-11}	5.2×10^{-11}
70	6.14×10^{-12}	2.1×10^{-11}	1.9×10^{-11}

6.3 Conclusions

Leaching of enargite in chloride media was studied with the addition of cupric and ferric ions as the oxidant. Based on the leaching experiments, enargite leaching is a very slow process without the use of a catalyst. Cupric ions were found to be the main oxidant of enargite in the leach process. The largest recovery for a test without AC was approximately 70% after 96 h at 90 °C. The leaching process was greatly enhanced in the presence of AC and AF 5 where 92% and 96% copper recovery respectively was achieved at 90 °C. The SCM presented a very good fit to the experimental leaching data, suggesting that the leaching control mechanism was diffusion through a solid product layer, which is believed to be a metal deficient sulfide layer. Low pulp density experiments were carried out to confirm that the diffusion through the metal deficient layer is the controlling step of the leach process. The effective oxidant is found to be the cupric ions and ferric is a much less effective oxidant in the leaching process. Diffusion of the Cu^{2+} ions through the metal deficient passivating layer is the slowest step through the process of enargite leaching. The diffusivity of Cu^{2+} was shown to increase by the application of catalysts, however the diffusion coefficient of Cu^{2+} remained at approximately $10^{-11} \text{ cm}^2/\text{s}$.

Chapter 7

Oxidative arsenic precipitation as scorodite during carbon catalyzed enargite leaching process

7.1 Introduction

Arsenic (As) is a highly toxic element, and very often occurs within secondary copper sulfide ores. Atmospheric leaching of enargite leads to a low copper recovery and a subsequent process is then required to immobilize arsenic into an environmentally stable residue. Arsenic immobilization as an environmentally stable residue prior to the discarding of waste has been a challenging subject for the metal and mining industry (Riveros and Dutrizac, 2008).

This study proposes a novel in-situ arsenic immobilization process in the form of scorodite precipitates during enargite leaching in a chloride media. In this process, AC and Lewatit® AF 5 were used to oxidize As(III) to As(V). Likewise, the effect of various operational conditions, such as temperature, oxygen rate, and ferric ion dosage on the scorodite precipitation process, were explored.

7.2 Results and discussion

7.2.1 Scorodite crystallization during enargite leaching with AC and AF 5

7.2.1.1 Effect of temperature on the arsenic recovery

The arsenic dissolution rate is often closely related to the copper leaching rate in the hydrometallurgical processing of enargite. Therefore, it is imperative to detail the mechanism of arsenic dissolution in the atmospheric leaching process. The reactions involved in the dissolution of copper and arsenic in a ferric sulfate media are illustrated in Equation 2-2 and Equation 2-3 (Dutrizac and MacDonald, 1972). In contrast to the sulfate media, the cupric ions are the main oxidant, rather than ferric ions, in chloride media and cuprous ions are subsequently formed as the

final enargite oxidation product (7-1) (Jahromi et al., 2017; Miki and Nicol, 2008; Parker et al., 1981). In order to improve the enargite leaching kinetics, both ferric and cupric ions were added to the chloride leach solution.



The effect of temperature on arsenic dissolution rate in the absence of a catalyst within 96 h is shown in Figure 7-1. The dissolution rate of arsenic is identical to that of copper at a temperature range of 60-90 °C. This is in accordance with the findings reported in the literature (Padilla et al., 2005a). As illustrated in Figure 7-1, increasing the temperature up to 90 °C improved the arsenic recovery from 24% to 70%. This implies that temperature has a pronounced effect on the arsenic dissolution in the atmospheric leaching processes.

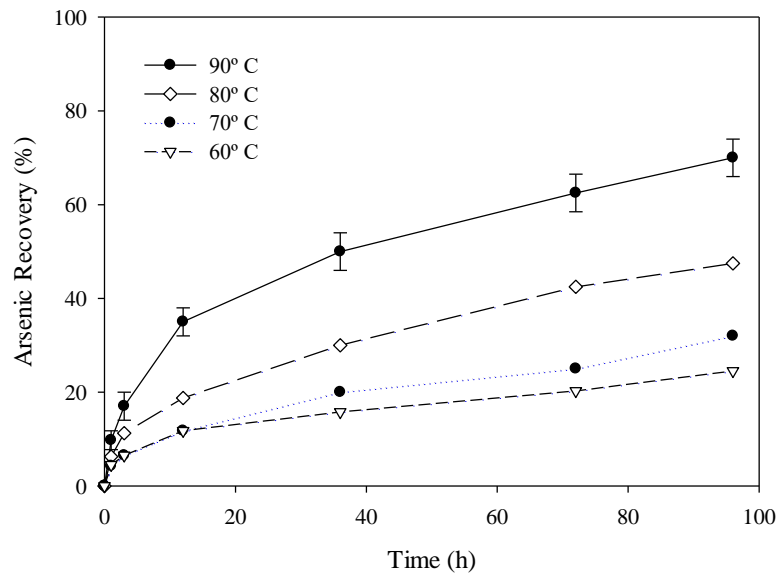


Figure 7-1. Effect of temperature on the arsenic recovery in the absence of catalyst (0.5 M HCl, 5 g/L ferric ions, 5 g/L cupric ions, 1.5 M Cl⁻)

The effect of temperature on the arsenic recovery percentage in the presence of AF 5 was examined at different temperatures (60-90 °C). As shown in Figure 7-2, at the temperature range of 60-70 °C the arsenic dissolution percentage improved with a slight slope within 96 h and the maximum

arsenic recovery was obtained at 70 °C (46%). Additionally, no scorodite precipitate was detected in the chemical analysis of leaching residue, which is assigned to the low arsenic supersaturation at the temperature range of 60-70 °C. Increasing the temperature to 80 °C significantly enhanced the arsenic recovery to nearly 80% within 72 h. However, a further increase in the leaching time drastically decreased the arsenic dissolution percentage attributed to the formation of the scorodite precipitates. At 90 °C, the arsenic leaching rate improved and the onset point, where scorodite precipitation commenced, decreased to 36 h. The results agreed with the findings reported by Le Berre et al. (2008) who illustrated that the lengths of both induction and acceleration periods for arsenic precipitation were highly dependent on the temperature (Le Berre et al., 2008). An increase in the temperature improved the kinetics of enargite leaching and, subsequently, arsenic dissolution. This caused the arsenic concentration to readily reach the critical saturation point (Demopoulos et al., 1995).

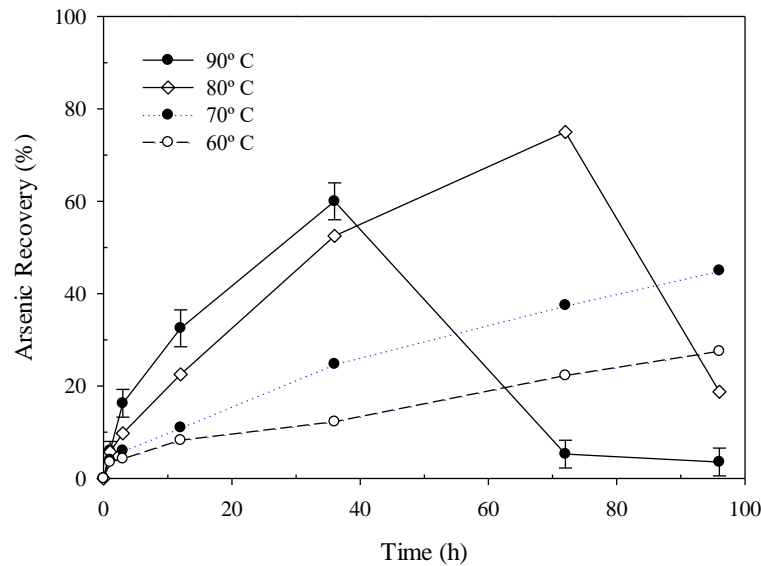


Figure 7-2. Effect of temperature on arsenic recovery in presence of AF5 (0.5 M HCl, 5 g/L ferric ions, 5 g/L cupric ions, 1.5 M Cl⁻, concentrate:AF 5 ratio 1:1, 0.1 L/min oxygen sparging rate)

7.2.1.2 Effect of carbon-based catalysts on the arsenic recovery

It has been shown that the carbon-based catalysts improve copper sulfide leaching kinetics by the regeneration of the leach oxidant (e.g. oxidizing ferrous to ferric ions) and/or by in-situ generation of hydrogen peroxide which in return can oxidize copper sulfides (Ahumada et al., 2002).

A series of enargite leaching experiments were conducted at 90 °C to probe the impact of different concentrate to AC ratios on the arsenic recovery. An increase in the leach time up to 96 h improved the arsenic dissolution percentage to nearly 75% at the concentrate:AC ratio of 2:1 (Figure 7-3). However, a decrease in the concentrate:AC ratio down to 1:4 markedly modified the trend of arsenic recovery. At a concentrate:AC ratio of 1:1, increasing the leaching time improved the arsenic dissolution and the maximum arsenic recovery (85%) was achieved after 72 h. However, an additional increase in the leaching time led to a drastic decrease in the arsenic concentration in the solution. This sudden decrease in As concentration is connected to the formation of scorodite particles, which were observed as a white precipitate in the leach solution, resulting in arsenic immobilization and consequently an abrupt decrease in the arsenic recovery. Likewise, a further decrease in the concentrate:AC ratio to 1:2 lowered the onset point, at which the scorodite precipitation commenced (36 h). At a concentrate:AC ratio of 1:4, no obvious change in the onset point was observed and most of the arsenic ions were fixed in the form of scorodite precipitates after 72 h (1.57% Arsenic recovery). It is evidenced from Figure 7-3 that AC plays a key role in the oxidation of the enargite and subsequently arsenic dissolution, through regeneration of oxidant and in-situ formation of hydrogen peroxide. At a low fraction of AC (concentrate:AC ratio of 2:1), AC only participated in the oxidation of enargite and subsequently generated trivalent arsenic in the leach solution. However, increasing the portion of AC led to the formation of an excess amount of in-situ hydrogen peroxide which oxidized As(III) to As(V) (Equation 7-2) (Radzinski, 2017). Furthermore, the addition of higher AC can increase the availability of nucleation sites. This suits

the condition for the heterogeneous nucleation and growth of the crystalline scorodite precipitates. The required energy for the heterogeneous precipitation on a foreign surface is much lower than the homogenous nucleation (Demopoulos et al., 1995). It is worth noting that the results were contrary to those reported by Rivera-Vasquez and Dixon (2015), as they did not report any scorodite precipitation in the sulfate leach solution in the presence of AC within 48 h (Rivera-Vasquez and Dixon, 2015).

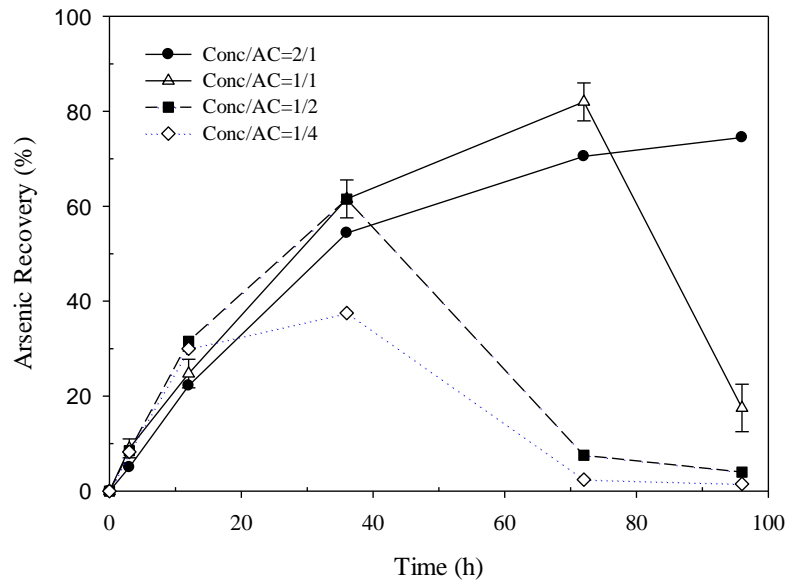
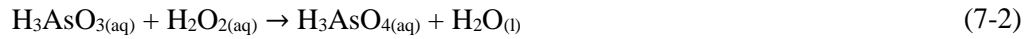


Figure 7-3. Effect of the AC addition on arsenic recovery (90 °C, 0.5 M HCl, 5 g/L ferric ions, 5 g/L cupric ions, 1.5 M Cl⁻, 0.1 L/min oxygen sparging rate)

Several atmospheric leaching experiments were carried out at various concentrate:AF 5 ratios to investigate the arsenic recovery. As presented in Figure 7-4, arsenic recovery at different ratios demonstrated a similar trend to that of AC. Increasing the leaching time elevated the arsenic recovery percentage to 75% at the concentrate:AF 5 ratio of 2:1. Similar to AC, a decrease in the concentrate:AF 5 ratio down to 1:2 caused a sharp decrease in the arsenic dissolution within 36 h, which is attributed to the formation of the scorodite precipitates. AF 5 exhibited a superior

functionality compared to that of AC. At the concentrate to catalyst ratio of 1:1, the onset point decreased to 36 h for AF 5 and scorodite precipitates were readily formed (Figure 7-4). This resulted from the higher surface area of AF 5 ($1154 \text{ m}^2/\text{g}$) compared to that of AC ($921 \text{ m}^2/\text{g}$) (Jahromi et al., 2017), which accelerated the catalytic reactions and consequent generation of in-situ hydrogen peroxide. The other reason for the rapid scorodite precipitation is assigned to the type of functional groups present on the AF 5's surface (Jahromi et al., 2017).

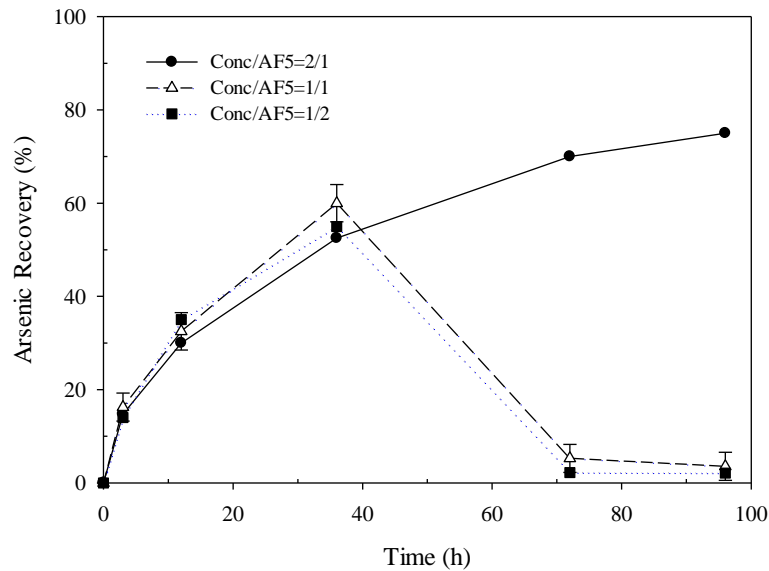


Figure 7-4. Effect of the AF 5 addition on the arsenic recovery from the enargite concentrate (90 °C, 0.5 M HCl, 5 g/L ferric ions, 5 g/L cupric ions, 1.5 M Cl⁻, 0.1 L/min oxygen sparging rate).

7.2.1.3 Effect of ferric ion on the arsenic recovery

Ferric ions have been deemed to be an effective oxidant in the hydrometallurgical process. In addition, they significantly function to immobilize arsenic through the formation of FH and scorodite. Initial ferric ion loading is a substantial parameter controlling both the atmospheric leaching of enargite and scorodite precipitation. The molar ratio of Fe:As in most of the arsenic precipitation methods is maintained above 3 to generate crystalline and more stable arsenic compounds (Krause and Ettel, 1989; Langmuir et al., 2006). This section elucidates the role of

ferric ions in the arsenic dissolution and scorodite formation processes. Ferric ions were added to the chloride media at different concentrations (0-10 g/L) in the presence of AF5 at 90 °C. As indicated in Figure 7-5, in the absence of ferric ions, arsenic recovery increased to 82% over 96 h and no scorodite precipitate was observed in the leach solution. However, increasing ferric ion dosage to 1 g/L and 5 g/L led to a drastic decrease in the dissolved arsenic concentration at 36 h, which is the onset point of scorodite formation. It is worth mentioning that, at the ferric ion dosage of 5 g/L, the molar ratio of Fe:As was 3.9. An additional rise in the ferric loading to 10 g/L chiefly lowered the onset point to 12 h. This is in compliance with the data in the literature that a higher ratio of Fe:As enhances the precipitation kinetics and efficiency in a chloride media due to the formation of weaker iron complexation (Demopoulos, 2009). However, the findings obtained in this section were in conflict with the observations reported by Singhania et al. (2006), where they studied the effect of various Fe:As molar ratios (1.5-3) on the extent of scorodite precipitates in a sulfate media (Singhania et al., 2006). It was concluded that increasing the Fe:As ratio retarded the precipitation process and subsequently reduced the scorodite precipitation yield.

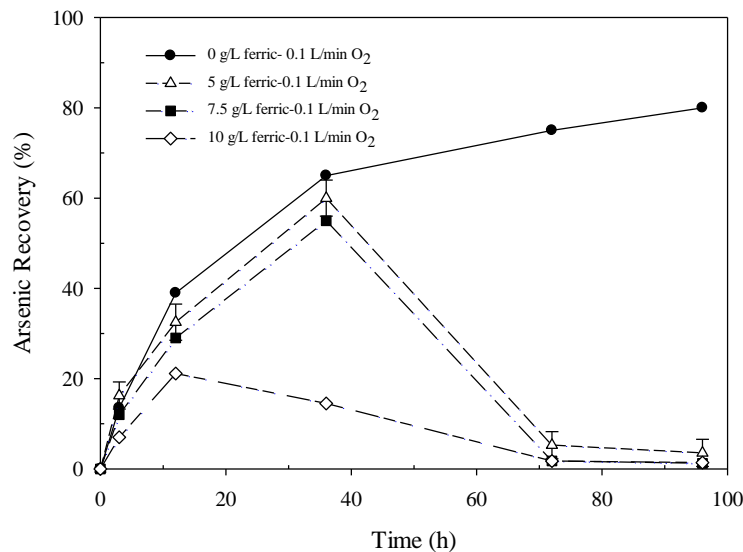


Figure 7-5. Effect of ferric ion dosage on the arsenic recovery in the presence of AF 5 (90° C, 0.5 M HCl, 5 g/L cupric ions, 1.5 M Cl⁻, concentrate:AF 5 ratio 1:1)

7.2.1.4 Effect of oxygen sparging rate on the arsenic recovery

Oxygen is an effective oxidant in the atmospheric leaching process, which controls the oxidation of ferrous and cuprous ions and the regeneration of ferric and cupric ions. Moreover, it plays a role in the catalytic activity of AC and AF 5 and generation of in-situ hydrogen peroxide as illustrated in Equation 2-15. Figure 7-6 presents the extent of arsenic recovery at various oxygen sparging rates. At an argon sparging rate of 0.1 L/min, the oxidation rate of enargite was slow and only 10% arsenic dissolution was achieved within 96 h. In the absence of oxygen, both the oxidant regeneration reactions and catalytic activity of AF 5 were retarded. In the presence of oxygen (0.1 L/min) arsenic recovery initially increased to 64% and then significantly decreased at 36 h, which was due to the formation of scorodite precipitates. However, a further increase in the oxygen sparging rate to 1 L/min at 5 g/L ferric ion concentration demonstrated no obvious effect on the arsenic recovery and scorodite precipitation. This also confirmed at the ferric concentration of 10 g/L, that the arsenic recovery at an oxygen sparging rate of 0.1 L/min exhibited a similar behavior to that at 1 L/min. These results indicated that the dissolved oxygen concentration in the solution reached an equilibrium value and increasing the oxygen sparging rate from 0.1 L/min to 1 L/min exhibited no significant effect on the arsenic dissolution and scorodite precipitation.

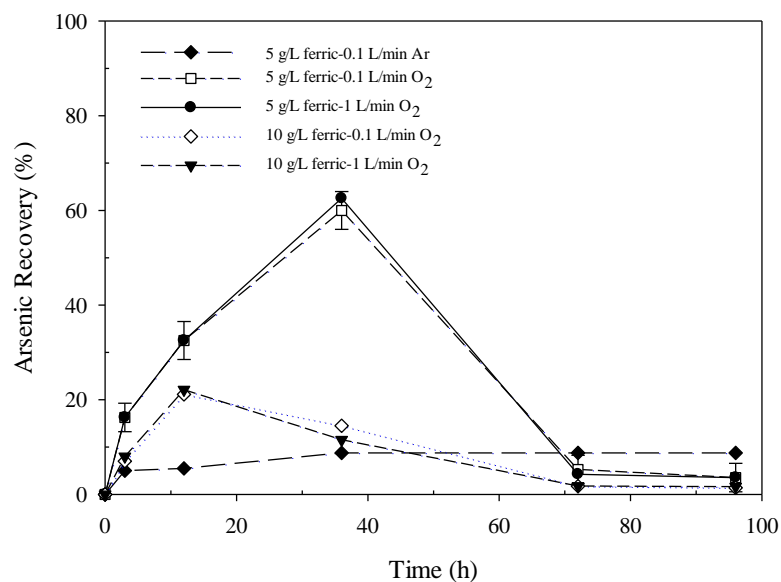


Figure 7-6. Effect of oxygen on arsenic recovery in the presence of AF 5 (90 °C, 0.5 M HCl, 5 g/L cupric ions, 1.5 M Cl, concentrate:AF 5 ratio 1:1)

7.2.1.5 Effect of seed addition on the arsenic recovery

To get insight into the effect of seed addition on the arsenic recovery and scorodite precipitation, different experiments were performed in the absence/presence of seed at the ferric ion dosage of 5 g/L. The surface energy for scorodite precipitation and the critical supersaturation value on a foreign surface (heterogeneous nucleation) is higher than the same kind surface nucleation (Demopoulos, 2009) (homogenous nucleation). Introduction of scorodite seed crystals reduces the required energy and results in a rapid and efficient arsenic precipitation during the leaching process. The scorodite precipitates, which were formed in the previous enargite leaching tests in the presence of AF 5, were used as the parent seeds. As illustrated in Figure 7-7, arsenic recovery in the absence of seed improved to 67% with an increase in the contact time and then it significantly decreased at 48 h, which was due to the formation of scorodite particles. In the presence of 5 g/L seed particles, the arsenic recovery increased to 22% within 6 h and then reduced with a slight slope to 4%. The seed addition significantly decreased the onset of scorodite precipitation to 6 h. In

addition, an increase in the initial dosage of ferric to 7.5 g/L demonstrated no significant effect on the arsenic recovery.

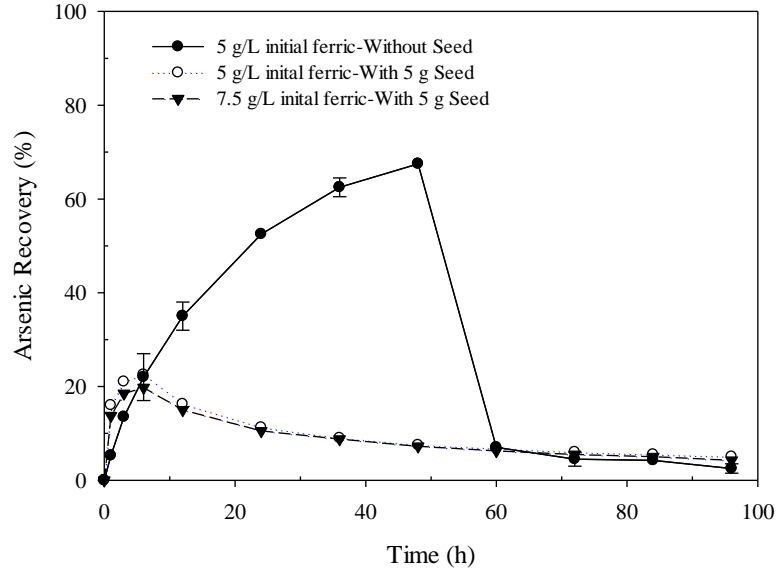


Figure 7-7. Effect of seed particle addition on arsenic recovery

7.2.1.6 Free acid concentration effect on the arsenic recovery

The pH can influence the arsenic dissolution and precipitation through manipulating the critical saturation of arsenic. A pH range of 0.3-1 is favorable to form the stable scorodite particles from a solution containing the ferric and arsenate ions (Fujita et al., 2009). In this study, free acid titration tests were conducted to probe the acidity of the leach solution and its effect on scorodite precipitation. Experiments were conducted in solutions with initial concentrations of 0.5 M hydrochloric acid, while pH adjustment was not performed during the tests.

The free acid titrations are shown in Figure 7-8, illustrated that the solution pH was lower than 0.5 in all the atmospheric leaching experiments. Free acid concentration was reduced by addition of the catalyst to the solution due to adsorption. The decrease in the free acid concentration continued with the dissolution of the enargite with, or without, catalyst. For the leaching experiments with AF 5, the acid consumption was stopped after 36 h and subsequently the free acid was re-generated

in the leach solution. This might be due to the dissolution of pyrite while the concentration of enargite decreased in the leaching reactors and catalyst is present.

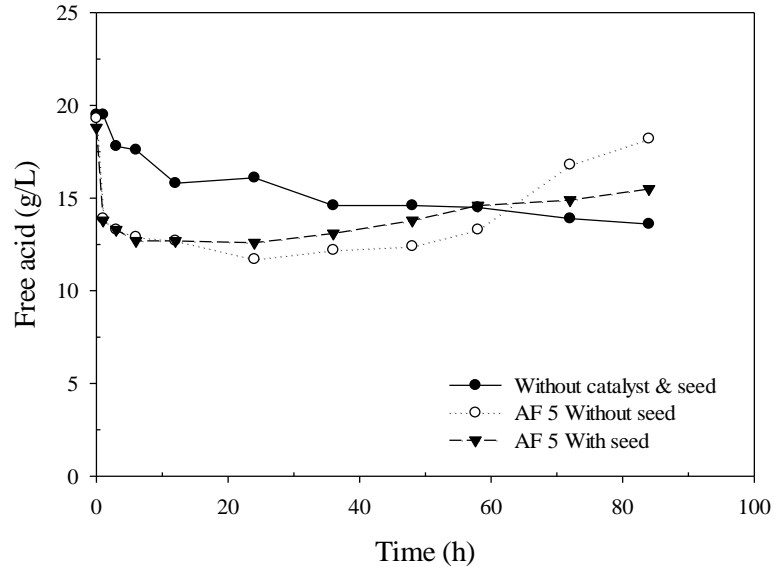


Figure 7-8. Free acid titration results during leaching without catalyst, with AF 5 and without seed and with AF 5 with scorodite seed addition (all the leaching experiments were performed with 5 g/L ferric ions, 5 g/L cupric ions at 90 °C)

7.2.2 The effect of iron on the precipitation and dissolution

Both a total iron concentration and a ferric to ferrous ion ratio are an indication of the overall oxidation occurring in a leach solution. Catalyst addition to the leach solution significantly improves the ferric to ferrous ion ratio by means of increasing the oxidation potential of the solution and regenerating the ferric and cupric ions (Ahumada et al., 2002). In the presence of catalyst, ferric ions at the concentration of 5 g/L were added in the form of ferric chloride salts to the solution. It is worth noting that an hour of time was given after the ferric addition to attain equilibrium conditions. The equilibrium concentrations of ferric to ferrous ions at various time intervals are depicted in Figure 7-9. As illustrated in Figure 7-9a, the initial equilibrium concentrations of ferric and ferrous ions were 3.15 g/L and 0.88 g/L, respectively, and the rest of Fe was adsorbed to the surface of AC. The leaching reaction proceeded rapidly within 5 h and the

ferric dosage sharply decreased. A further increase in the contact time leads to the regeneration of the ferric ions and the concentration, subsequently, had increased to 6.5 g/L at 84 h. In contrast to ferric ions, the ferrous ion concentration increased with a steep slope to 3 g/L within 1 h and then slightly decreased, which was due to the oxidation of ferrous to ferric ions. A plateau was eventually obtained after 36 h (Figure 7-9a). An increase in the ferric ion dosage, while ferrous ion concentration was constant, demonstrated that a fraction of pyrite is being leached into the chloride media and subsequently adds ferrous ions to the solution. This implies the significant role of pyrite in the enargite leaching process. The generated ferrous ions were then oxidized via sparged oxygen and in-situ hydrogen peroxide, which formed on the surface of AC. After 84 h of leaching, a sharp decrease in the ferric ion concentration resulted from the formation of scorodite precipitates.

The equilibrium concentrations of ferric and ferrous ions in the presence of AF 5 exhibited a similar behavior to that of AC (Figure 7-9b), however they were distinguishable in the initial equilibrium ferric ion concentration and the onset of scorodite precipitation. The initial concentration of ferric and ferrous ions was 1.67 g/L and 2.24 g/L, respectively, and the rest was adsorbed to the surface of AF 5. It was evident that the fraction of the iron adsorbed to both of the catalysts was about 1 g/L. The ferric ion concentration decreased to 1.6 g/L in an hour due to the rapid leaching reactions occurring on the fresh surfaces of the mineral. However, an increase in the leaching time promoted the ferric ion concentration to 5.2 g/L at 48 h. A significant decrease in the ferric concentration from 48 h to 60 h was assigned to the precipitation of scorodite. Contrary to ferric ions, the concentration of ferrous ions increased from 2.2 g/L to about 3.1 g/L within 1 h due to the ferric ion reduction reaction and then decreased to 1.8 g/L at 24 h.

In order to understand the effect of temperature on the ferric-ferrous ion ratio during the enargite leaching process, an atmospheric leaching experiment was performed at 70 °C in the presence of AF 5. As shown in Figure 7-9c, the initial equilibrium concentration of ferric and ferrous ions was 1.2 g/L and 2.6 g/L, respectively, and the rest was adsorbed to the AF 5, which was greater

compared to that at 90 °C. The ferric ion concentration initially increased within 6 h, which was due to the slow rate of the leaching reaction at 70 °C. The ferrous ion dosage initially dropped to 1.7 g/L at 6 h and then a plateau was reached. The pyrite leaching in tandem with the ferrous ion oxidation resulted in a gradual increase in the ferric ion concentration above 6 h. The total ferric ion concentration at 70 °C was lower than that at 90 °C, which was assigned to the higher rate of pyrite dissolution at 90 °C.

This section presents the effect of ferric ion addition on the Fe dissolution rate and total ferric ion concentration. A series of experiments were performed at the cupric ion concentration of 5 g/L in the presence of AF 5 at 90 °C. As illustrated in Figure 7-10a, in the absence of Fe salt, the Fe dissolution was directly proportional to the leaching time and gradually increased within 96 h. As stated previously, the increase in the Fe leaching percentage was due to the dissolution of pyrite in the chloride media. Additionally, the addition of the ferric salts, at a concentration of 2.5 g/L, led to a slight increase in the pyrite leaching rate and subsequent Fe dissolution percentage. It was also illustrated that no scorodite precipitate was observed at the ferric ion dosage range of 0-2.5 g/L.

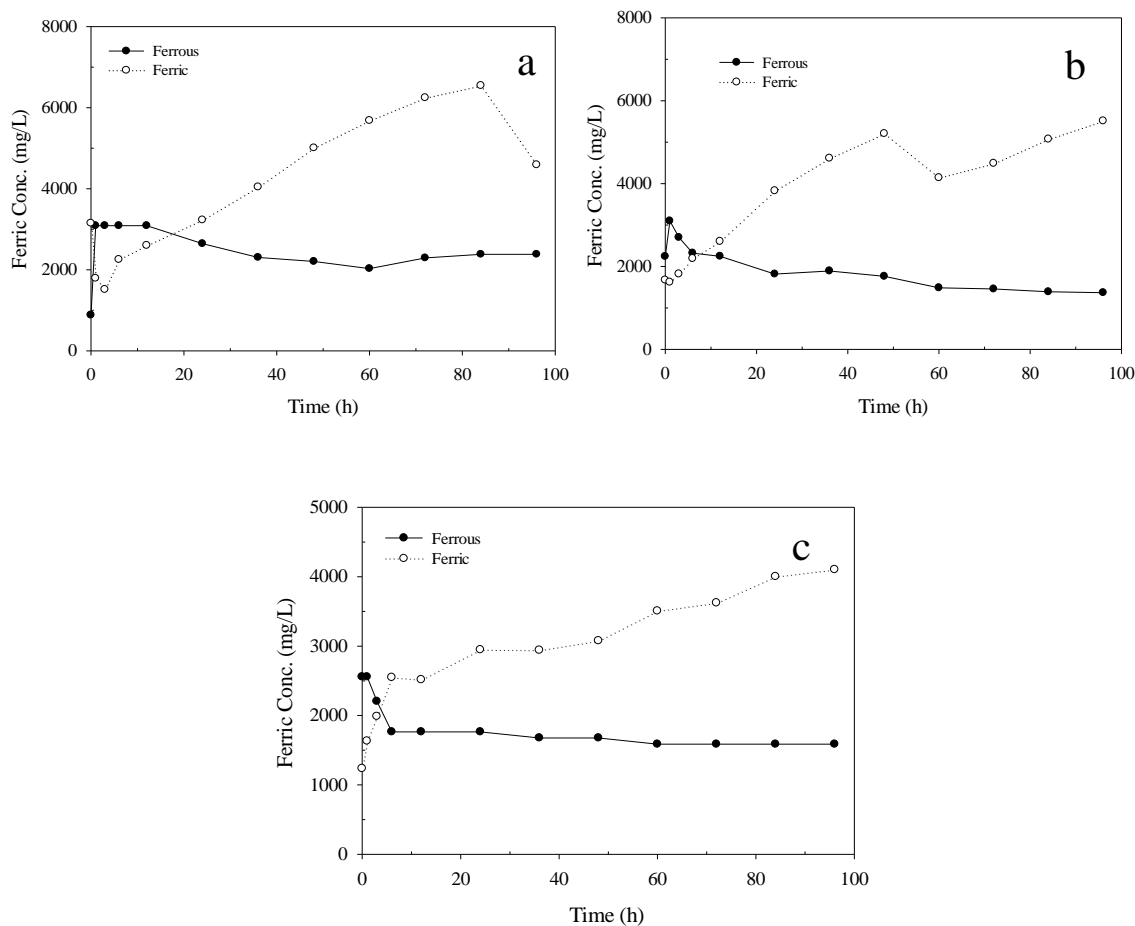


Figure 7-9. Ferric/ferrous ion concentration in the presence of (a) AC at 90 °C, (b) AF 5 at 90 °C and (c) of AF 5 at 70 °C

Figure 7-10b demonstrates that the addition of ferric ions at 2.5 g/L improved the total ferric ion dosage at different time intervals. A further rise in the ferric ion dosage up to 10 g/L significantly modified the trend of total Fe dissolution percentage. The Fe leaching percentage initially improved within a certain time and then sharply decreased. The decrease in the Fe concentration was attributed to the formation of scorodite precipitates. Increasing the ferric ion concentration lowered the onset point, at which time the scorodite precipitation started. For example, the scorodite formation process at the ferric concentration of 5 g/L was much slower (48 h) than the one at 10 g/L (6 h). The rate of total Fe dissolution was similar at the concentration range of 5 g/L-10 g/L. In addition, at the ferric ion concentration range of 0-10 g/L, the trend of total iron dissolution

percentage was in agreement with those of the total ferric ion concentration. This pointed out that the drastic decrease in the total iron was influenced by the ferric role in the scorodite precipitation process.

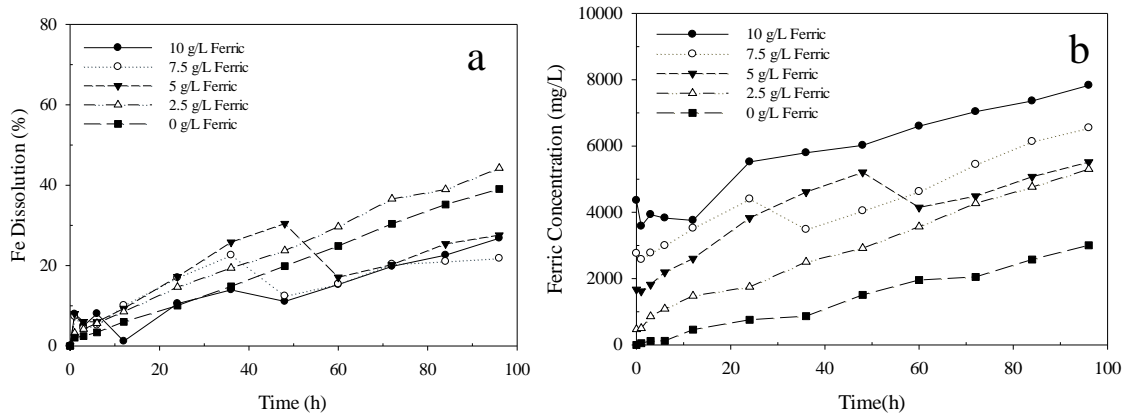


Figure 7-10. Effect of initial ferric concentration on: (a) final iron dissolution and (b) ferric ion concentration

The effect of AF 5 addition on the total ferric ion concentration is investigated in this part. The experiments were implemented at different fractions of AF 5 (25g-100g) while keeping ferric ion concentrations constant at 5 g/L. As illustrated in Figure 7-11, the fraction of AF 5 added to the leach solution significantly influenced the initial ferric ion concentrations. Increasing the portion of AF 5 from 25 g to 100 g reduced the initial ferric ion concentration from 2.5 g/L to 0.74 g/L. At the AF 5 amount of 25 g, the concentration of ferric ions increased intermittently at various time intervals. Also, an additional rise in the AF 5 amount (50 g-100g) led to a significant change in the trend of ferric concentration within 96 h. The ferric ion concentration increased up to a certain point and then appreciably decreased, which is attributed to the scorodite precipitation process. The onset point was moved to a lower time value when the amount of AF 5 in chloride media was increased. After the completion of scorodite precipitation, the ferric ion concentration increased. At a low fraction of AF 5 (25 g), AF 5 is only capable of oxidizing the pyrite and enargite and subsequently generating ferric and trivalent arsenic ions in the leach solution. However, increasing the ratio of

AC in the chloride solution caused an excess amount of in-situ hydrogen peroxide generation, which oxidized As(III) to As(V). Furthermore, AC increased the availability of nucleation sites. This suits the condition for the heterogeneous nucleation and growth of the crystalline scorodite precipitates.

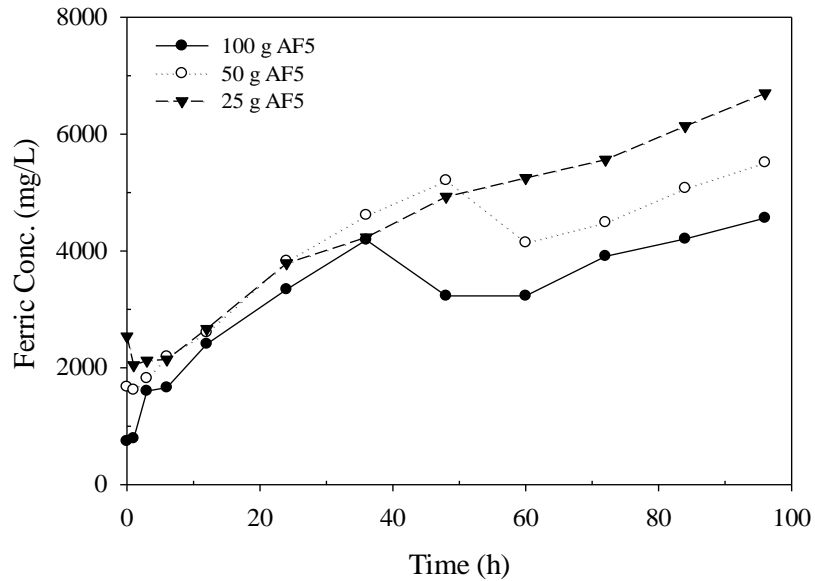


Figure 7-11. Effect of different AF5 ratios on ferric concentration

7.2.3 Scorodite characterization

Figure 7-12 shows the XRD patterns of the solid residue obtained after 60 h and 96 h of leaching at 90 °C with 5 g/L ferric ions, 5 g/L cupric ions, and at a concentrate to AF 5 ratio of 1:1. The XRD analysis clearly confirms the presence of the crystalline scorodite precipitates in the solid residue for both samples. It is also evident from Figure 7-12 that the enargite peaks have disappeared from the solid residue obtained after 96 h. In addition, the Rietveld refinement technique confirmed 7.7% enargite present in the solid residue after 60 h of leaching.

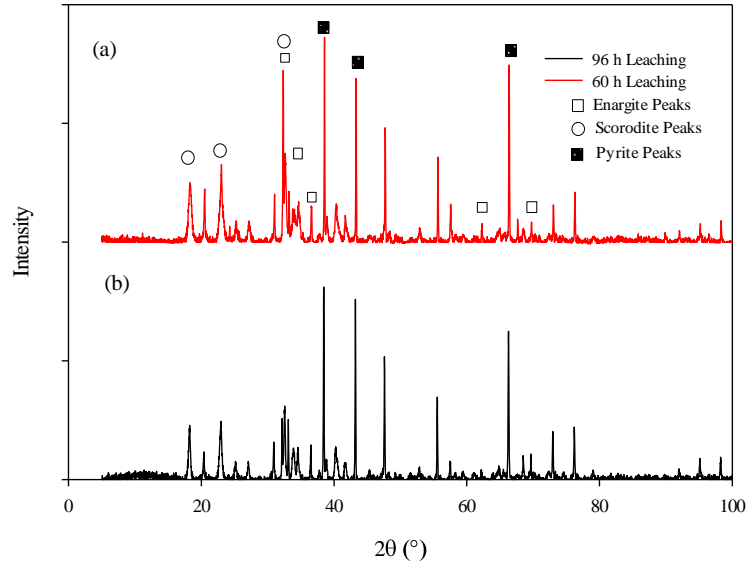


Figure 7-12. XRD patterns of the solid residue with 5 g/L ferric ions, 5 g/L cupric ions, concentrate: AF 5 1:1 at 90 °C (a) after 60 h of leaching (b) after 96 h of leaching

The XRD patterns of the solid residues obtained from different experimental conditions are illustrated in Figure 7-13. The XRD patterns of (a), (b), (c) and (d) demonstrated the presence of pyrite and scorodite as the major mineral phases. However, the scorodite peaks were not observed in the XRD analyses of (e), (f) and (g).

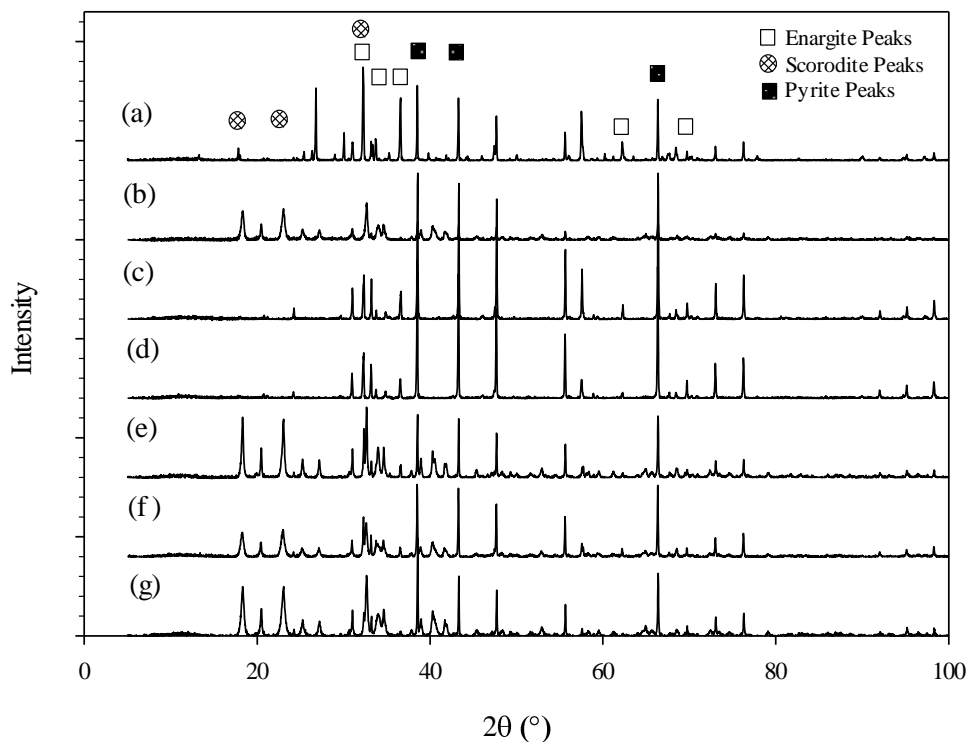


Figure 7-13. XRD patterns of solid residue with: (a) 5 g/L ferric ions, 5 g/L cupric ions, without catalyst (b) 5 g/L ferric ions , 5 g/L cupric ions and 200 g AC (c) 5g/L ferric ions, 5 g/L cupric ions and 25 g AF 5 (d) 2.5 g/L ferric ions, 5 g/L cupric ions and 50 g AF 5 (e) 10 g/L ferric ions, 5 g/L cupric ions and 50 g AF 5 (f) 5 g/L ferric ions, 0 g/L cupric ions and 50 g AF 5, (g) 5 g/L ferric ions, 5 g/L cupric ions and 50 g AF 5

The quantitative analysis of the scorodite phase, which was performed by the Rietveld refinement method, is given in Table 7-1. It is worth mentioning that the carbon weight was subtracted from the residue weight. Scorodite content in the residue varied between 63%-77% based on the experimental conditions (Table 7-1). The arsenic precipitation yield was in the range of 93%-100% which was in agreement with the data obtained from the solution analysis.

Table 7-1. Comparison between the arsenic precipitation recovery from solid and solution analysis

Sample	Solid Residue Weight (g)	Scorodite in Residue (%)	As Precipitation Yield from Solid (%)	As Precipitation Yield from Solution (%)
Without catalyst	19.1	0.0	0.0	0.0
200 g AC	20.9	63.0	100.0	98.5
25 g AF 5	7.5	0.0	0.0	0.0
2.5 g/L Ferric ions	7.8	0.0	0.0	0.0
10 g/L Ferric ions	16.9	77.4	99.0	98.6
0 Cupric ions	18.8	65.7	93.0	95.2
Control Test	16.8	77.2	99.0	96.5

The thermogravimetric analysis (TGA) was applied to measure the number of molecular waters attached to the ferric arsenate species in the scorodite residue (x value in the $\text{FeAsO}_4 \cdot x\text{H}_2\text{O}$ precipitates). TGA is a method wherein the mass of a sample is calculated at different time intervals as the temperature rises. It provides valuable information about the extent of crystallization and nature of water content in the residue (Le Berre et al., 2008). TGA of the solid residue is presented in Figure 7-14. The first sample mass loss (7-10%) between 170 °C-200 °C is assigned to the evaporation of crystalline water, which is characteristic of crystalline scorodite (Bluteau and Demopoulos, 2007). However, in poorly crystalline material, the evaporation of water occurs before 170 °C (Subrt et al., 1992). The second mass loss at 500 °C is attributed to the scorodite decomposition or the transformation of pyrite to pyrrhotite (Lambert et al., 1998).

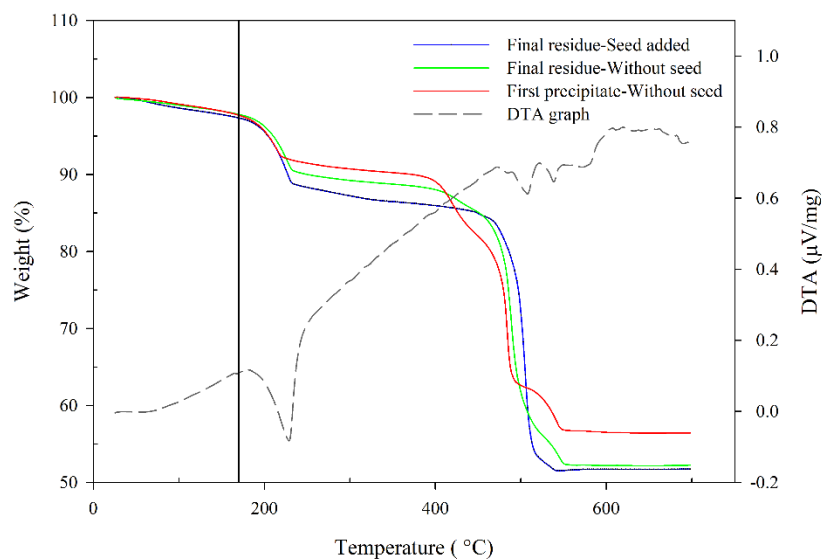


Figure 7-14. TGA curve of final leaching residue on the final leaching residue with and without the seed and on the initial precipitation solid after 60 h of leaching in the nitrogen environment (90 °C with 5 g/L ferric ions, 5 g/L cupric ions and concentrate: AF 5 1:1)

Figure 7-15 illustrates the SEM micrographs of the solid residue obtained after 50 h and 96 h of leaching in the absence/presence of seed crystals. As shown in Figure 7-15a, in the absence of seed crystals, the sub-micron scorodite precipitates were formed after 50 h on the surface of the enargite and pyrite particles. It is also evident from Figure 7-15b that the size of sub-micron scorodite precipitates increased over the leaching time and the particles were densely stacked. However, in the presence of seed crystals, the sizes of the scorodite particles were larger compared to those in the absence of seed crystals and the morphology of the precipitates changed from plate-like to a spherical-like structure (Figure 7-15c and d). The spherical-shaped scorodite precipitates demonstrated a higher dissolution rate than that of the plate-like scorodite particles (Caetano et al., 2009).

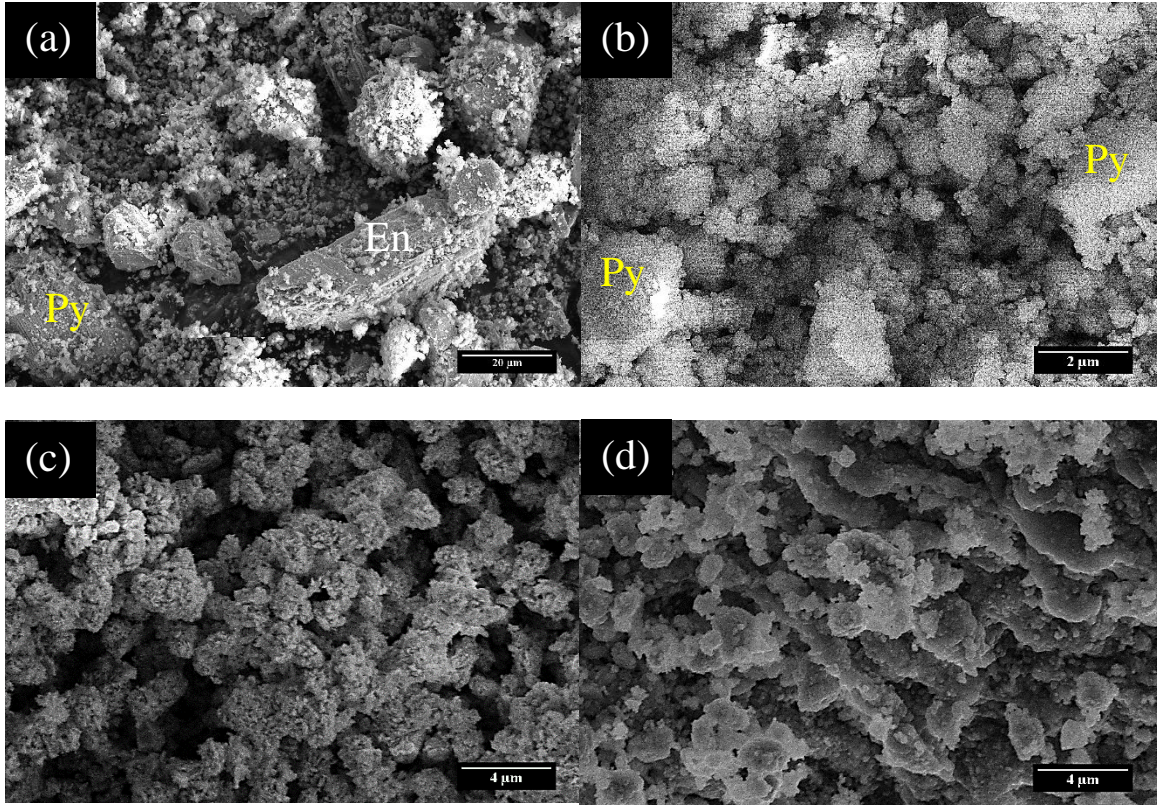


Figure 7-15. SEM micrograph of the precipitates obtained (a) after 50 hours of leaching (b) after 96 h of leaching (c) after 50 h of leaching in the presence of seed crystals (d) after 96 h of leaching in the presence of seed crystals (at ferric ion dosage of 5 g/L, in the presence of AF 5 at 90 °C)

Figure 7-16 clearly illustrates the optical microscopy micrograph of the greyish-white scorodite precipitates obtained after 96 h of enargite leaching. Also, the golden yellow color is referred to the pyrite particles, which were not leached in the chloride media.



Figure 7-16. Optical microscopy micrograph of the precipitated scorodite

The arsenic solubility of the arsenic-bearing residue is one of the significant parameters which must be assessed in the arsenic immobilization process. The degree of stability is measured using the toxicity characteristic leaching procedure (TCLP) that was developed by the United States Environmental Protection Agency (US EPA) in 1992. A series of TCLP tests on the scorodite precipitates demonstrated a low arsenic release ranging from 0.2 mg/L to 0.7 mg/L at pH 2.8-5.3 (U.S. Environmental Protection Agency, 1992). This indicated that the formed scorodite particles passed the EPA TCLP test limit of 5 mg/L As. It is worth noting that the seed crystal addition illustrated no significant impact on the dosage of arsenic release.

7.3 Conclusions

In this study, in-situ precipitation of the scorodite particles was investigated during the enargite leaching in the absence and presence of two carbon-based catalysts. The XRD and TGA results clearly affirmed the presence of the crystalline scorodite particles in the solid residue. It was demonstrated that the catalyst played a significant role in the arsenic dissolution, oxidation and immobilization. AF 5 showed a superior functionality compared to that of AC. At the concentrate to catalyst ratio of 1:1, the onset point at which the scorodite precipitation commenced decreased to 36 h for AF 5 and scorodite precipitates were readily formed. Ferric ion concentration had a

significant effect on the arsenic dissolution and arsenic immobilization process. No scorodite precipitate was observed at the ferric dosage range of 0-2.5 g/L. A further increase in the ferric ion concentration in the solution from 5 g/L to 10 g/L lowered the onset point. At the temperature range of 60-70 °C in the presence of AF 5 the arsenic dissolution percentage improved with a slight slope within 96 h and no scorodite precipitate was identified in the leaching residue. However, increasing the temperature from 80 °C to 90 °C not only significantly enhanced the arsenic recovery, but also lowered the onset of scorodite precipitation. In contrast to the hydrochloric media, no scorodite precipitate was detected in the sulfate media. It was also concluded that arsenic dissolution in the sulfuric acid solution was faster than that in the chloride media. SEM micrographs illustrated that, in the presence of seed, the size of the scorodite particles was larger compared to that in the absence of seed and the morphology of the precipitates changed from plate-like to a spherical-like structure.

Chapter 8

Effect of surface modification with different acids on the catalytic properties of AF 5 during atmospheric leaching of enargite

8.1 Introduction

A CBC, such as activated carbon (AC) and AF 5, are often porous materials with a high surface area and high chemical resistance. One of the most important properties of the CBC is the oxidation property in the presence of oxygen, making the CBC an efficient catalyst in the hydrometallurgical leaching processes (Cowan et al., 2017; Jahromi et al., 2017).

The catalytic properties of the CBC are connected to the functional groups on its surface. Through chemical pre-treatment processes it is possible to increase the density of functional groups on the CBC surface and improve its catalytic properties. The chemical pre-treatment processes can be low cost and convenient to implement, as very often it only involves contacting the CBC with an oxygenated acidic solution. The oxygen functional groups such as hydroquinone and quinone groups on a CBC surface have been proven to facilitate reversible reduction oxidation (redox) reactions (Andreas and Conway, 2006; Karatepe et al., 2008; Montes-Morán et al., 2004). The redox reactions are not limited to the oxygen functionalities, and the negatively charged nitrogen functionalities also can execute reversible redox reactions (Hulicova-Jurcakova et al., 2009). Some of the oxygen functional groups that might be available on the surface of a CBC are shown in Figure 8-1. As the pre-treatment media, the solutions of nitric acid, sulfuric acid, sodium hypochlorite, permanganate, bichromate, hydrogen peroxide, transition metals, and ozone-based gas mixtures can be used as oxidants for chemical oxidation of a CBC to generate oxygen functionalities (Shim et al., 2001). During the nitric acid pre-treatment process the nitration mechanism and the generation of oxygen functionalities take place simultaneously. Nitration treatment can form nitrogen functionalities such as pyridine structures, nitro groups, pyrrole-like

groups, lactam, imides, amines, and pyridine-N-oxide species (Bandosz and Ania, 2006). It has been shown that the existence of nitrogen functionalities on a CBC surface enhances its hydrogen sulfide and sulfur dioxide removal processing capabilities and increases its sorption capacity for anions (Bandosz and Ania, 2006). The mechanism associated with the sulfur fixation is proposed to be through capillary condensation, adsorption, chemisorption, and solution in structure (Bandosz and Ania, 2006; Boudou et al., 2003; Mangun et al., 2001; Rosas et al., 2017; Sun et al., 2015). CBCs such as AF 5 and AC have been employed in hydrometallurgy processes to catalyze the oxidative leaching of refractory sulfide minerals (Cowan et al., 2017; Jahromi et al., 2017). The application of a CBC during the enargite leaching process in chloride media is shown to increase the copper recovery from 69% (no CBC) to 92% (with AC or AF 5) in 96 h (Jahromi et al., 2017). Ahumada et al. (2002) have shown that some of CBC can produce in-situ H_2O_2 and HO_2^- in the presence of oxygen and this phenomenon can be explained by the availability of chromene and quinone groups on the surface of the catalyst, as shown in Reactions 2-15 and 2-16 (Ahumada et al., 2002).

The aim of this study was to investigate the effect of different chemical treatment and leaching environments on the surface functional groups and oxidation capability of AF 5. The effects of leaching environment and pretreatment of AF 5 were studied on enargite leaching with respect to the dissolution and speciation of copper, iron, arsenic, and finally the sulfur department.

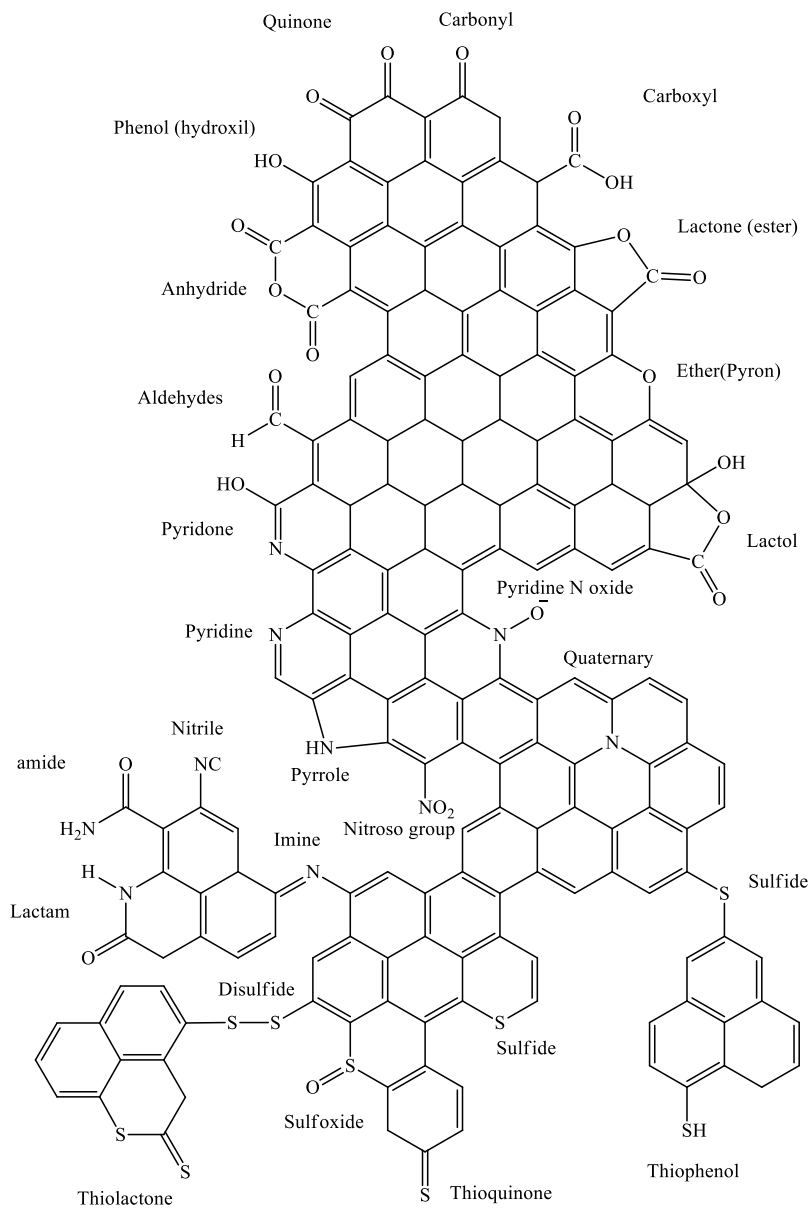


Figure 8-1. Oxygen, sulfur and nitrogen functional groups on the surface of CBC

8.2 Results and discussion

8.2.1 Pre-treated AF 5 surface Characterization

8.2.1.1 Infrared (IR) Spectroscopy

The IR analysis was applied to study the surface of AF 5 after different pre-treatment processes. It is worth noting that the IR analysis is often carried out as a qualitative analysis method rather than a quantitative method (Biniak et al., 1997). The transmission IR spectra of fresh AF 5 and hydrochloric, nitric and sulfuric acid treated AF 5 are presented in Figure 8-2. In all of the measurements, a band of O-H stretching vibrations exists between 3200-3600 cm^{-1} . This band is related to the surface carboxylic groups and chemisorb water (Biniak et al., 1997). The adsorption bands at 1700 cm^{-1} and in the 1570-1620 cm^{-1} range, which were observed in all the catalyst analysis, likely are due to the stretching vibrations of C=O in carboxylic, ester lactones, quinone and radical structures (Biniak et al., 1997; Shim et al., 2001). The absorption band in the 1300-1000 cm^{-1} range is likely connected to the overlapping peaks of absorption of ethers, epi-oxides and phenolic structures existing in different environments or the existence of C-N stretching vibrations overlapping the carbon structure (Pevida et al., 2008). The absorption band around 800 cm^{-1} can be the result of cyclic compounds containing C=C and C=N (Biniak et al., 1997; Chingombe et al., 2005).

The nitric acid treatment on a CBC can evolve the oxygen containing functionalities and nitro groups on the surface of the carbonaceous materials which can be detected by an absorption band in the range of 1330-1530 cm^{-1} (Bandosz and Ania, 2006; Biniak et al., 1997). The nitric acid treatment can form a pyridine structure on the surface of the carbon. In the band range of 1380-1470 cm^{-1} carboxyl carbonate structures, absorption hydroxyl groups, C=C-H structures and C-N vibrations can show up in the nitric acid treated AF 5 (Bandosz and Ania, 2006; Biniak et al., 1997). The absorption sharp band at 1076-1014 cm^{-1} in sulfuric acid-treated AF 5 can be due to the C-O stretching band due to the sulfuric acid oxidation process (Shin et al., 1997). Also, the band at 590

cm^{-1} Which appeared in the sulfuric acid-treated AF 5 is related to the sulfate and bisulfate ions (Terzyk, 2001). The nitric acid and sulfuric acid treatment of AF 5 resulted in the formation of the carboxylic structures and surface oxygen complexes (Bandosz and Ania, 2006).

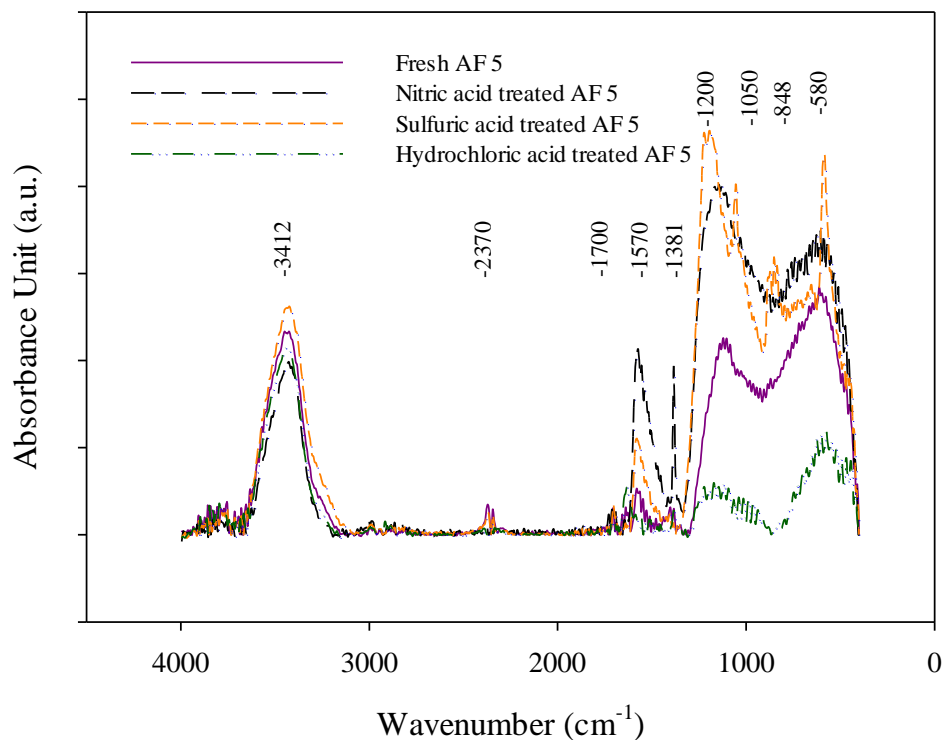


Figure 8-2. DRIFT spectra of the treated AF 5 in the 4000-450 cm^{-1}

8.2.1.2 Surface analysis by XPS

The XPS spectra of AF 5 catalyst indicated the presence of carbon, oxygen, silicon, and sulfur in the acid-treated samples, and nitrogen and chlorine in some of the samples based on the chemical treatment. The different detected species are presented in in Figure 8-3.

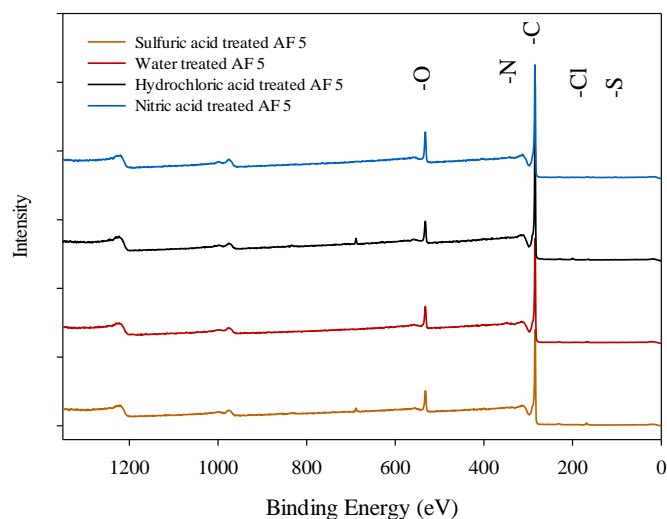


Figure 8-3. XPS spectra of AF 5 with different pre-treatment

The XPS spectra of O 1s excitation of carbon-based catalyst can be concluded of five main components of oxygen doubly bonded to carbon in quinone-like structures with a binding energy of 531.0-531.9 eV (Hulicova-Jurcakova et al., 2009; Zhou et al., 2007), carbonyl, anhydrides and hydroxyl groups at 532.3-532.8 eV (Hulicova-Jurcakova et al., 2009; Kundu et al., 2008; Zhou et al., 2007), non-carbonyl oxygen atoms in anhydrides and esters at 533.1–533.8 eV (Hulicova-Jurcakova et al., 2009; Kundu et al., 2008), oxygen in carboxyl groups at 534.3–535.4 eV (Kundu et al., 2008) and chemisorbed water or oxygen at 536.0–536.5 eV (Bandosz and Ania, 2006; Hulicova-Jurcakova et al., 2009; Kundu et al., 2008; Zhou et al., 2007). Most of the O 1s deconvolution peaks are located between 531 and 534 eV, and a shift of these peaks to a higher binding energy might be an indication of declining of amide type or carboxylic groups or increasing of ethers and the hydroquinone group. It is worth mentioning that, in the characterization of oxygen functionalities, it is more convenient to use C 1s instead of O 1s electron peaks since the difference in binding energies of electronegative elements is quite small (Bandosz and Ania, 2006; Kundu et al., 2008). High resolution XPS spectra of the O 1s peak for different treatments of AF 5 are shown in Figure 8-4. For all of the AF 5 investigated samples, three forms of oxygen peaks can be found

including: (1) an oxygen peak in quinone-like structures observed at 530.8-531.3 eV (Hulicova-Jurcakova et al., 2009; Zhou et al., 2007), (2) carbonyl oxygen peaks in ester and anhydrides observed at 532.4-532.6 eV (Hulicova-Jurcakova et al., 2009; Kundu et al., 2008; Zhou et al., 2007), and (3) non-carbonyl oxygen atoms in ester and anhydrides which were found at 533.4-533.7 eV (Bandosz and Ania, 2006; Hulicova-Jurcakova et al., 2009; Kundu et al., 2008; Zhou et al., 2007).

The relative content of oxygen peaks is reported in Table 8-1. In the water treated samples, the O 1s peak was deconvoluted to an evenly distributed mix of peaks 1, 2, and 3. By sulfuric acid treatment, the relative content of the peaks 1 and 3 was increased from 36.8% and 32.5% (water treated) to 45.4% and 37.3% respectively, indicating an increase in the quinone-like structures, ester and quinone on the surface of AF 5. On the other hand, the hydrochloric acid treatment declined the relative content of the quinone-like structures from 36.8 to 29.8%. The other substantial change in the oxygen functional groups was attributed to the nitric acid treatment. The nitric acid pretreatment can also cause the formation of surface defects, increase the porosities and reveal fresh new surfaces with high potentials of activation (Kundu et al., 2008). The relative content of peaks 1 and 2 were decreased significantly when the peak 2 content had increased from 30.7 to 49%. This increase can be related to the oxygen and nitrogen bindings.

Table 8-1. Relative content of functional groups in O 1s peak

Sample	O 1s relative concentration (%)		
	Peak 1	Peak 2	Peak 3
Water treated	36.8	30.7	32.5
Hydrochloric acid treated	29.8	33.9	36.3
Sulfuric acid treated	45.4	17.3	37.3
Nitric acid treated	23.5	49.0	27.5

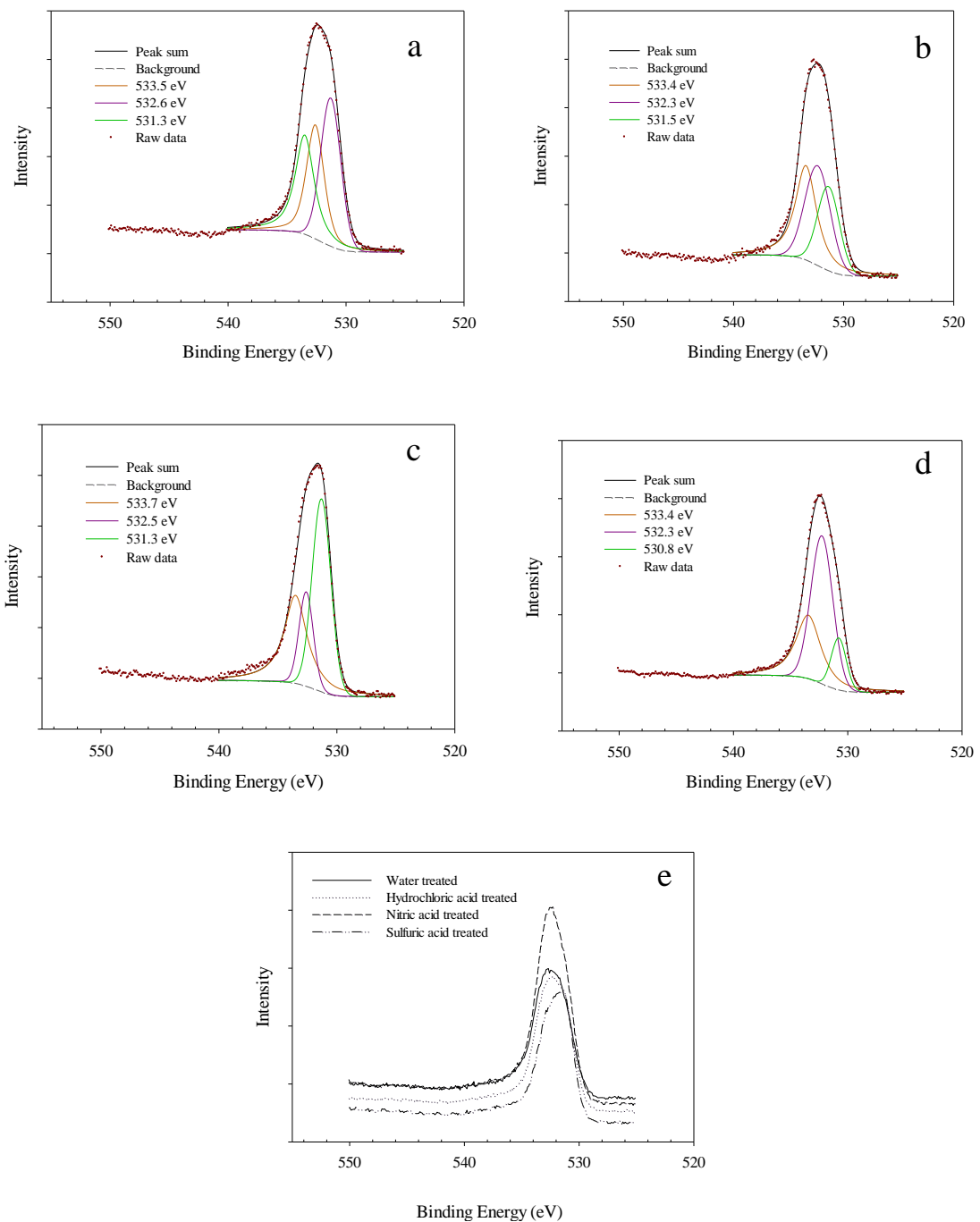


Figure 8-4. XPS spectra of oxygen 1s peak for different AF 5 treatments: (a) Water treated (b) Hydrochloric acid treated, (c) Sulfuric acid treated, (d) Nitric acid treated, (e) Raw data comparison

The high resolution XPS spectra of S 2p can contain up to 6 main peaks related to thiol; carbon bisulfide and SH group bonded to the phenol ring at 163.1-163.7 eV (Bandosz and Ania, 2006;

Hulicova-Jurcakova et al., 2009; Terzyk, 2001); sulfides and thioether groups at 164.3 eV (Bandosz and Ania, 2006; Hulicova-Jurcakova et al., 2009; Terzyk, 2001); sulfoxides and sulfite groups at 167.5-167.2 eV (Hulicova-Jurcakova et al., 2009); sulfone at 168.0 eV (Bandosz and Ania, 2006; Terzyk, 2001); and sulfate, sulfite, and sulfonic acid groups at 169 eV (Bandosz and Ania, 2006; Hulicova-Jurcakova et al., 2009; Terzyk, 2001). It should be noted that fresh AF 5 contains 1.06% sulfur in its structure. In the water treated AF 5, four peaks were detected: (1) SH group bound to the phenol ring at 163.7 eV (Bandosz and Ania, 2006; Hulicova-Jurcakova et al., 2009; Terzyk, 2001), (2) sulfur bonded to the carbon in the structure of C-S-C and R-S-S-OR at 164.9 eV (Bandosz and Ania, 2006; Hulicova-Jurcakova et al., 2009; Terzyk, 2001), (3) R₂S=O, R-SO₂-R groups at 168 eV (Bandosz and Ania, 2006; Hulicova-Jurcakova et al., 2009; Terzyk, 2001), and (4) SO₄²⁻, SO₃²⁻ ions, and RO₂-S-S-R groups at 169 eV (Bandosz and Ania, 2006; Hulicova-Jurcakova et al., 2009; Terzyk, 2001). The hydrochloric acid treatment of AF 5 in Figure 8-5b clearly shows peaks 1 and 2; however, peaks 3 and 4 were not detectable and a sulfonate and sulfite peak was observed because of dissolution. The sulfuric acid treated AF 5 showed the four general types of sulfur peaks; nonetheless, the concentrations of peaks 3 and 4 showed an increase. Furthermore, nitric acid pretreatment did not make a considerable change in the type of sulfur functional groups; however, peaks 3 and 4 concentrations declined when peaks 1 and 2 increased compared to the water treated AF 5.

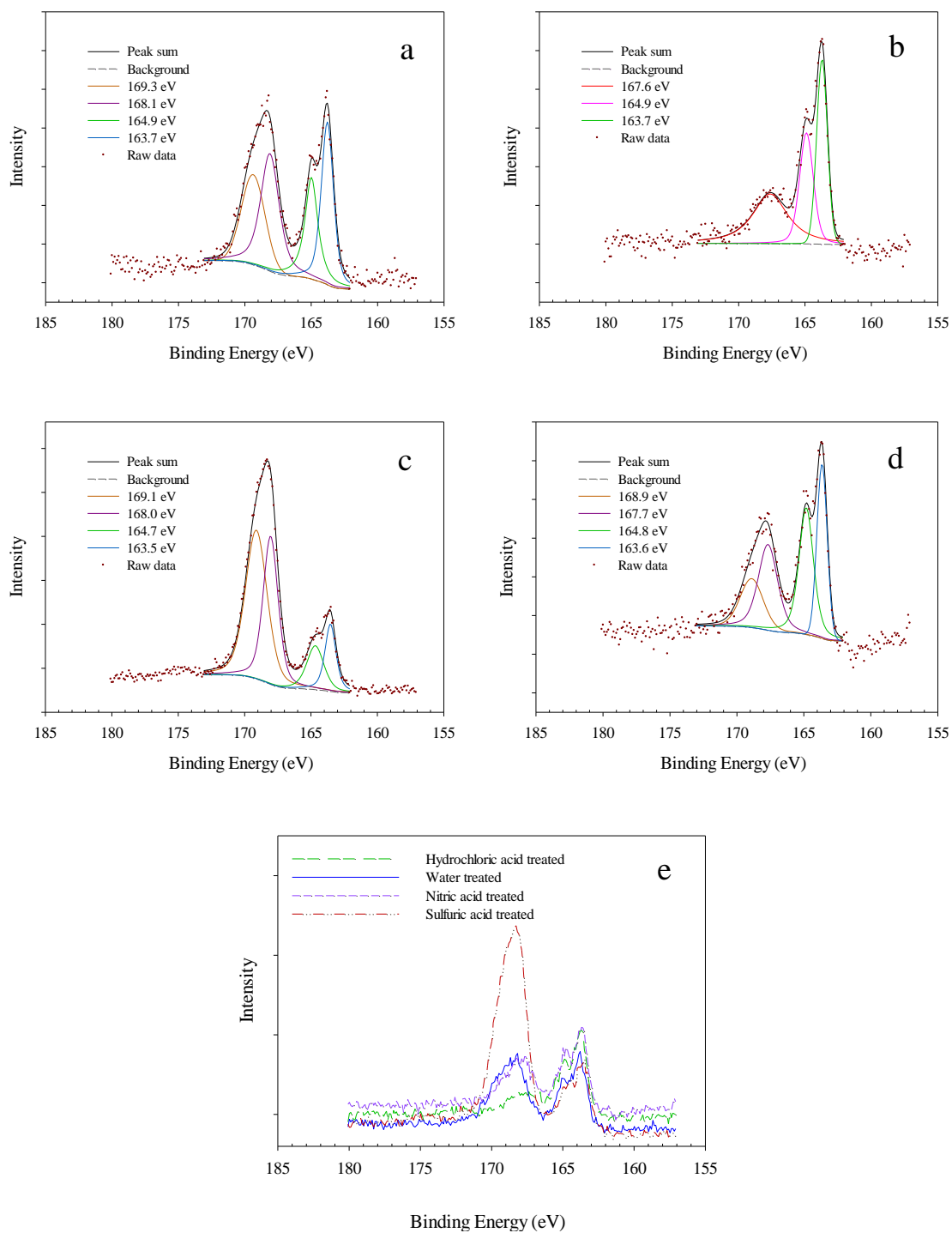


Figure 8-5. XPS spectra of sulfur 2p peak for different AF 5 treatments: (a) Water treated (b) Hydrochloric acid treated, (c) Sulfuric acid treated, (d) Nitric acid treated, (e) Raw data comparison

The carbon 1s XPS spectra of carbon-based catalysts can be deconvoluted into several peaks including carbon with a graphite structure at 284.5 eV (Hulicova-Jurcakova et al., 2009; Terzyk, 2001), carbon singly bonded to oxygen in phenols and ethers in the form of (C-O) at 286.1 eV (Bandosz and Ania, 2006; Terzyk, 2001), carbon double bonded to oxygen (C=O) in ketones and quinones at 287.5 eV (Hulicova-Jurcakova et al., 2009), carbon nitrogen structures at 286.3-287.5 eV (Bandosz and Ania, 2006; Terzyk, 2001), carbonyls at 287.3 eV (Bandosz and Ania, 2006; Hulicova-Jurcakova et al., 2009; Terzyk, 2001), carbon bonded with two oxygens in the form of –COO such as carboxyls, esters and anhydrides at 288.7 eV (Bandosz and Ania, 2006; Hulicova-Jurcakova et al., 2009; Terzyk, 2001) and the shake-up line for carbon in an aromatic compound (π - π^* transition) at 290.5 eV (Figueiredo et al., 1999; Figueiredo and Pereira, 2010; Hulicova-Jurcakova et al., 2009; Puziy et al., 2008). As shown in Figure 8-6, all of the carbon peaks were observed in different treatments of AF 5, however, some shifts in peak positions were detected, specifically in the case of hydrochloric acid-treated AF 5 (Kundu et al., 2008; Pevida et al., 2008; Puziy et al., 2008). All of the above carbon deconvoluted XPS spectra for AF 5 samples clearly incorporate five main peaks of (1) graphitic carbon (Bandosz and Ania, 2006; Hulicova-Jurcakova et al., 2009; Terzyk, 2001), (2) carbon species in phenols, alcohols and ethers (Bandosz and Ania, 2006; Hulicova-Jurcakova et al., 2009; Terzyk, 2001), (3) carbon in quinones, ketones and carbonyls or carbon nitrogen bonding (Bandosz and Ania, 2006; Hulicova-Jurcakova et al., 2009; Terzyk, 2001), (4) carboxyl, anhydrides and ester groups (Bandosz and Ania, 2006; Hulicova-Jurcakova et al., 2009; Terzyk, 2001), and (5) shake up satellite due to the transition in aromatic rings with a shift in some cases (Bandosz and Ania, 2006; Hulicova-Jurcakova et al., 2009; Terzyk, 2001), as shown in Figure 8-6. Based on the deconvoluted C 1s peak, the relative concentrations of different functional groups are demonstrated in Table 8-2. Peaks 2, 3, and 4 indicate the oxygenated carbon peaks, and an increase in the sum of those peaks indicates the efficient degree of oxidation by oxidative pretreatment (Puziy et al., 2008). In general, the sulfuric acid and nitric acid treatment

had increased carboxylic and quinone-like structures and reduced the phenol type functional groups. The oxidative pretreatment likely oxidized graphite and phenolic groups to carboxylic and quinone-like structures (Kundu et al., 2008).

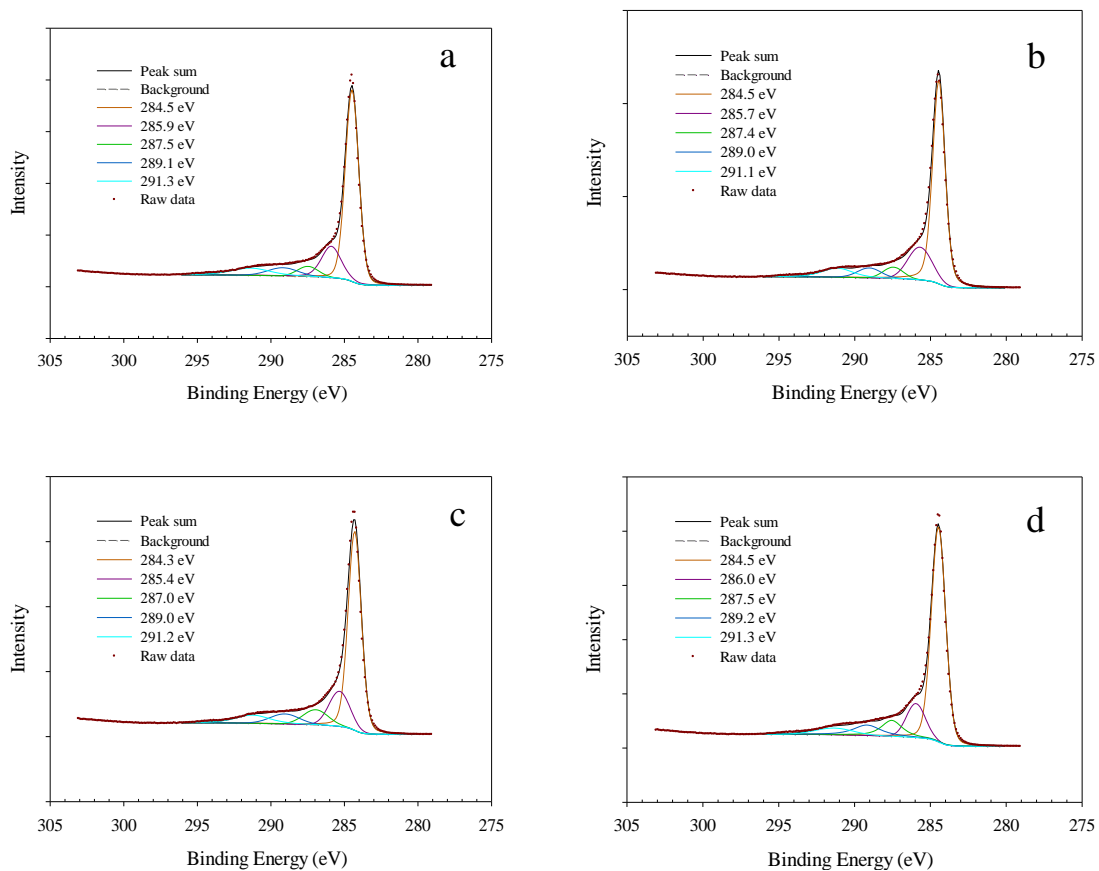


Figure 8-6. XPS spectra of carbon 1s peak for different AF 5 treatments (a) Water treated (b) Hydrochloric acid treated, (c) Sulfuric acid treated, (d) Nitric acid treated, (e) Raw data comparison

Table 8-2. Relative concentration of different groups in C 1s peak

Sample	C 1s relative concentration (%)					Oxygenated carbon
	Peak 1	Peak 2	Peak 3	Peak 4	Peak 5	
Water treated	64.7	16.2	5.1	5.9	8.1	27.2
Hydrochloric acid treated	64.3	17.7	5.1	5.6	7.3	28.3
Sulfuric acid treated	61.8	15.9	8.3	6.5	7.5	30.6
Nitric acid treated	65.7	12.8	8.7	7.7	5.1	29.2

The analysis of N 1s of a carbon-based catalyst can be assigned to main peaks of pyrrolic nitrogen and pyridines in the form of (C-N-C) at 399.6-400.5 eV (Bandosz and Ania, 2006; Hulicova-Jurcakova et al., 2009; Terzyk, 2001), quaternary (N-Q) nitrogen, protonated pyridinic, nitrogen atoms replacing carbon in graphene in the form of (C-N⁺H-C) at 401.3 eV, and oxidized nitrogen functionalities or NO₂ groups at 402-405 eV and 405.1 eV (Figure 8-7) (Hulicova-Jurcakova et al., 2009; Terzyk, 2001). A nitrogen 1s excitation peak was only found in the nitric acid treated AF 5 sample and deconvoluted to three main peaks at 405.6, 401.3 and 399.7 eV (Bandosz and Ania, 2006; Hulicova-Jurcakova et al., 2009; Terzyk, 2001) which is the characteristic of the above three peaks. The contribution of oxidized nitrogen functionalities is high at 52.8% in this sample indicating the oxidation associated with the generation of nitrogen functional groups on the surface of AF 5 by nitric acid oxidative pre-treatment.

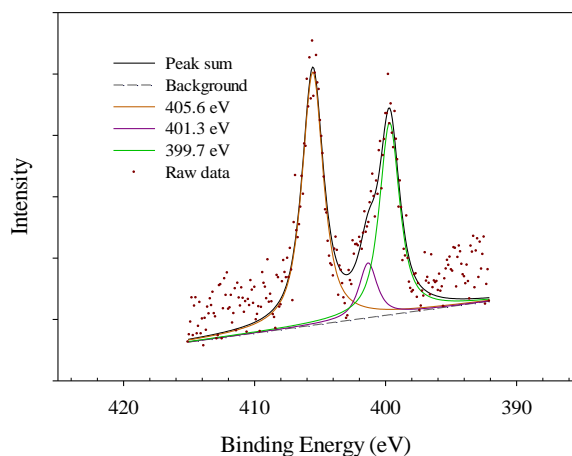


Figure 8-7. XPS spectra of nitrogen 1s peak for nitric acid treated AF 5

8.2.1.3 Sulfur analysis

The sulfur content of different pre-treated AF 5 samples is listed in Table 8-3. An untreated AF 5 samples contains 1.06% sulfur. The sulfur content in AF 5 had increased to 2.12% after the sulfuric acid treatment, whereas the hydrochloric acid and nitric acid treatment had removed sulfur from AF 5 reducing the AF 5 sulfur content to 0.97 and 0.88%, respectively. The tendency of a CBC for sulfur adsorption has been previously shown, where the adsorption of hydrogen sulfide can proceed until the adsorbed sulfur blocks the porosities and prohibits further adsorption (Bandosz and Ania, 2006).

Table 8-3. Sulfur content in AF 5 samples

Catalyst	Sulfur Content (%)
Fresh AF 5	1.06
Sulfuric acid treated AF 5	2.12
Hydrochloric acid treated AF 5	0.97
Nitric acid treated AF 5	0.88

8.2.2 Adsorption and oxidation

8.2.2.1 Adsorption

The physical and/or chemical ion adsorption is one of the important characteristics of a CBC such as AF 5 (Park et al., 2015; Reddad et al., 2002; Roy et al., 2014). The physical adsorption is dependent on various factors such as the concentration of the adsorbate and the surface area of the catalyst, whereas the chemical adsorption is mostly dependent on the functional groups on the surface of the CBC. The adsorption rate is also dependent on the temperature and its rate usually increases at elevated temperatures owing to the higher diffusion rate (Arcibar-Orozco et al., 2014; Bandoz and Ania, 2006; Chang et al., 2010; Di Natale et al., 2013; Park et al., 2015).

It is shown that some ions such as copper, iron and arsenic adsorb onto the AF 5 surface during the AF 5 assisted leaching processes (Cowan et al., 2017; Jahromi et al., 2017). To better understand the adsorption characteristics, the adsorption of copper, iron, and arsenic on an AF 5 sample were studied in synthesized solutions of 0.5 M hydrochloric acid and 1.5 M Cl^- ion concentration with different concentrations of Fe, Cu and As.

The effect of initial concentration of iron and copper on their adsorption on AF 5 was studied and the results are presented in Figure 8-8. The copper adsorption on AF 5 varied between 12-18% when contacting AF 5 with a 5 g/L copper solution (Figure 8-8a). The iron adsorption on AF 5 catalyst varied between 18-24% when contacted with a 5 g/L ferric ion containing solution (Figure 8-8b). The adsorption capacity of the AF 5 for iron was calculated to be in the range of 18 to 24 mg/g, and the copper adsorption capacity was calculated as 12 to 18 mg/g. Arsenic adsorption was measured to be around 10%, which was 200 ppm of the initial 2 g/L As(III) ions in the solution with the adsorption capacity of 4 mg/g. In this set of experiments no adsorption was observed after 60 min of the AF 5 and solution contact time, meaning that the adsorption process was virtually complete at the 60 min mark.

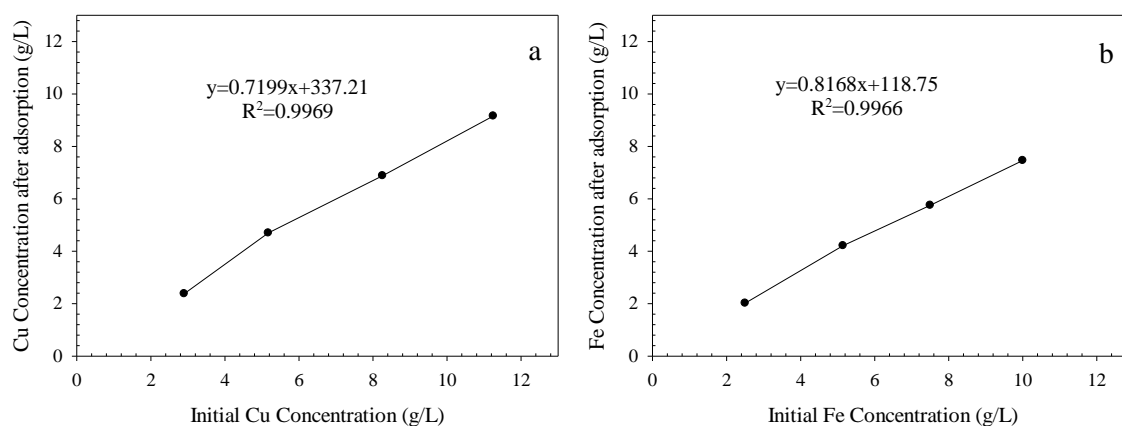


Figure 8-8. (a) Copper adsorption values for different initial concentration of copper on AF 5, (b) iron adsorption values for different initial concentration of iron on AF 5 (0.5 M hydrochloric acid, 1 L solution, 1.5 M Cl⁻ and 50 g AF 5 at 90 °C)

The relationship between the Cu concentration of the solution after the adsorption to AF 5 versus its initial concentration (Figure 8-8a) demonstrated a linear trend with the R² value of 0.997 and the slope of 0.81. In the case of ferric a linear trend similar to that of copper was observed with an identical R² value and a slope of 0.72. The linear trend of adsorption on the surface of the AF 5 shows that the adsorption is concentration dependent in this case. These results are also in agreement with those of Radzinski (Radzinski, 2017), which indicated the ratio of the adsorbed arsenic concentration to the initial arsenic concentration had a linear proportion to the initial concentration of the arsenic in the solution.

8.2.2.2 The AF 5 catalysis of oxidation process

The contact of AF 5 with oxygen in acidic solutions generates in-situ hydrogen peroxide which is a strong oxidant (Radzinski, 2017). In order to study the oxidative catalysis properties of AF 5 on Fe species oxidation in chloride media, the oxidation of iron was studied by measuring the concentration of Fe(II) and Fe(III) ions in the test solution during the oxidation process. The concentration of Fe(II) and Fe(III) ions in the solution in the presence of AF 5 catalysts are shown in Figure 8-9a and b respectively.

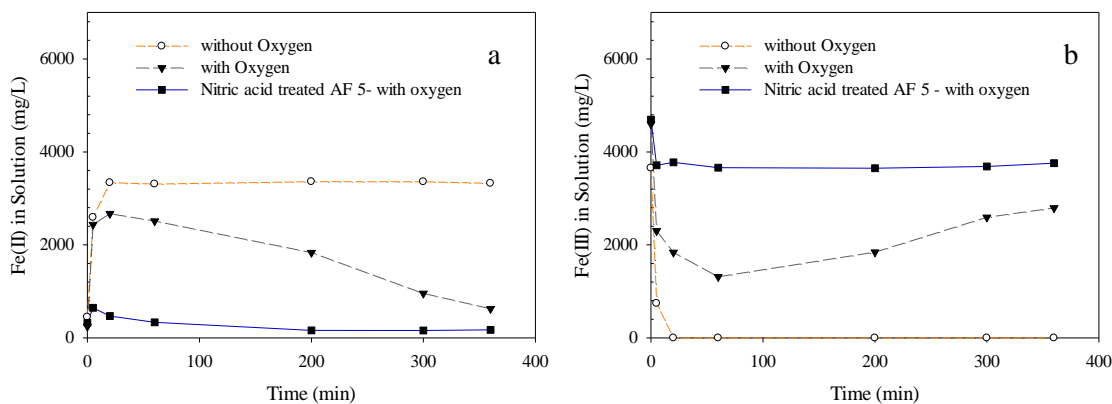


Figure 8-9. (a) Concentration of Fe(II) ions in the solution versus time, (b) concentration of Fe(III) ions in the solution versus time (0.5 M hydrochloric acid, 5 g/L initial cupric and ferric ion concentration, 0.1 L solution, 1.5 M Cl⁻ and 5 g AF 5 at 90 °C)

Immediately after the AF 5 addition to the test solutions, the Fe(III) reduces to Fe(II). This reduction occurs in less than 20 min on the surface of the AF 5, and proceeds near to completion if no oxygen is added to the system. The reduction of Fe(III) was minimized when AF 5 was treated with nitric acid (Figure 8-9a). It appears that the functional groups on AF 5 for reduction of Fe(III) are significantly decreased by the nitric acid treatment. The nitric acid treatment increases the acidity and especially the concentration of carboxylic acids (Figueiredo et al., 2006, 1999). The CBC in general, and AF 5 particularly, can either reduce or oxidize the redox species depending on the condition and the availability of certain functional groups on its surface (Figueiredo et al., 2006). It is also noted by several authors that the Fe(III) reduction on a CBC surface can potentially form oxygen containing functionalities on the catalyst (Martin-Gullon and Menendez-Diaz, 2006; Moreno-Piraján and Giraldo, 2013; Shah et al., 2015). Ferric chloride has been proven to activate the CBC and improve its adsorption efficiency (Martin-Gullon and Menendez-Diaz, 2006; Moreno-Piraján and Giraldo, 2013; Shah et al., 2015). The addition of oxygen to the test solution can facilitate the oxidation reactions by AF 5. In the tests with oxygen sparging in the reactor, the initial ferric reduction had decreased from near 100% to only 59% (Figure 8-9) and the oxidation of the reduced Fe(II) was then observed. In conclusion, the oxidation experiments generally confirmed

that Fe(III) was initially reduced to Fe(II) creating oxygen functional groups on the surface of AF 5, and the continuation of the oxygen gas sparging created the catalytic functional groups on AF 5 that were needed for Fe(II) oxidation back to Fe(III). However from Figure 8-9 the Fe(III) reduction was impeded when the AF 5 was treated with nitric acid, likely due to the formation of oxygen and nitrogen functional groups on the surface of AF 5.

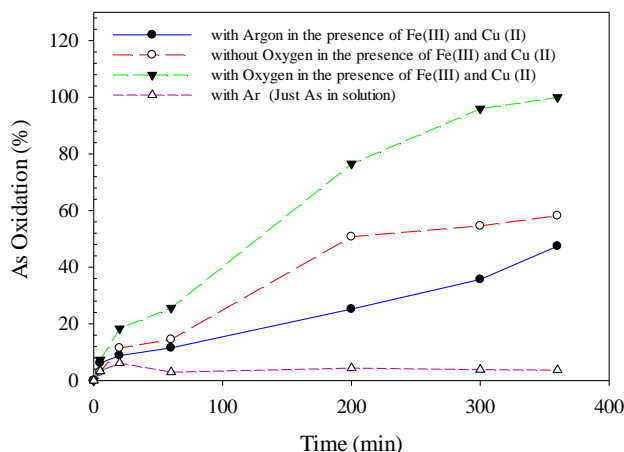


Figure 8-10 . Oxidation of As versus time in the presence of the catalysts, 5 g/L iron and copper in chloride media with 2 g/L As(III) initial concentration at 80 °C

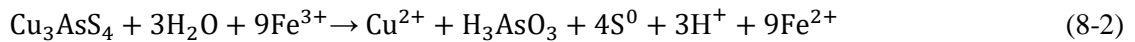
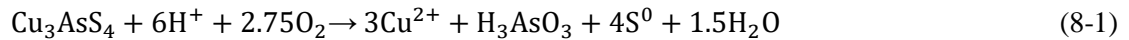
The effect of AF 5 on the As(III) oxidation is presented in Figure 8-10. With no oxygen addition the catalyst can only generate limited hydrogen peroxide and oxidize a small amount of As(III) (Radzinski, 2017), whereas, with oxygen addition, the catalyst effectively oxidizes arsenic. As shown in Figure 8-10, with no oxygen addition, only about 50% of the As(III) was oxidized and the reaction was stalled after about 200 min. In another experiment, Ar gas was sparged through the wetted AF 5 for 3 h before the oxidation experiment began to remove the oxygen from the porosities of AF 5. As a result, around 40% of As(III) oxidation was observed in 6 h at 80 °C in the presence of initial 5 g/L Fe(III) and Cu(II) ions. This experiment showed that not only the oxygen is important and effective in the formation of the oxygen functional groups on the AF 5 surface, but also Fe(III) can activate the AF 5 surface for oxidation catalysis. This finding was further followed by an experiment with the same content of As(III) (2 g/L) in the solution with argon

sparging and without the existence of ferric ions. The result of this experiment showed only a negligible arsenic oxidation in the solution (0.15%). Moreover, oxygen availability is a key for rapid oxidation of all the ions in the presence of AF 5, and without oxygen addition the kinetics of the oxidation process decreases considerably. When oxygen is added to the reactor the As(III) oxidation efficiency proceeded to completion in 6 h. The oxidation of As(III) to As(V) is one of the most important advantages of using AF 5 and other CBC in the leaching of arsenic-bearing copper sulfide minerals.

8.2.3 Effect of catalyst pre-treatment and leaching media on enargite leaching

8.2.3.1 Oxidative enargite leaching with AF 5 catalyst

The oxidative leaching of enargite in an acidic ferric sulfate solution can be presented by the following reactions (Ruiz et al., 2011; Safarzadeh et al., 2012):



It has been shown that AF 5 can catalyze this leaching reaction (Cowan et al., 2017; Jahromi et al., 2017). The main purposes of the AF 5 application, as a catalyst, in the enargite leaching process are: (1) to increase the leaching process kinetics and recovery of a high percentage of the copper to the pregnant leach solution (PLS), (2) to oxidize the arsenic in the leach solution, and (3) to collect the elemental sulfur product of enargite leaching on AF 5. As presented in the proceeding sections, the AF 5 catalyst pre-treatment with chemicals changes the functional groups on its surface and it is desired to demonstrate the impact of those changes on the catalytic leaching of enargite with AF 5 as well as its capacity for the elemental sulfur adsorption. The type of dissolution media can also have a significant effect on the leaching kinetics. In order to study the effect of the catalyst pre-treatment and dissolution media, three sets of enargite leaching experiments were carried out: (a) leaching in sulfate solution with water-treated AF 5, (b) leaching in chloride solution with water-treated AF 5, and finally (c) leaching in sulfate solution with nitric acid-treated AF 5. The leaching

condition was similar in these experiments including 5 g/L initial ferric ion concentration with 50 g AF 5 at 90 °C. The copper recoveries versus time are presented in Figure 8-11 for these tests. In sulfuric acid leaching cases, the dissolution of copper is comparable with and without nitric acid catalyst pre-treatment. The copper dissolution rate in sulfuric acid leaching had increased from 97.1% to 98.8% when the nitric acid pre-treated AF 5 was used. The copper recovery with the water treated catalyst in hydrochloric acid was only 88.6% (Figure 8-11).

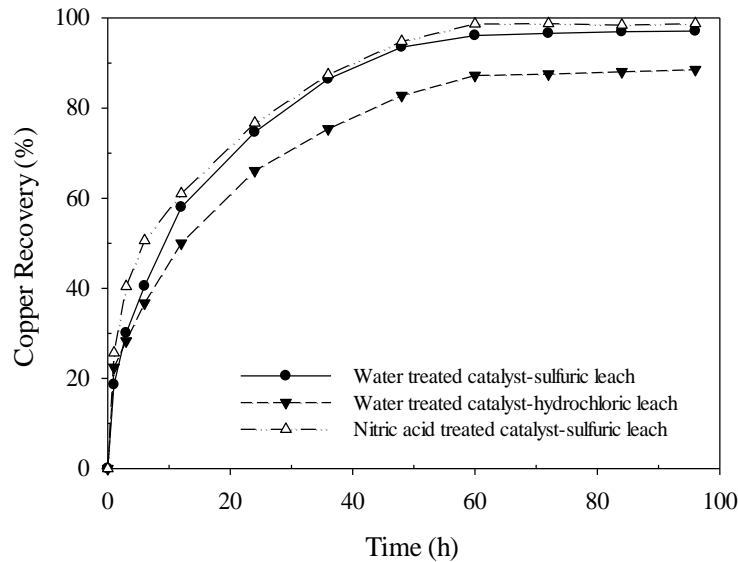


Figure 8-11. Effect of acid type and catalyst pretreatment on copper recovery

8.2.3.2 Arsenic oxidation with AF 5 catalyst

The type, ionic strength of the dissolution media, and AF 5 pre-treatment process are important parameters which can affect both the arsenic leaching into the PLS and the arsenic immobilization reactions during the enargite leaching process. It has been shown that arsenic can be immobilized in the enargite leaching process according to Reaction 2-17, if the arsenic is present as the As(V) species.

Solubility of arsenic species is dependent on the ionic strength and the composition of the leaching media. As illustrated in Figure 8-12, arsenic leaching kinetics within 96 h shows two steps for both AF 5 and nitric acid treated AF 5 in the sulfuric acid solution: (i) a sharp increase in the arsenic recovery within 36 h; (ii) a slow increase in the arsenic dissolution after which equilibrium was reached. For nitric acid treated AF 5, arsenic recovery at different time intervals was greater than that of un-treated AF 5 due to the higher catalytic activity of the oxidized surface of AF 5 and availability of the higher number of functional groups on the AF 5 surface. The final arsenic dissolution of 87.1% was achieved when the un-treated AF 5 was used in the leach tests (Figure 8-12), and the arsenic recovery was 92.1% when the AF 5 was pre-treated with nitric acid. In addition, no scorodite or other ferric arsenate precipitates were identified in the residue of the sulfate media leach tests. However, in the chloride leach solution, arsenic dissolution initially increased with a steep slope and the maximum arsenic recovery was reached at 48 h (70%). Further increase in the leach time significantly dropped the arsenic concentration, which was assigned to the formation of scorodite/ferric arsenate particles. The critical supersaturation of the chloride media is much lower than that of the sulfate media, thus the formation of scorodite occurs in the chloride leach solution (Demopoulos, 2009).

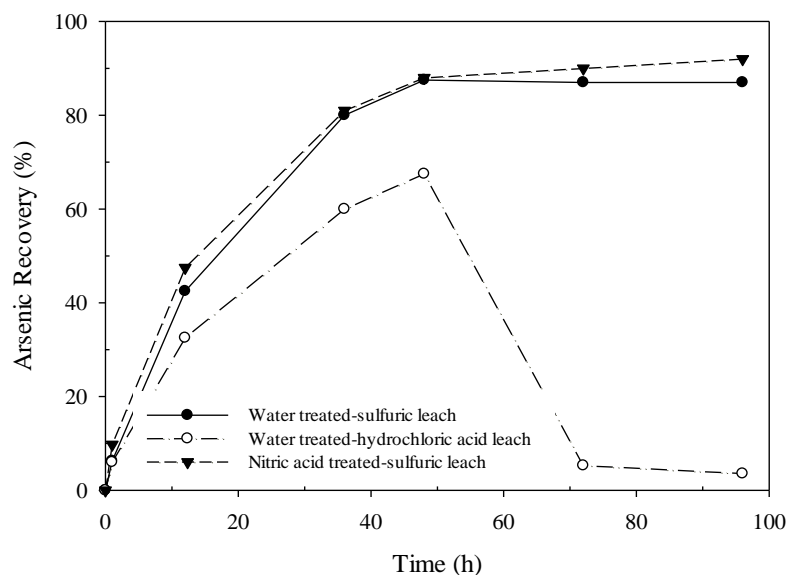


Figure 8-12. Effect of acid type and catalyst pretreatment on arsenic recovery

8.2.3.3 Iron oxidation with AF 5 catalyst

The enargite concentrate which was used in the leaching experiments contained 43% pyrite and 20.1% iron. The leach conditions that are designed for the oxidative enargite leaching also oxidize a proportion of the pyrite. The iron dissolution rates in the leaching experiments in different media are presented in Figure 8-13. The iron dissolution in chloride media was rapid for the first hour and then followed a linear trend up to 36 h when the precipitation of iron with arsenic started. After the initial precipitation stage, the iron concentration rose in the solution again with the linear trend up to 27.6% at the end of the test. The iron dissolution in the sulfate media (Figure 8-13) was faster than that in the chloride media. In the experiment with water-treated AF 5, the iron dissolution rate showed a steep curve reaching up to 82.5% iron recovery. When the nitric acid-treated AF 5 was used in the sulfate leaching media, the iron dissolution rate increased drastically for the first 3 h (73.5%) which might be due to the evolution of pyrrolic nitrogen, pyridines, quaternary nitrogen, and protonated pyridinic functional groups generated on the surface of the AF 5. It is also worth noting that the enargite leaching rate was not as impacted as the pyrite oxidation rate in this

experiment. In addition, no sign of iron precipitation was observed in the sulfate media leaching experiments. The free acid concentrations in the leaching experiments were measured by a free acid titration method to develop a better understanding of the acidity level of the solution and monitoring the generation or consumption of the acid. In the chloride media leach experiments, a 0.5 M hydrochloric acid solution was used at the leach media, while in the rest of the experiments, a solution with 1 M sulfuric acid concentration was used.

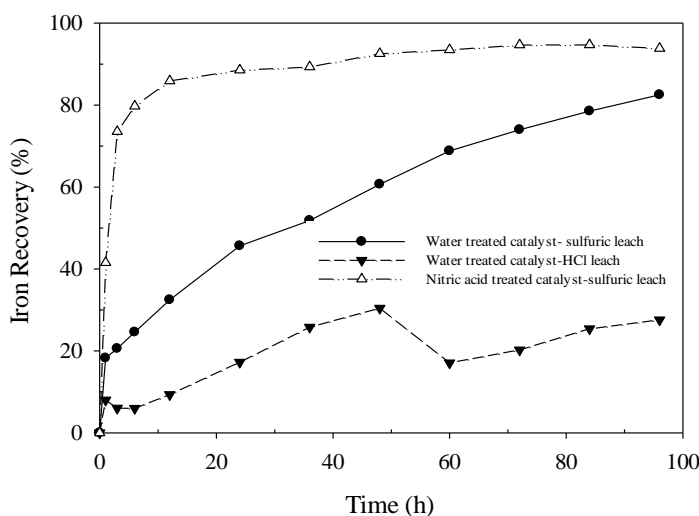


Figure 8-13. Effect of acid type and catalyst pretreatment on iron recovery (50 g enargite, concentrate to AF 5 ratio 1:1, 90 °C for 96 h)

It can be inferred from comparing the leaching and XPS results that, leaching in sulfuric acid can act as a sulfuric acid pre-treatment and generate oxygen functional groups including carbonyl, non-carbonyl and quinone groups on the surface of the catalyst and improve both copper and iron leaching. Furthermore, nitric acid pre-treated AF 5 in sulfuric acid leach can enhance iron dissolution significantly due to the generation of nitrogen-oxygen functionalities in addition to the oxygen functionalities evolves in a sulfuric acid leach.

As is reported in Table 8-4, the adsorption of H^+ ions occurred once the acidic solution was added to the pre-wetted or pre-treated catalysts. The free acid concentration in the chloride media leaching test decreased for the first 24 h from 19.3 g/L to 11.7 g/L, and then experienced an increase to 19

g/L. In the sulfate media leaching test, the free acid concentration declined regardless of the excess pyrite dissolution during the experiments. The leaching experiment with nitric acid treated AF 5 resulted in higher free acid in the solution which can be justified by the higher pyrite dissolution rate.

Table 8-4. The free acid concentration in leaching solution

Experiment Time	Water treated AF 5 in hydrochloric acid leaching	Water treated AF 5 in sulfuric acid leaching	Nitric acid treated AF 5 in sulfuric acid leaching
Before catalyst addition	19.3	96.2	99.0
After catalyst addition	16.6	94.6	91.7
1	13.9	92.9	88.3
3	13.3	85.3	88.6
6	12.9	85.1	87.6
12	12.7	84.2	87.8
24	11.7	83.9	87.3
36	12.2	75.6	87.8
48	12.4	74.2	86.0
58	13.3	73.5	82.7
72	16.8	72.5	82.4
84	18.2	73.1	82.6
96	19.0	72.0	83.0

8.2.3.4 Elemental sulfur adsorption onto AF 5 during leaching tests

One of the advantages of using AF 5 over other CBC is its unique sulfur collection capability. The sulfur adsorption on AF 5 potentially reduces sulfur oxidation to sulfate and consequently decreases the neutralization cost associated with generated acid during the atmospheric pyrite leaching process. In addition, the sulfur removal from the leach residue, via its adsorption onto AF 5, makes

the treatment of the residue in the downstream operations simpler (for instance the presence of elemental sulfur in a cyanidation circuit can be an issue). The mechanism of the sulfur collection process on AF 5 is not well understood yet; however, it might be due to the physical absorption through AF 5 mesopores, chemical absorption by the functional groups or oxidation-reduction of other sulfur by products on the surface of the catalyst or a combination of all (Bandosz and Ania, 2006). The sulfur balance results in the leaching experiments are provided in Table 8-5. The sulfur collection results showed that using a sulfate leach media drastically increased the sulfur yield over sulfate formation. The sulfur collection on the water-treated AF 5 was higher than that on the nitric acid treated AF 5 by 6%, confirming the free acid titration results. Furthermore, the nitrogen functional groups can increase the desulfurization activity of CBC (Figueiredo and Pereira, 2010).

Table 8-5. Sulfur balance of the leaching experiments

Experiment	S in residue (%)	S in solution (%)	S collected by AF 5 (%)
Water treated AF 5 hydrochloric acid leach	16.9	51.8	30.9
Water treated AF 5 sulfuric acid leach	9.5	39.2	51.1
Nitric acid treated AF 5 sulfuric acid leach	0.4	54.6	45.1

The sulfate formed in the chloride leaching media was 12.6% higher than was formed in the sulfate media leaching experiments. In summary, the utilization of the sulfate media increases the sulfur yield on the surface of the AF 5 catalyst; however, the nitric acid pretreatment of AF 5 shows a negative effect on the sulfur yield or the leach process.

8.2.3.5 XPS study of the residue and the post leaching catalysts

The XPS spectra of the leaching residues in the hydrochloric leaching experiment for arsenic 3d, iron 2p, and sulfur 2p peaks are shown in Figure 8-14. For the arsenic 3 d peak, the binding energies

of the different species can be listed as: As at 41.6 eV (Kloprogge and Wood, 2017a), As_2O_3 at 44.2-45.0 eV (Kloprogge and Wood, 2017a), and As_2O_5 at 45.9-46.5 eV (Kloprogge and Wood, 2017a). The arsenic 3d deconvolution peak includes a single peak at 46.5 eV which is attributed to the As(V) bond to oxygen (AsO_4^- bearing phases) and approves the oxidation state of arsenic in scorodite precipitate (Kloprogge and Wood, 2017a). In iron 2p spectra, five peaks were used to fit the XPS spectrum. The iron band at 725 eV and 720 eV are attributed to the Fe $2p_{1/2}$ band (Garavelli et al., 2009; Kloprogge and Wood, 2017b). In the Fe $2p_{3/2}$ band, the 707.2 eV peak is related to the ferrous in the pyrite residue remained from the leaching, the ferric band has shown up in 712.4 eV with a shakeup satellite band at 714.9 eV, which was reported before by Kloprogge and Wood, 2017 (Garavelli et al., 2009; Kloprogge and Wood, 2017b). The results for the iron 2P band confirmed previous results from Frau et al. (2005) that reported ferric arsenate bonding in scorodite for iron is at 712 eV (Frau et al., 2005). The interpretation of sulfur deconvolution peaks is more challenging due to the overlaps in different sulfur species; S^{2-} at 161.3 eV (Kloprogge and Wood, 2017a), S_2^{2-} at 161.8-162.5 eV (Kloprogge and Wood, 2017a), S_n^{2-} at 163.3-163.8 eV (Kloprogge and Wood, 2017a), AsS^{2-} at 162.4 eV (Kloprogge and Wood, 2017a), S^0 at 163.7-164.8 eV (Kloprogge and Wood, 2017a), SO_3^{2-} and at 166-167 eV (Kloprogge and Wood, 2017a) and SO_4^{2-} at 168.4-169.4 eV (Fantauzzi et al., 2015; Zhu et al., 2014). Three major peaks were fitted in the residue XPS spectra located at (i) 169.4 eV (Kloprogge and Wood, 2017a), (ii) 164 eV (Kloprogge and Wood, 2017a), and (iii) 162.7-164 eV (Kloprogge and Wood, 2017a). Peak (i) can be assigned to the SO_4^{2-} group as a product of the leaching (Kloprogge and Wood, 2017a), peak (ii) might be attributed to the generated elemental sulfur (Kloprogge and Wood, 2017a), and peak (iii) can be assigned to the S_2^{2-} as a part of un-leached pyrite (Kloprogge and Wood, 2017a).

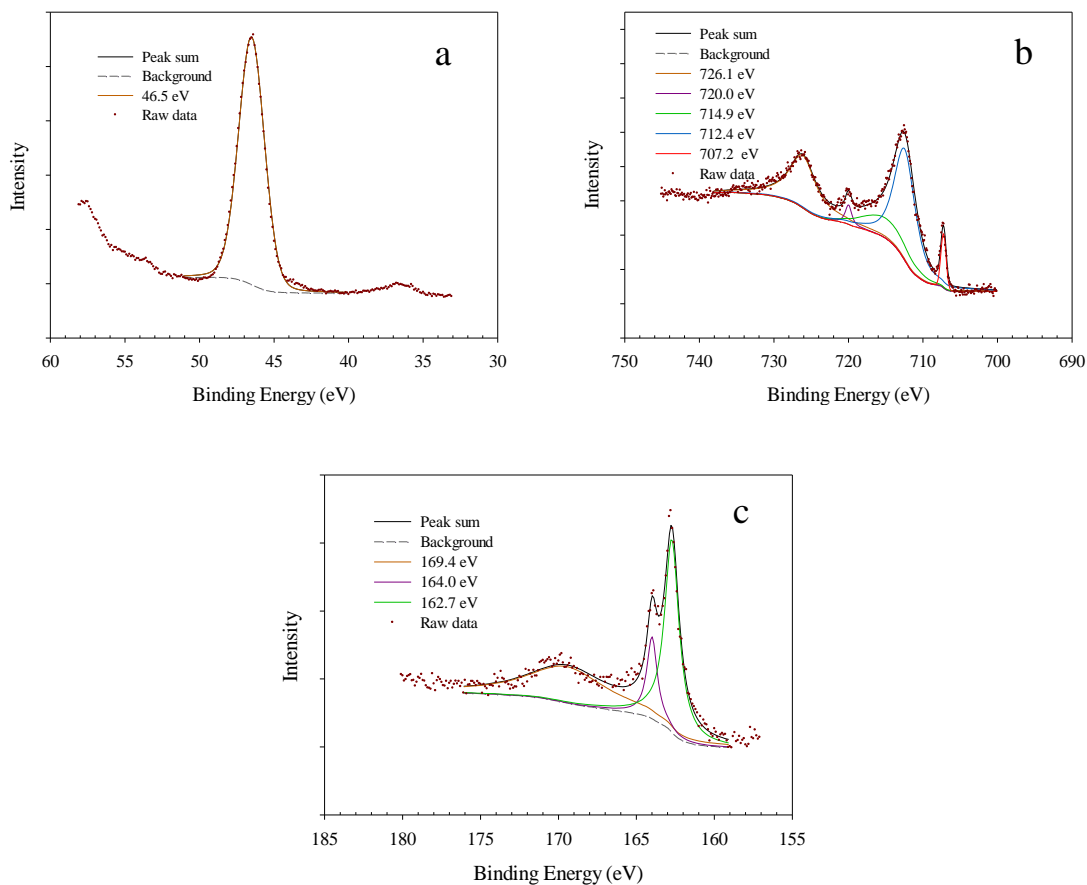


Figure 8-14. XPS spectra of the leaching residue from hydrochloric acid experiment for (a) arsenic 3d, (b) iron 2p, (c) sulfur 2p

The XPS spectra of the AF 5 catalyst after the leaching experiment for arsenic 3d, iron 2p, sulfur 2p and oxygen 1s peaks in Figure 8-15 validates the existence of As(V) on the catalyst at 45.9 eV (Zhu et al., 2014). For iron 2p spectra, three peaks were fitted with and without the Fe 2p_{3/2} was located at 712.3 eV assigned to the existence of ferric ions on the catalyst surface (Zhu et al., 2014). Some of the peaks for sulfur groups are difficult to distinguish because of the complicated bonding and overlaps of bands, and the existence of initial functional groups makes it even more intricate (Zhu et al., 2014). The sulfur fitted peaks are located at 168.8 (Zhu et al., 2014), 164.8 (Zhu et al., 2014), and 163.8 eV (Zhu et al., 2014), similar to the initial sulfur peaks on the surface of AF 5 but with much higher intensities. These peaks are assigned to the sulfate, elemental sulfur, and

polysulfide groups collected by AF 5 by adsorption of polymeric chain or capillary adsorption. One of the possible mechanisms which can be proposed for the sulfur collection is the adsorption of meta-stable polysulfide groups which were evolved as the result of leaching by the polymeric adsorption of the sulfur groups on the surface of the catalyst.

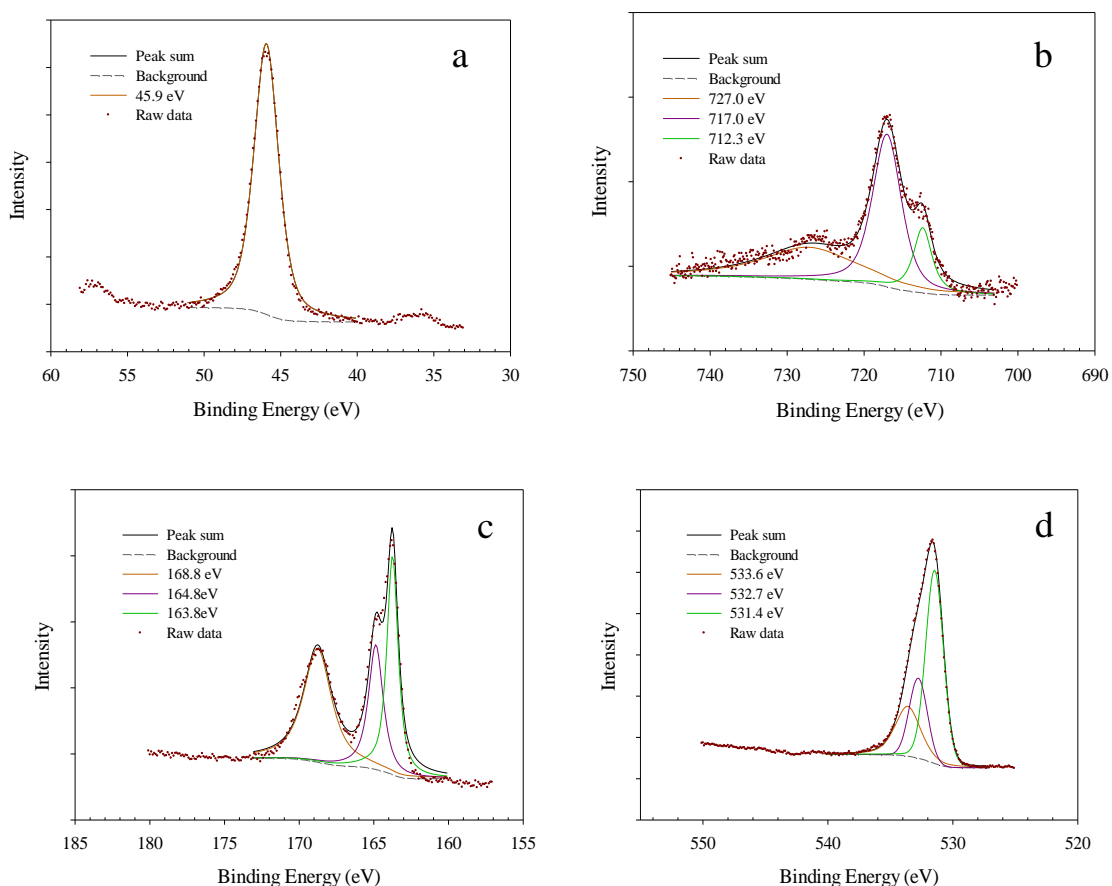


Figure 8-15. XPS spectra of the AF 5 used in leaching experiment for (a) arsenic 3d, (b) iron 2p, (c) sulfur 2p, (d) oxygen 1s

The XPS spectra of nitric acid-treated AF 5 after the leaching experiment are similar to the other post-leaching AF 5 samples, however the availability of oxygen functional groups are different. The nitrogen 1s spectra presented in Figure 8-16 can be deconvoluted to three main peaks similar to prior leaching peaks at 405.6, 402, and 400.1 eV. These peaks confirm the existence of generated functional groups on the surface of the catalyst even after 96 h of leaching. However, the

contribution of these groups has significantly changed, and peak intensities are considerably reduced. The contribution of oxidized nitrogen functionalities reduced from 52.8% to 32.2%.

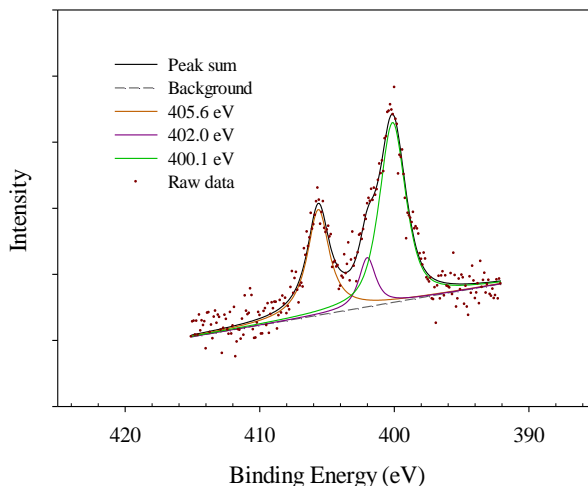


Figure 8-16. XPS spectra of nitrogen 1s peak for nitric acid treated AF 5 after 96 h of leaching

8.3 Conclusions

AF 5 is a carbon-based catalyst which can effectively increase the oxidative leaching kinetics of sulfide minerals, including enargite and pyrite. The catalytic effect of carbon-based catalysts such as AF 5 in leaching processes is attributed to their surface functional groups, and chemical pre-treatment is a viable method to alter the functional groups on the surface of catalysts. In the present study AF 5 was pre-treated with different acidic solutions and the functional groups on its surface was studied. The AF 5 surface characterization after different chemical pre-treatments confirmed that nitric acid and sulfuric acid pre-treatment processes both could introduce functional groups such as nitrogen and thiol on its surface, as well as increase the oxygen functional groups. The oxygen functional groups that form with the oxidative pre-treatment results in the formation of more oxygen double bonds such as quinone groups which can significantly increase the catalytic capability of AF 5 for oxidation reactions. The treatment of AF 5 with ferric ion, in the presence of oxygen, resulted in the reduction of 60% of ferric to ferrous. This initial ferric reduction was

decreased to only 14% when the AF 5 was pre-treated with nitric acid, and it was increased to 100% when the oxygen was not present in the system. The existence of oxygen is found to be the key for arsenic oxidation, although the presence of ferric and cupric ions can also enhance the As(III) to As(V) oxidation to some limited extent.

The AF 5 catalysts with different pre-treatment were used in enargite leaching tests. The nitric acid pre-treated AF 5 showed superior enargite leaching catalytic properties, where 98.8% copper and 93.8% iron could be recovered into the pregnant leach solution. However, the precipitation of arsenic in the form of scorodite solely occurred in the leaching tests in the chloride media. In addition, the sulfuric acid leaching led to 97.1% copper recovery as well as a pyrite oxidation of about 82.5%. The lowest copper recovery was obtained in the leaching tests in the chloride media, with only 88.6% Cu recovery.

One unique property of AF 5 is its sulfur adsorption capacity. More elemental sulfur was collected on AF 5 when the leach tests were carried out in sulfuric acid solution and the AF 5 was pre-treated in sulfuric acid. It is believed that the sulfur adsorption to AF 5 potentially occurs by the chemical or physical adsorption of meta-stable polysulfide groups on the surface of the catalyst.

The XRD study on the post leaching residue indicated the existence of scorodite and pyrite. Based on the XPS spectra of the post leaching catalyst surface, the nitrogen functionalities concentration, specially oxidized nitrogen functionalities, were reduced on the surface of the nitric acid pre-treated AF 5.

Chapter 9

General conclusions and recommendations

9.1 Conclusions

The aim of this study was to understand the dissolution of enargite in the presence of the two carbon-based catalysts: activated carbon (AC) and AF 5. The catalysts were applied to improve the enargite leaching rate as well as to immobilize arsenic during the leach process. This thesis research work was carried out in 5 main sections focusing on (1) catalyst characterization, (2) the study of process parameters of the leaching process, (3) kinetics of leaching in the presence of the catalysts, (4) arsenic behavior and arsenic fixation mechanism during the catalytic leach process, and finally (5) the study of the effect of chemical pre-treatment of the catalysts on leaching kinetics.

The enargite leaching process kinetics was enhanced significantly in the presence of AC and AF 5 catalysts. Both of the catalysts were proven to be very efficient and increased the copper recovery from 69% (no catalyst) to 92% (AF 5) and 96% (AC) in 96 h of leaching. Several effective parameters were discussed in Chapter 4, of which, among those, the most important parameters were found to be the temperature, catalyst addition, oxidant and oxygen presence. By increasing the catalyst ratio the copper recovery improved, however, a concentrate to catalyst ratio of 1:2 for AC and 1:1 for AF 5 were found to be sufficient for acceptable leaching kinetics. Further investigation showed that oxygen is a key factor for catalytic activity of AC and AF 5, however, higher sparging rates than 0.1 L/min did not show a significant effect on the recovery.

Temperature has a profound effect on the recovery, and the best leaching results, regardless of catalyst type and addition, were achieved at 90 °C.

Higher surface area might be one of the reasons behind higher catalytic effect of AF 5 compare to AC. By increasing the surface area of the catalyst, the copper recovery improves. Therefore CBC with higher surface area is more desirable for leaching catalysis.

The shrinking core model was used as the general kinetic model to study the enargite leaching kinetics at different temperatures. In the chloride media cupric ions were proven to be more effective than the ferric ions as the result of the strong bonding and stable species of copper in the chloride solution. It was shown that the diffusion of cupric ions through the product layer on partially leached enargite particles is the controlling step. It was confirmed that the addition of the AC and AF 5 catalysts did not change the process reaction controlling mechanism. The formation of the product layer on the mineral surface was confirmed with electrochemical chronoamperometry tests. Scanning electron microscopy images of the partially leached minerals confirmed that no impermeable elemental sulfur layer was formed on the enargite surface.

In the enargite leaching tests with a catalyst in chloride media the arsenic could precipitate in the leaching reactor in the form scorodite. The temperature, oxygen sparging rate, the different fractions of the catalyst and ferric ions were effective parameters on the scorodite precipitation process. Crystalline scorodite was precipitated out of the leach solution in the absence of seed at temperatures above 80 °C where the ratio of both AF5 to concentrate and AC to concentrate were 1:2 and 1:1, respectively. The minimal dosage of ferric ions to form the scorodite residue was 5 g/L. The seed addition facilitated the scorodite precipitation process where the primary scorodite particles precipitated after 6 h of enargite leaching. The ferric-ferrous titration indicated a sharp decline in the ferric concentration while forming the scorodite precipitates. It was shown that the residual concentration of arsenic in the pregnant leach solution was as low as <50 mg/L. A series of the toxicity characteristic leaching procedure (TCLP) tests on the residue scorodite exhibited a low arsenic release ranging from 0.2 to 0.7 mg/L, showing an acceptable stability of the scorodite residue.

The surface study of the AF 5 catalyst revealed that oxygen and sulfur functional groups were available on the surface of the catalyst. The chemical pre-treatment methods increased the concentration of the oxygen functional groups and evolved other functional groups such as

nitrogen. By pre-treatment the ability of the catalyst increased significantly and not only the copper dissolution rate increased in the nitric acid pretreatment, but also iron dissolution from pyrite increased significantly.

Generally, sulfate media showed a better dissolution environment than the chloride media for copper and specially iron in the same leaching condition (with just ferric as the oxidant). However, the scorodite formation was not observed in the sulfate system and, the sulfate leaching system seemed to improve the sulfur yield on the AF 5 catalyst. The collection of elemental sulfur by AF 5 catalyst in different leaching media varied from 31% in the chloride media to 51% in sulfate system.

9.2 Recommendations

The recommended for future work are the following:

- The effect of cupric and ferric ions on the dissolution of enargite in the presence of catalyst should be studied in electrochemical kinetic experiments to investigate the effect of these ions on the enargite dissolution process.
- The mechanism of elemental sulfur deposition on the AF 5 catalysts has been not fully understood and therefore needs further investigation.
- The recycling process for AF 5 needs further investigation and possible recycling paths should be studied.
- The oxidation potential of recycled AF 5 needs to be studied.
- The link between Cu/Fe ratio, synergetic effect of Cu and Fe and total iron and copper in leach solution should be studied.

References

- Ahumada, E., Lizama, H., Orellana, F., Suarez, C., Huidobro, A., Seouveda-Escribano, A., Rodriquez-Reinoso, F., 2002. Catalytic oxidation of Fe (II) by activated carbon in the presence of oxygen . Effect of the surface oxidation degree on the catalytic activity. *Carbon* N. Y. 40, 2827–2834.
- Akilan, C., Nicol, M.J., 2016. Kinetics of the oxidation of iron(II) by oxygen and hydrogen peroxide in concentrated chloride solutions - A re-evaluation and comparison with the oxidation of copper(I). *Hydrometallurgy* 166, 123–129.
doi:10.1016/j.hydromet.2016.10.014
- Al-Harashseh, M., Kingman, S., Al-Harashseh, A., 2008. Ferric chloride leaching of chalcopyrite: Synergetic effect of CuCl₂. *Hydrometallurgy* 91, 89–97.
doi:10.1016/j.hydromet.2007.11.011
- Andreas, H.A., Conway, B.E., 2006. Examination of the double-layer capacitance of an high specific-area C-cloth electrode as titrated from acidic to alkaline pHs. *Electrochim. Acta* 51, 6510–6520. doi:10.1016/j.electacta.2006.04.045
- Arcibar-Orozco, J.A., Josue, D.-B., Rios-Hurtado, J.C., Rangel-Mendez, J.R., 2014. Influence of iron content, surface area and charge distribution in the arsenic removal by activated carbons. *Chem. Eng. J.* 249, 201–209. doi:10.1016/j.cej.2014.03.096
- Aylmore, M., 2012. Evaluating process options for treating some refractory ores, in: ALTA. Perth, Australia.
- Baláž, P., Achimovičová, M., 2006. Selective leaching of antimony and arsenic from mechanically activated tetrahedrite, jamesonite and enargite. *Int. J. Miner. Process.* 81, 44–50. doi:10.1016/j.minpro.2006.06.004

- Baláž, P., Achimovičová, M., Bastl, Z., Ohtani, T., Sánchez, M., 2000a. Influence of mechanical activation on the alkaline leaching of enargite concentrate. *Hydrometallurgy* 54, 205–216. doi:10.1016/S0304-386X(99)00071-7
- Baláž, P., Achimovičová, M., Bastl, Z., Ohtani, T., Sánchez, M., 2000b. Influence of mechanical activation on the alkaline leaching of enargite concentrate. *Hydrometallurgy* 54, 205–216. doi:10.1016/S0304-386X(99)00071-7
- Bandosz, T.J., Ania, C.O., 2006. Activated Carbon Surfaces in Environmental Remediation. *Interface Sci. Technol.* 7, 159–229. doi:10.1016/S1573-4285(06)80013-X
- Barr, G., Defreyne, J., Jones, D., Mean, R., 2005a. On-site processing vs. sale of copper concentrates, in: ALTA. Perth, Australia, pp. 1–78.
- Barr, G., Defreyne, J., Mayhew, K., 2005b. CESL copper process - an economic alternative to smelting, CESL Engineering.
- Batty, J.D., Rorke, G. V., 2006. Development and commercial demonstration of the BioCOP thermophile process. *Hydrometallurgy* 83, 83–89. doi:10.1016/j.hydromet.2006.03.049
- Bhatia, S.K., Perlmutter, D.D., 1981. A random pore model for fluid-solid reactions: II. Diffusion and transport effects. *AIChE J.* 27, 247–254. doi:10.1002/aic.690270211
- Biegler, T., 1977. Reduction kinetics of a chalcopyrite electrode surface. *J. Electroanal. Chem. Interfacial Electrochem.* 85, 101–106. doi:10.1016/S0022-0728(77)80155-1
- Biegler, T., Horne, M.D., 1985. The Electrochemistry of Surface Oxidation of Chalcopyrite. *J. Electrochem. Soc.* 132, 1363–1369. doi:10.1149/1.2114117
- Biniak, S., Szymański, G., Siedlewski, J., Świątkoski, A., 1997. The characterization of activated carbons with oxygen and nitrogen surface groups. *Carbon N. Y.* 35, 1799–1810. doi:10.1016/S0008-6223(97)00096-1
- Bluteau, M.-C., Demopoulos, G.P., 2007. The incongruent dissolution of scorodite — Solubility, kinetics and mechanism. *Hydrometallurgy* 87, 163–177.

doi:10.1016/j.hydromet.2007.03.003

Boudou, J.-P.P., Chehimi, M., Broniek, E., Siemienińska, T., Bimer, J., 2003. Adsorption of H₂S or SO₂ on an activated carbon cloth modified by ammonia treatment. *Carbon N. Y.* 41, 1999–2007.

Bowen, P., Hourn, M.M., 2015. Treatment of sulphidic materials. US 8999274 B2.

doi:10.1016/j.(73)

Bruce, R., Mayhew, K., Demopoulos, G.P., Heidel, A., 2010. Arsenic stability and characterization of CESL process residues, in: COM. Niagra Falls.

Caetano, M.L., Ciminelli, V.S.T., Rocha, S.D.F., Spitale, M.C., Caldeira, C.L., 2009. Batch and continuous precipitation of scorodite from dilute industrial solutions. *Hydrometallurgy* 95, 44–52. doi:10.1016/j.hydromet.2008.04.010

Callister, W., Rethwisch, D., 2007. Materials science and engineering: an introduction, *Materials Science and Engineering*. John Wiley & Sons, Inc. doi:10.1016/0025-5416(87)90343-0

Chang, Q., Lin, W., Ying, W., 2010. Preparation of iron-impregnated granular activated carbon for arsenic removal from drinking water. *J. Hazard. Mater.* 184, 515–22.

doi:10.1016/j.jhazmat.2010.08.066

Chingombe, P., Saha, B., Wakeman, R.J., 2005. Surface modification and characterisation of a coal-based activated carbon. *Carbon N. Y.* 43, 3132–3143.

doi:10.1016/j.carbon.2005.06.021

Christov, C., 2001. Thermodynamic study of the K-Mg-Al-Cl-SO₄-H₂O system at the temperature 298.15 K. *Calphad Comput. Coupling Phase Diagrams Thermochem.* 25, 445–454. doi:10.1016/S0364-5916(01)00063-3

Córdoba, E.M., Muñoz, J. a., Blázquez, M.L., González, F., Ballester, a., 2008a. Leaching of chalcopyrite with ferric ion. Part III: Effect of redox potential on the silver-catalyzed process. *Hydrometallurgy* 93, 97–105. doi:10.1016/j.hydromet.2007.11.006

- Córdoba, E.M., Muñoz, J. a., Blázquez, M.L., González, F., Ballester, a., 2008b. Leaching of chalcopyrite with ferric ion. Part IV: The role of redox potential in the presence of mesophilic and thermophilic bacteria. *Hydrometallurgy* 93, 106–115.
doi:10.1016/j.hydromet.2007.11.005
- Córdoba, E.M., Muñoz, J.A., Blázquez, M.L., González, F., Ballester, A., 2008c. Leaching of chalcopyrite with ferric ion. Part I: General aspects. *Hydrometallurgy* 93, 81–87.
doi:10.1016/j.hydromet.2008.04.015
- Cowan, D.H., Jahromi, F.G., Ghahreman, A., 2017. Atmospheric oxidation of pyrite with a novel catalyst and ultra-high elemental sulphur yield. *Hydrometallurgy* 173, 156–169.
doi:10.1016/j.hydromet.2017.07.003
- Dean, J.A., 1999. *Lange's handbook of chemistry*, 15th ed, McGraw-Hill.
doi:10.1080/10426919008953291
- Debekaussen, R., Droppert, D., Demopoulos, G.P., 2001. Ambient pressure hydrometallurgical conversion of arsenic trioxide to crystalline scorodite. *CIM Bull.* 94, 116–122.
- Demopoulos, G.P., 2009. Aqueous precipitation and crystallization for the production of particulate solids with desired properties. *Hydrometallurgy* 96, 199–214.
doi:10.1016/j.hydromet.2008.10.004
- Demopoulos, G.P., Droppert, D.J., Van Weert, G., 1995. Precipitation of crystalline scorodite ($\text{FeAsO} \cdot 2\text{H}_2\text{O}$) from chloride solutions. *Hydrometallurgy* 38, 245–261.
- Di Natale, F., Erto, A., Lancia, A., 2013. Desorption of arsenic from exhaust activated carbons used for water purification. *J. Hazard. Mater.* 260, 451–458.
doi:10.1016/j.jhazmat.2013.05.055
- Dixon, D.G., Mayne, D.D., Baxter, K.G., 2008. GalvanoxTM – a Novel Galvanically-Assisted Atmospheric Leaching Technology for Copper Concentrates. *Can. Metall. Q.* 47, 327–336.
doi:10.1179/000844308794408317

- Dixon, D.G., Rivera-Vasquez, B., 2012. Leaching process for copper concentrates with a carbon catalyst. US 2012/0279357.
- Dreisinger, D., 2014. Hydrometallurgical treatment of arsenic containing materials, in: Com 2014.
- Droppert, D.J., 1996. The ambient pressure precipitation of crystalline scorodite ($\text{FeAsO}_4 \cdot 2\text{H}_2\text{O}$) from sulphate solutions. McGill.
- Dutrizac, J., 1990. Elemental sulphur formation during the ferric chloride leaching of chalcopyrite. *Hydrometallurgy* 23, 153–176. doi:10.1016/0304-386X(90)90002-J
- Dutrizac, J.E., 1992. The leaching of sulfide minerals in chloride media. *Hydrometallurgy* 29, 1–45. doi:10.1016/0304-386X(95)00003-Y
- Dutrizac, J.E., 1989. Elemental Sulphur Formation During the Ferric Sulphate Leaching of Chalcopyrite. *Can. Metall. Q.* 28, 337–344. doi:10.1179/000844389795576230
- Dutrizac, J.E., Jambor, J.L., 1988. The synthesis of crystalline scorodite. *Hydrometallurgy* 19, 377–384.
- Dutrizac, J.E., Jambor, J.L., 1987. The behaviour of arsenic during jarosite precipitation: Arsenic precipitation at 97°C from sulphate or chloride media. *Can. Metall. Q.* 26, 91–101. doi:10.1179/cm.1987.26.2.91
- Dutrizac, J.E., MacDonald, R.J.C., 1972. The kinetics of dissolution of enargite in acidified ferric sulphate solutions. *Can. Metall. Q.* 11, 469–477.
- Escobar, B., Huenupi, E., Godoy, I., Wiertz, J. V., 2000. Arsenic precipitation in the bioleaching of enargite by *Sulfolobus* BC at 70 °C. *Biotechnol. Lett.* 22, 205–209. doi:10.1023/A:1005610226677
- Fantauzzi, M., Elsener, B., Atzei, D., Rigoldi, A., Rossi, A., 2015. Exploiting XPS for the identification of sulfides and polysulfides. *RSC Adv.* 5, 75953–75963. doi:10.1039/C5RA14915K

- Figueiredo, J., Pereira, M.F., Freitas, M.M., Órfão, J.J., Jansen, R.J.J., van Bekkum, H., Chingombe, P., Saha, B., Wakeman, R.J., Biniak, S., Szymański, G., Siedlewski, J., Świątkoski, A., Bandosz, T.J., Ania, C.O., Jia, Q., Ramaswamy, N., Tylus, U., Strickland, K., Li, J., Serov, A., Artyushkova, K., Atanassov, P., Anibal, J., Gumeci, C., Barton, S.C., Sougrati, M.T., Jaouen, F., Halevi, B., Mukerjee, S., Menéndez-Díaz, J.A., Martín-Gullón, I., Inagaki, M., Tascón, J.M.D., Bandosz, T.J., 2006. Activated Carbon Surfaces in Environmental Remediation. *Interface Sci. Technol.* 7, 65–82. doi:10.1016/S0008-6223(98)00333-9
- Figueiredo, J.L., Pereira, M.F.R., 2010. The role of surface chemistry in catalysis with carbons. *Catal. Today* 150, 2–7. doi:10.1016/j.cattod.2009.04.010
- Figueiredo, J.L., Pereira, M.F.R., Freitas, M.M. a, Órfão, J.J.M., 1999. Modification of the surface chemistry of activated carbons. *Carbon N. Y.* 37, 1379–1389. doi:10.1016/S0008-6223(98)00333-9
- Filippou, D., Demopoulos, G.P., 1997. Arsenic immobilization by controlled scorodite precipitation. *Jom* 49, 52–55. doi:10.1007/s11837-997-0034-3
- Frau, F., Rossi, A., Ardaù, C., Biddau, R., Da Pelo, S., Atzei, D., Licheri, C., Cannas, C., Capitani, G., 2005. Determination of arsenic speciation in complex environmental samples by the combined use of TEM and XPS. *Microchim. Acta* 151, 189–201. doi:10.1007/s00604-005-0399-3
- Fujita, T., Taguchi, R., Abumiya, M., Matsumoto, M., Shibata, E., Nakamura, T., 2009. Effect of pH on atmospheric scorodite synthesis by oxidation of ferrous ions: Physical properties and stability of the scorodite. *Hydrometallurgy* 96, 189–198. doi:10.1016/j.hydromet.2008.10.003
- Fujita, T., Taguchi, R., Abumiya, M., Matsumoto, M., Shibata, E., Nakamura, T., 2008. Effects of zinc, copper and sodium ions on ferric arsenate precipitation in a novel atmospheric

- scorodite process. *Hydrometallurgy* 93, 30–38. doi:10.1016/j.hydromet.2008.02.016
- Garavelli, A., Pinto, D., Vurro, F., Mellini, M., Viti, C., Balić-Žunić, T., Ventura, G. Della, 2009. Yukonite from the grota della monaca cave, sant'agata di esaro, Italy: characterization and comparison with cotype material from the daulton mine, Yukon, Canada. *Can. Mineral.* 47, 39–51. doi:10.3749/canmin.47.1.39
- Gbor, P.K., Jia, C.Q., 2004. Critical evaluation of coupling particle size distribution with the shrinking core model. *Chem. Eng. Sci.* 59, 1979–1987. doi:10.1016/j.ces.2004.01.047
- Georgiou, D., Papangelakis, V.G., 1998. Sulphuric acid pressure leaching of a limonitic laterite: chemistry and kinetics. *Hydrometallurgy* 49, 23–46. doi:10.1016/S0304-386X(98)00023-1
- Ghahreman, A., 2018. Hydrometallurgy of copper concentrates : opportunities and complexities, in: *Copper Workshop*. Santiago, pp. 1–60.
- Ghahremaninezhad, A., Dixon, D.G., Asselin, E., 2012. Kinetics of the ferric–ferrous couple on anodically passivated chalcopyrite (CuFeS₂) electrodes. *Hydrometallurgy* 125, 42–49. doi:10.1016/j.hydromet.2012.05.004
- Ghahremaninezhad, A., Radzinski, R., Gheorghiu, T., Dixon, D.G., Asselin, E., 2015. A model for silver ion catalysis of chalcopyrite (CuFeS₂) dissolution. *Hydrometallurgy* 155, 95–104. doi:10.1016/j.hydromet.2015.04.011
- Ghanad, I., 2011. Atmospheric leaching of enargite in iron sulphate solutions catalyzed by activated carbon. University of British Columbia.
- Gupta, M.Z., 2010. An investigation into the leaching of enargite under atmospheric condition.
- Harvey, T.J., Holder, N., Stanek, T., 2002. Thermophilic Bioleaching of Chalcopyrite Concentrates with GEOCOAT Process, in: *ALTA*. pp. 1–19.
- Harvey, T.J., Ph, D., Shield, J.W., Crowell, R.M., 1999. GEOCOAT™ Biooxidation Demonstration at Ashanti Goldfields ' Obuasi Operations , Ghana , West Africa 1–8.
- Haver, F.P., Wong, M.M., 1971. Recovery of copper, iron, and sulphur from chalcopyrite

- concentrate using ferric chloride leach. *J. Met.* 23, 25–29.
- Henke, K.R., 2009. *Arsenic: environmental chemistry, health threats and waste treatment*, Wiley.
doi:10.1002/9780470741122
- Herreros, O., Quiroz, R., Hernandez, M.C., Viñals, J., 2002. Dissolution kinetics of enargite in dilute Cl₂/Cl media. *Hydrometallurgy* 64, 153–160.
- Hiroyoshi, N., Arai, M., Miki, H., Tsunekawa, M., Hirajima, T., 2002. A new reaction model for the catalytic effect of silver ions on chalcopyrite leaching in sulfuric acid solutions. *Hydrometallurgy* 63, 257–267. doi:10.1016/S0304-386X(01)00228-6
- Hiroyoshi, N., Kuroiwa, S., Miki, H., Tsunekawa, M., Hirajima, T., 2007. Effects of coexisting metal ions on the redox potential dependence of chalcopyrite leaching in sulfuric acid solutions. *Hydrometallurgy* 87, 1–10. doi:10.1016/j.hydromet.2006.07.006
- Hiroyoshi, N., Kuroiwa, S., Miki, H., Tsunekawa, M., Hirajima, T., 2004. Synergistic effect of cupric and ferrous ions on active-passive behavior in anodic dissolution of chalcopyrite in sulfuric acid solutions. *Hydrometallurgy* 74, 103–116. doi:10.1016/j.hydromet.2004.01.003
- Hourn, M., Turner, D.W., Hourn, M., 2012. Commercialisation of the Albion Process, in: *ALTA*. Perth, Australia, pp. 1–19.
- Hulicova-Jurcakova, D., Seredych, M., Lu, G.Q., Bandosz, T.J., 2009. Combined effect of nitrogen- and oxygen-containing functional groups of microporous activated carbon on its electrochemical performance in supercapacitors. *Adv. Funct. Mater.* 19, 438–447.
doi:10.1002/adfm.200801236
- Hyvärinen, O., Hämäläinen, M., 2005. HydroCopper™ - A new technology producing copper directly from concentrate. *Hydrometallurgy* 77, 61–65. doi:10.1016/j.hydromet.2004.09.011
- Jahromi, F.G., Cowan, D.H., Ghahreman, A., 2017. Lanxess Lewatit® AF 5 and activated carbon catalysis of enargite leaching in chloride media; a parameters study. *Hydrometallurgy* 174, 184–194. doi:10.1016/j.hydromet.2017.10.012

- Karatepe, N., Orbak, I., Yavuz, R., Özyuğuran, A., 2008. Sulfur dioxide adsorption by activated carbons having different textural and chemical properties. *Fuel* 87, 3207–3215.
doi:10.1016/j.fuel.2008.06.002
- Kloprogge, J.T., Wood, B.J., 2017a. X-ray Photoelectron spectroscopic and Raman spectroscopic study of bayldonite from Wheal Carpenter, Cornwall, UK. *Vacuum* 141, 49–56.
doi:10.1016/j.vacuum.2017.03.018
- Kloprogge, J.T., Wood, B.J., 2017b. X-ray Photoelectron Spectroscopic and Raman microscopic investigation of the variscite group minerals: Variscite, strengite, scorodite and mansfieldite. *Spectrochim. Acta - Part A Mol. Biomol. Spectrosc.* 185, 163–172.
doi:10.1016/j.saa.2017.05.042
- Krause, E., Ettel, V.A., 1989. Solubilities and stabilities of ferric arsenate compounds. *Hydrometallurgy* 22, 311–337. doi:10.1016/0304-386X(89)90028-5
- Kundu, S., Wang, Y., Xia, W., Muhler, M., 2008. Thermal Stability and Reducibility of Oxygen-Containing Functional Groups on Multiwalled Carbon Nanotube Surfaces : A Quantitative High-Resolution XPS and TPD / TPR Study. *J. Phys. Chem. C* 112, 16869–16878.
doi:10.1021/jp804413a
- Lambert, J.M., Simkovich, G., Walker, P.L., 1998. The kinetics and mechanism of the pyrite-to-pyrrhotite transformation. *Metall. Mater. Trans. B* 29, 385–396. doi:10.1007/s11663-998-0115-x
- Langmuir, D., Mahoney, J., Rowson, J., 2006. Solubility products of amorphous ferric arsenate and crystalline scorodite (FeAsO₄·2H₂O) and their application to arsenic behavior in buried mine tailings. *Geochim. Cosmochim. Acta* 70, 2942–2956. doi:10.1016/j.gca.2006.03.006
- Lattanzi, P., Da Pelo, S., Musu, E., Atzei, D., Elsener, B., Fantauzzi, M., Rossi, A., 2008. Enargite oxidation: A review. *Earth-Science Rev.* 86, 62–88.
doi:10.1016/j.earscirev.2007.07.006

- Le Berre, J.F., Gauvin, R., Demopoulos, G.P., 2008. A study of the crystallization kinetics of scorodite via the transformation of poorly crystalline ferric arsenate in weakly acidic solution. *Colloids Surfaces A Physicochem. Eng. Asp.* 315, 117–129.
doi:10.1016/j.colsurfa.2007.07.028
- Levenspiel, O., 1999. *Chemical reaction engineering*, 3rd ed. John Wiley & Sons, New York.
doi:10.1016/0009-2509(64)85017-X
- Liddicoat, J., Dreisinger, D., 2007. Chloride leaching of chalcopyrite. *Hydrometallurgy* 89, 323–331. doi:10.1016/j.hydromet.2007.08.004
- Lundström, M., 2009. *Chalcopyrite dissolution in cupric chloride solutions*. Helsinki University of Technology.
- Lundström, M., Aromaa, J., Forsén, O., 2009. Redox potential characteristics of cupric chloride solutions. *Hydrometallurgy* 95, 285–289. doi:10.1016/j.hydromet.2008.06.009
- Lundström, M., Aromaa, J., Forsén, O., Hyvärinen, O., Barker, M.H., 2007. Cathodic reactions of Cu^{2+} in cupric chloride solution. *Hydrometallurgy* 85, 9–16.
doi:10.1016/j.hydromet.2006.07.002
- Lundström, M., Aromaa, J., Forsén, O., Hyvärinen, O., Barker, M.H., 2005. Leaching of chalcopyrite in cupric chloride solution. *Hydrometallurgy* 77, 89–95.
doi:10.1016/j.hydromet.2004.10.013
- Mangun, C.L., DeBarr, J.A., Economy, J., 2001. Adsorption of sulfur dioxide on ammonia-treated activated carbon fibers. *Carbon N. Y.* 39, 1689–1696. doi:10.1016/S0008-6223(00)00300-6
- Martin-Gullon, I., Menendez-Diaz, J.A., 2006. *Types of Carbon Adsorbents and their Properties, Activated Carbon Surfaces in Environmental Remediation*.
- Martinez-Gomez, V.J., Fuentes-Aceituno, J.C., Perez-Garibay, R., Lee, J.C., 2016. A phenomenological study of the electro-assisted reductive leaching of chalcopyrite.

- Hydrometallurgy 164, 54–63. doi:10.1016/j.hydromet.2016.05.008
- Mayhew, K., Mean, R., Miller, C., Thompson, J., Barrios, P., Koenig, C., Omaynikova, V., Wagner, O., 2010. CESL Teck – Aurubis : An integrated mine to metal approach to develop high arsenic copper deposits usin.
- McDonald, G.W., Udovic, T.J., Dumesic, J.A., Langer, S.H., 1984. Equilibria associated with cupric chloride leaching of chalcopyrite concentrate. *Hydrometallurgy* 13, 125–135. doi:10.1016/0304-386X(84)90022-7
- Miki, H., Nicol, M., 2008. The kinetics of the copper-catalysed oxidation of iron(II) in chloride solutions, in: *Hydrometallurgy 2008: 6th International Symposium*. Phoenix, AZ, pp. 971–979.
- Molnar, R.E., Verabaan, N., 2003. Extraction of Copper At Elevated Feed Concentrations.
- Montes-Morán, M.A., Suárez, D., Menéndez, J.A., Fuente, E., 2004. On the nature of basic sites on carbon surfaces: an overview. *Carbon N. Y.* 42, 1219–1225. doi:10.1016/j.carbon.2004.01.023
- Moreno-Piraján, J.C., Giraldo, L., 2013. Activated carbon from bamboo waste modified with iron and its application in the study of the adsorption of arsenite and arsenate. *Cent. Eur. J. Chem.* 11, 160–170. doi:10.2478/s11532-012-0138-7
- Nadkarni, R., Kusik, C., 1988. Hydrometallurgical removal of arsenic from copper concentrates. *Arsen. Metall. Fundam. Appl.* 263–286.
- Narita, E., Lawson, F., Han, K.N., 1983. Solubility of oxygen in aqueous electrolyte solutions. *Hydrometallurgy*. doi:10.1016/0304-386X(83)90074-9
- Nazari, A.M., Radzinski, R., Ghahreman, A., 2017. Review of arsenic metallurgy: Treatment of arsenical minerals and the immobilization of arsenic. *Hydrometallurgy* 174, 258–281. doi:10.1016/j.hydromet.2016.10.011
- Nazari, G., Dixon, D.G., Dreisinger, D.B., 2012. The mechanism of chalcopyrite leaching in the

- presence of silver-enhanced pyrite in the Galvanox process. *Hydrometallurgy* 113–114, 122–130. doi:10.1016/j.hydromet.2011.12.011
- Nazari, G., Dixon, D.G., Dreisinger, D.B., 2011. Enhancing the kinetics of chalcopyrite leaching in the Galvanox™ process. *Hydrometallurgy* 105, 251–258. doi:10.1016/j.hydromet.2010.10.013
- Padilla, R., Girón, D., Ruiz, M.C., 2005a. Leaching of enargite in H₂SO₄–NaCl–O₂ media. *Hydrometallurgy* 80, 272–279. doi:10.1016/j.hydromet.2005.08.006
- Padilla, R., Girón, D., Ruiz, M.C., 2005b. Leaching of enargite in H₂SO₄–NaCl–O₂ media. *Hydrometallurgy* 80, 272–279. doi:10.1016/j.hydromet.2005.08.006
- Padilla, R., Rivas, C.A., Ruiz, M.C., 2008a. Kinetics of pressure dissolution of enargite in sulfate-oxygen media. *Metall. Mater. Trans. B Process Metall. Mater. Process. Sci.* 39, 399–407. doi:10.1007/s11663-008-9151-9
- Padilla, R., Rivas, C.A., Ruiz, M.C., 2008b. Kinetics of pressure dissolution of enargite in sulfate-oxygen media. *Metall. Mater. Trans. B Process Metall. Mater. Process. Sci.* 39, 399–407. doi:10.1007/s11663-008-9151-9
- Padilla, R., Rodríguez, G., Ruiz, M.C., 2010. Copper and arsenic dissolution from chalcopyrite – enargite concentrate by sulfidation and pressure leaching in H₂SO₄ – O₂. *Hydrometallurgy* 100, 152–156. doi:10.1016/j.hydromet.2009.11.006
- Palmer, C.M., Johnson, G.D., 2005. The Activox process: Growing significance in the nickel industry. *J. Miner. Met. Mater. Soc.* 57, 40–47. doi:10.1007/s11837-005-0251-6
- Parada, F., Jeffrey, M.I., Asselin, E., 2014. Leaching kinetics of enargite in alkaline sodium sulphide solutions. *Hydrometallurgy* 146, 48–58. doi:10.1016/j.hydromet.2014.03.003
- Park, H., Koduru, J.R., Choo, K., Lee, B., 2015. Activated carbons impregnated with iron oxide nanoparticles for enhanced removal of bisphenol A and natural organic matter. *J. Hazard. Mater.* 286, 315–324. doi:10.1016/j.jhazmat.2014.11.012

- Park, K.-H., Lee, C.-H., Ryu, S.-K., Yang, X., 2007. Zeta-potentials of Oxygen and Nitrogen Enriched Activated Carbons for Removal of Copper Ion. *Carbon Lett.* 8, 321–325.
doi:10.5714/CL.2007.8.4.321
- Parker, A.J., Paul, R.L., Power, G.P., 1981. Electrochemical aspects of leaching copper from chalcopyrite in ferric and cupric salt solutions. *Aust. J. Chem.* 34, 13–34.
doi:10.1071/CH9810013
- Peacey, J.G., Gupta, M.Z., Ford, K.J.R., 2010. Review of Process Options to Treat Enargite Concentrates, in: *Copper*. pp. 1–17.
- Pevida, C., Plaza, M.G., Arias, B., Feroso, J., Rubiera, F., Pis, J.J., 2008. Surface modification of activated carbons for CO₂ capture. *Appl. Surf. Sci.* 254, 7165–7172.
doi:10.1016/j.apsusc.2008.05.239
- Puziy, A.M., Poddubnaya, O.I., Socha, R.P., Gurgul, J., Wisniewski, M., 2008. XPS and NMR studies of phosphoric acid activated carbons. *Carbon N. Y.* 46, 2113–2123.
doi:10.1016/j.carbon.2008.09.010
- Radzinski, R.L., 2017. An investigation in to the carbon-catalyzed arsenic oxidation process. Queen’s University.
- Raghavan, S., Gajam, S., 1983. A kinetic study of enargite dissolution in ammoniacal solutions. *Int. J. Miner. Process.* 10, 113–129.
- Rawlings, D.E., Johnson, D.B., 2007. *Biomining*, 1st ed. Springer. doi:10.1007/978-3-540-34911-2
- Reddad, Z., Gerente, C., Andres, Y., Le Cloirec, P., 2002. Adsorption of several metal ions onto a low-cost biosorbent: kinetic and equilibrium studies. *Environ. Sci. Technol.* 36, 2067–2073.
doi:Doi 10.1021/Es0102989
- Rivera-Vasquez, B.F., Dixon, D., 2015. Rapid atmospheric leaching of enargite in acidic ferric sulfate media. *Hydrometallurgy* 152, 149–158. doi:10.1016/j.hydromet.2014.12.012

- Riveros, P.A., Dutrizac, J.E., 2008. The leaching of tennantite, tetrahedrite and enargite in acidic sulphate and chloride media. *Can. Metall. Q.* 47, 235–244.
doi:10.1179/000844308794408227
- Robins, R.G., 1987. Solubility and stability of scorodite, $\text{FeAsO}_4 \cdot 2\text{H}_2\text{O}$: Discussion. *Am. Mineral.* 72, 842–844.
- Rohner, P., Bartsch, P., Ngoviky, K., 2012. Benefits of Using the Albion Process for a North Queensland Project, and a Case Study of Capital and Operating Cost Benefits Versus Bacterial Oxidation and Pressure Oxidation. Perth, Australia.
- Rosas, J.M., Ruiz-Rosas, R., Rodríguez-Mirasol, J., Cordero, T., 2017. Kinetic study of SO_2 removal over lignin-based activated carbon. *Chem. Eng. J.* 307, 707–721.
doi:10.1016/j.cej.2016.08.111
- Roy, P., Mondal, N.K., Das, K., 2014. Modeling of the adsorptive removal of arsenic: A statistical approach. *J. Environ. Chem. Eng.* 2, 585–597. doi:10.1016/j.jece.2013.10.014
- Ruiz, M.C., Vera, M. V., Padilla, R., 2011. Mechanism of enargite pressure leaching in the presence of pyrite. *Hydrometallurgy* 105, 290–295. doi:10.1016/j.hydromet.2010.11.002
- Ruiz, M.C., Vera, M. V., Padilla, R., 2011. Hydrometallurgy Mechanism of enargite pressure leaching in the presence of pyrite. *Hydrometallurgy* 105, 290–295.
doi:10.1016/j.hydromet.2010.11.002
- Safari, V., Arzpeyma, G., Rashchi, F., Mostoufi, N., 2009. A shrinking particle—shrinking core model for leaching of a zinc ore containing silica. *Int. J. Miner. Process.* 93, 79–83.
doi:10.1016/j.minpro.2009.06.003
- Safarzadeh, M.S., City, S.L., Moats, M.S., 2012. Preprint 12-068 EVALUATION OF SULFURIC ACID BAKING AND LEACHING OF ENARGITE CONCENTRATES 1–6.
- Safarzadeh, M.S., Moats, M.S., Miller, J.D., 2012. Recent Trends in the Processing of Enargite Concentrates. *Miner. Process. Extr. Metall. Rev.* 121016112728008.

doi:10.1080/08827508.2012.725683

Safarzadeh, M.S., Moats, M.S., Miller, J.D., 2012. An Update to “Recent Trends in the Processing of Enargite Concentrates.” *Miner. Process. Extr. Metall. Rev.*

121016112728008. doi:10.1080/08827508.2012.725683

Safarzadeh, M.S., Moats, M.S., Miller, J.D., 2012. Hydrometallurgy Acid bake-leach process for the treatment of enargite concentrates. *Hydrometallurgy* 119–120, 30–39.

doi:10.1016/j.hydromet.2012.03.002

Shah, I., Adnan, R., Ngah, W.S.W., Mohamed, N., 2015. Iron impregnated activated carbon as an efficient adsorbent for the removal of methylene blue: Regeneration and kinetics studies.

PLoS One 10, 1–23. doi:10.1371/journal.pone.0122603

Shim, J.W., Park, S.J., Ryu, S.K., 2001. Effect of modification with HNO₃ and NaOH on metal adsorption by pitch-based activated carbon fibers. *Carbon N. Y.* 39, 1635–1642.

doi:10.1016/S0008-6223(00)00290-6

Shin, S., Jang, J., Yoon, S.-H., Mochida, I., 1997. A study on the effect of heat treatment on functional groups of pitch based activated carbon fiber using FTIR. *Carbon N. Y.* 35, 1739–

1743. doi:10.1016/S0008-6223(97)00132-2

Singhania, S., Wang, Q., Filippou, D., Demopoulos, G.P., 2006. Acidity, valency and third-ion effects on the precipitation of scorodite from mixed sulfate solutions under atmospheric-

pressure conditions. *Metall. Mater. Trans. B Process Metall. Mater. Process. Sci.* 37, 189–197. doi:10.1007/BF02693148

Souza, A.D., Pina, P.S., Leão, V.A., Silva, C.A., Siqueira, P.F., 2007. The leaching kinetics of a zinc sulphide concentrate in acid ferric sulphate. *Hydrometallurgy* 89, 72–81.

doi:10.1016/j.hydromet.2007.05.008

Stieper, G., 2018. Sable Plant, Zambia An Industrial Facility Transformation to Treat Complex Chalcopyrite Copper Concentrates Using Albion Process™ Technology, in: *Hydroprocess.*

- Subrt, J., Stengl, V., Skokanek, M., 1992. Decomposition of ferrihydrite prepared from $\text{Fe}(\text{NO}_3)_3$ aqueous solutions under varying pH. *Thermochim. Acta* 211, 107–119. doi:10.1016/0040-6031(92)87011-X
- Sun, F., Gao, J., Liu, X., Tang, X., Wu, S., 2015. A systematic investigation of SO_2 removal dynamics by coal-based activated cokes: The synergic enhancement effect of hierarchical pore configuration and gas components. *Appl. Surf. Sci.* 357, 1895–1901. doi:10.1016/j.apsusc.2015.09.118
- Swash, P.M., Monhemius, A.J., 1994. Hydrothermal precipitation from aqueous solutions containing iron(III), arsenate and sulphate, in: *Hydrometallurgy '94: Papers Presented at the International Symposium 'Hydrometallurgy '94' Organized by the Institution of Mining and Metallurgy and the Society of Chemical Industry, and Held in Cambridge, England, from 11 to 15 July, 1994.* Springer Netherlands, Dordrecht, pp. 177–190. doi:10.1007/978-94-011-1214-7_10
- Takatsugi, K., Sasaki, K., Hirajima, T., 2011. Mechanism of the enhancement of bioleaching of copper from enargite by thermophilic iron-oxidizing archaea with the concomitant precipitation of arsenic. *Hydrometallurgy* 109, 90–96. doi:10.1016/j.hydromet.2011.05.013
- Technologies, M.I.M.P., 1991. *IsaMill Ultrafine Grinding for a Sulphide Leach Process. Analysis.*
- Terzyk, A.P., 2001. The influence of activated carbon surface chemical composition on the adsorption of acetaminophen (paracetamol) in vitro. Part II. TG, FTIR, and XPS analysis of carbons and the temperature dependence of adsorption kinetics at the neutral pH. *Colloids Surfaces A Physicochem. Eng. Asp.* 177, 23–45. doi:10.1016/S0927-7757(00)00594-X
- Tromans, D., 1998a. Oxygen solubility modeling in inorganic solutions: concentration, temperature and pressure effects. *Hydrometallurgy* 50, 279–296. doi:10.1016/S0304-386X(98)00060-7

- Tromans, D., 1998b. Temperature and pressure dependent solubility of oxygen in water: a thermodynamic analysis. *Hydrometallurgy* 48, 327–342. doi:10.1016/S0304-386X(98)00007-3
- U.S. Environmental Protection Agency, 1992. Toxicity characteristic leaching procedure (Method 1311).
- Voigt, P., Hourn, M., Mallah, B., Turner, D., 2015. Commissioning and ramp-up of the Albion Process at the GPM Gold Project, in: *ALTA*. pp. 207–219.
- Wagman, D.D., Evans, W.H., Parker, V.B., Schumm, R.H., Halow, I., Bailey, S.M., Churney, K.L., Nuttall, R.L., 1982. The NBS tables of chemical thermodynamic properties. *J. Phys. Chem. Ref. Data*.
- Wang, J., 2006. *Analytical Electrochemistry*, Third Edit. ed, A John Wiley & Sons, Inc. John Wiley & Sons, Inc, Hoboken, New Jersey. doi:10.1017/CBO9781107415324.004
- Wang, S., 2005. Copper leaching from chalcopyrite concentrates. *Jom* 57, 48–51. doi:10.1007/s11837-005-0252-5
- Wilson, J.P., Fisher, W.W., 1981. Cupric chloride leaching of chalcopyrite. *J. Met.* 33, 52–57.
- Winand, R., 1991. Chloride hydrometallurgy. *Hydrometallurgy* 27, 285–316. doi:10.1016/0304-386X(91)90055-Q
- Yévenes, L.V., Miki, H., Nicol, M., 2010. The dissolution of chalcopyrite in chloride solutions. *Hydrometallurgy* 103, 80–85. doi:10.1016/j.hydromet.2010.03.004
- Yu, Y., Zhang, C., Yang, L., Paul Chen, J., 2016. Cerium oxide modified activated carbon as an efficient and effective adsorbent for the rapid uptake of arsenate and arsenite: material development and study of performance and mechanisms. *Chem. Eng. J.* 315, 630–638. doi:10.1016/j.cej.2016.09.068
- Zhou, J.H., Sui, Z.J., Zhu, J., Li, P., Chen, D., Dai, Y.C., Yuan, W.K., 2007. Characterization of surface oxygen complexes on carbon nanofibers by TPD, XPS and FT-IR. *Carbon N. Y.* 45,

785–796. doi:10.1016/j.carbon.2006.11.019

Zhu, T., Lu, X., Liu, H., Li, J., Zhu, X., Lu, J., Wang, R., 2014. Quantitative X-ray photoelectron spectroscopy-based depth profiling of bioleached arsenopyrite surface by *Acidithiobacillus ferrooxidans*. *Geochim. Cosmochim. Acta* 127, 120–139. doi:10.1016/j.gca.2013.11.025